รายงานวิจัยฉบับสมบูรณ์

การพัฒนาฟิลม์บางของโบรอน-โดปไดมอนด์โดยการแอโนไดซ์

Development of Boron-Doped Diamond Thin Film by Anodization

รศ.ดร.อรวรรณ ชัยลภากุล

31 สิงหาคม 2550

กิตติกรรมประกาศ

ขอขอบคุณ
สำนักงานกองทุนสนับสนุนการวิจัย
จุฬาลงกรณ์มหาวิทยาลัย

สัญญาเลขที่ RSA4780027

รายงานวิจัยฉบับสมบูรณ์

การพัฒนาฟิล์มบางของโบรอน-โดปไดมอนด์โดยการแอโนไดซ์

Development of Boron-Doped Diamond Thin Film by Anodization

รศ.ดร.อรวรรณ ชัยลภากุล

ภาควิชาเคมี คณะวิทยาศาสตร์ จุฬาลงกรณ์มหาวิทยาลัย

สนับสนุนโดยสำนักงานกองทุนสนับสนุนการวิจัย

บทคัดย่อ

รหัสโครงการ RSA4780027

ชื่อโครงการ: การพัฒนาฟิลม์บางของโบรอน-โดปไดมอนด์โดยการแอโนไดซ์

E-mail Address: corawon@chula.ac.th

ระยะเวลาที่ทำการวิจัย: 3 ปี

ในงานวิจัยนี้ได้มุ่งเน้นไปที่การพัฒนาการใช้ฟิล์มบางของโบรอน-โดปไดมอนด์ซึ่งผ่านการดัดแปรผิวหน้าด้วยการแอโนไดซ์และการฝังโลหะนิกเกิลสำหรับการหาปริมาณของสารในกลุ่มเตตร้าไซคลิน โดยทำการศึกษาเคมีไฟฟ้าของสารเตตร้าไซคลินที่ขั้วไฟฟ้าฟิล์มบางของโบรอน-โดปไดมอนด์ซึ่งผ่านการแอโนไดซ์ด้วยไซคลิกโวลแทมเมทรีและโฟลว์อินเจคชัน ซึ่งต่อกับระบบตรวจวัดทางเคมีไฟฟ้า เปรียบเทียบผลการทดลองโดยไซคลิกโวลแทมเมทรีกับขั้วไฟฟ้ากลาสสิคาร์บอนและขั้วไฟฟ้าฟิล์มบางของโบรอน-โดปไดมอนด์ พบว่าขั้วไฟฟ้าฟิล์มบางของโบรอน-โดปไดมอนด์ซึ่งผ่านการแอโนไดซ์จะให้ผลของไซคลิกโวลแทมโมแกรมสำหรับปฏิกิริยาออกซิเดชันของสารเตตร้าไซคลินแบบไม่ผันกลับที่ชัดเจนและให้สัญญาณกระแสไฟฟ้าสูงสุดเมื่อเปรียบเทียบกับขั้วไฟฟ้ากลาสสิคาร์บอนและขั้วไฟฟ้าฟิล์มบางขอโบรอน-โดปไดมอนด์ วิธีดังกล่าวสามารถนำไปประยุกต์ใช้กับการตรวจวัดสารเตตร้าไซคลินในตัวอย่างยาเตรียมได้ จากการศึกษาร้อยละการกลับคืนของสารมาตรฐานที่เติมในตัวอย่าง พบว่าผลการทดลองที่ได้เป็นที่น่าพอใจมีความสอดคล้องกับค่าที่ระบุในฉลาก สำหรับการวิเคราะห์ทางเคมีไฟฟ้าของสารเตตร้าไซคลินด้วยขั้วไฟฟ้าฟิล์มบางของโบรอน-โดปไดมอนด์ซึ่งผ่านการฝังโลหะนิกเกิล เปรียบเทียบผลการทดลองกับขั้วไฟฟ้าฟิล์มบางของโบรอน-โดปไดมอนด์ พบว่าที่ขั้วไฟฟ้าฟิล์มบางของโบรอน-โดปไดมอนด์ซึ่งผ่านการฝังด้วยโลหะนิกเกิลให้ผลของไซคลิกโวลแทมโมแกรมสำหรับปฏิกิริยาออกซิเดชันของสารเตตร้าไซคลินแบบไม่ผันกลับที่ชัดเจนและให้สัญญาณกระแสไฟฟ้าที่สูงกว่า นอกจากนี้ ได้นำขั้วไฟฟ้าฟิล์มบางของโบรอน-โดปไดมอนด์ซึ่งผ่านการฝังโลหะนิกเกิลไปใช้เป็นตัวตรวจวัดในระบบโฟลว์อินเจคชันเพื่อหาปริมาณของสารเตตร้าไซคลินในสารตัวอย่างยาด้วย และในส่วนสุดท้ายแสดงถึงผลที่ได้จากการนำขั้วไฟฟ้าฟิล์มบางของโบรอน-โดปไดมอนด์ซึ่งผ่านการฝังโลหะนิกมาใช้เป็นตัวตรวจวัดสารเตตร้าไซคลินที่ผ่านการแยกจากระบบไฮเปอร์ฟอร์มานซ์ลิควิดโครมาโทกราฟี ภายใต้ภาวะคือทำการแยกด้วยคอลัมน์ C18 ใช้เฟสเคลื่อนที่ที่ประกอบด้วยสารละลายฟอสเฟสบัพเฟอร์ (พีเอช 2.5) และแอซิโทรไนไตร์ ในอัตราส่วน 80:20 และตรวจวัดที่ 1.55 โวลต์ จากการสอบทวนในช่วงความเข้มข้น 0.05-100 พีพีเอ็ม ได้ค่าร้อยละการกลับคืนระหว่าง 83.3 – 102.5 ด้วยค่าเบี่ยงเบนมาตรฐานสัมพัทธ์ต่ำกว่า 10 เปอร์เซ็นต์ จากการนำวิธีนี้ไปใช้สำหรับการหาปริมาณสารเตตร้าไซคลินในสารตัวอย่างกุ้ง พบว่าวิธีที่เสนอนี้เป็นวิธีที่มีความเที่ยง ความแม่น และมีความไวต่อการหารปริมาณเตตร้าไซคลิน

คำสำคัญ: เตตร้าไซคลิน, ฟิล์มบางของโบรอน-โดปไดมอนด์ซึ่งผ่านการแอโนไดซ์, ฟิล์มบางของโบรอน-โดปไดมอนด์ซึ่งผ่านการฝังโลหะนิกเกิล, ไซคลิกโวลแทมเมทรี, โฟลอินเจคชัน, ไฮเปอร์ฟอร์มานลิควิดโครมาโทกราฟี, แอมเพอโรเมทรี

Abstract

Project code: RSA/21/2547

Project Title: Development of Boron-Doped Diamond Thin Film by Anodization

E-mail Address: corawon@chula.ac.th

Project period: 3 years

This research focused on the development of employing the modified boron-doped diamond thin film (BDD) including anodized BDD and Ni-implanted (Ni-DIA) BDD electrodes for the determination of tetracyclines (TCs). The electrochemistry of TCs was studied at an anodized BDD electrode using cyclic voltammetry and flow injection (FI) with electrochemical detector. At anodized BDD electrode, comparative experiments by cyclic voltammetry were performed at polishing glassy carbon (GC) and as-deposited BDD electrodes. The anodized BDD electrode exhibited well-defined irreversible cyclic voltammograms for the oxidation of TCs with the highest current signals compared to the as-deposited BDD and GC electrodes. The proposed method was also applied to determine TCs in pharmaceutical formulations. Recoveries of spiked standard solution were determined. The results obtained were satisfactory with label. For the electrochemical analysis of TCs using Ni-DIA BDD electrode, comparison experiments were carried out using as-deposited BDD electrode. Ni-DIA BDD electrode provided well-resolved oxidation irreversible cyclic voltammograms and the higher current signals when compared to those of as-deposited BDD electrode. Results using Ni-DIA BDD electrode in FI system coupled with amperometric detection were illustrated for the determination of TCs in drug samples. Moreover, in the last part, HPLC with amperometric detection using Ni-DIA electrode was also demonstrated. The chromatography was performed using a commercially available Inertsil C18 column, with the mobile phase being: 80% phosphate buffer (pH 2.5)–20% acetonitrile and detected at 1.55V. The methods were validated over the concentration range 0.05–100 ppm with the overall average recoveries from 83.3 to 102.5% and R.S.D. of less than 10%. The proposed method was further applied to analyze shrimp samples. The results obtained showed that this method is precise, accurate, and sensitive for the determination of TCs.

Keywords: TETRACYCLINES, ANODIZED BORON-DOPED DIAMOND THIN FILM ELECTRODE, Ni-IMPLANTED DIAMOND ELECTRODE, CYCLIC VOLTAMMETRY, FLOW INJECTION SYSTEM, HPLC, AMPEROMETRIC DETECTION

Executive Summary

วัตถุประสงค์

1. ศึกษาลักษณะของขั้วไฟฟ้าฟิล์มบางโบรอนโดปไดมอนด์ที่ได้พัฒนาโดยการแอโนไดซ์และโดยการฝังด้วยโลหะนิกเกิล
2. ศึกษาภาวะที่เหมาะสมสำหรับการใช้งานของขั้วไฟฟ้าฟิล์มบางโบรอนโดปไดมอนด์ที่ผ่านการแอโนไดซ์ และโดยการฝังด้วยโลหะนิกเกิล ตัวอย่างเช่น ผลของ pH สารละลายอิเล็กโทรไลท์ อัตราการสแกน เป็นต้น
3. ประยุกต์ใช้ขั้วไฟฟ้าฟิล์มบางโบรอนโดปไดมอนด์ที่ได้ดัดแปรโดยการแอโนไดซ์และโดยการฝังด้วยโลหะนิกเกิล กับการวิเคราะห์เชิงปริมาณ
4. ตรวจสอบอุปกรณ์ตรวจวัดที่ประกอบจากโบรอนโดปไดมอนด์อิเล็กโทรดที่ผ่านการดัดแปรเข้ากับระบบของไหลและระบบที่มีการแยก หาภาวะที่เหมาะสมในการวิเคราะห์แล้วนำไปทดลองใช้หาปริมาณของสารตัวอย่างจริง

การดำเนินงานวิจัย และผลงานวิจัยที่ได้รับอย่างย่อ ๆ

1. ค้นคว้าข้อมูลและเอกสารที่เกี่ยวข้อง
2. ตรวจสอบสารเตตร้าไซคลิน ใช้ขั้วไฟฟ้าฟิล์มบางโบรอน-โดปไดมอนด์ที่ได้ดัดแปรโดยการแอโนไดซ์ และโดยการฝังด้วยโลหะนิกเกิล ด้วยเทคนิค ไซคลิกโวลแทมเมทรี และแอมเพอโรเมทรี
3. หาภาวะที่เหมาะสมในการวิเคราะห์เตตร้าไซคลิน เพื่อปรับปรุงวิธีการวิเคราะห์ให้สามารถวิเคราะห์ได้ที่ความเข้มข้นต่ำ และเปรียบเทียบสมบัติทางเคมีไฟฟ้าของสารเตตร้าไซคลินเมื่อใช้ขั้วไฟฟ้าฟิล์มบางโบรอน-โดปไดมอนด์ที่ได้ดัดแปรโดยการแอโนไดซ์ ขั้วไฟฟ้าฟิล์มบางโบรอน-โดปไดมอนด์ และขั้วไฟฟ้ากลาสิคาร์บอนโดยใช้เทคนิคไซคลิกโวลแทมเมทรี จากการทดลองพบว่า สารเตตร้าไซคลินสามารถเกิดปฏิกิริยาผันกลับไม่ได้ที่ขั้วไฟฟ้าทั้งสามชนิด แต่ขั้วไฟฟ้าฟิล์มบางโบรอน-โดปไดมอนด์ที่ได้ดัดแปรโดยการแอโนไดซ์ จะให้ค่าสัญญาณของกระแสต่อพื้นหลังที่สูงกว่าขั้วไฟฟ้าฟิล์มบางโบรอน-โดปไดมอนด์และขั้วไฟฟ้ากลาสิคาร์ ค่า pH ที่เหมาะสมที่ให้สัญญาณในการตรวจวัดสูงสุดสำหรับเตตร้าไซคลิน ได้แก่ 2.0 สำหรับการหาภาวะที่เหมาะสมในการวิเคราะห์เตตร้าไซคลินด้วยขั้วไฟฟ้าฟิล์มบางโบรอน-โดปไดมอนด์ที่ได้ดัดแปรโดยการฝังด้วยโลหะนิกเกิล เมื่อเปรียบเทียบสัญญาณที่ได้จากปฏิกิริยาออกซิเดชันเมื่อใช้ขั้วไฟฟ้าฟิล์มบางโบรอน-โดปไดมอนด์ พบว่า ที่ขั้วไฟฟ้าฟิล์มบางโบรอน-โดปไดมอนด์ที่ได้ดัดแปรโดยการฝังด้วยโลหะนิกเกิล ให้สัญญาณที่สูงกว่าที่ค่า pH ของสารละลายเท่ากับ 2.0 เช่นกัน

4. หาภาวะที่เหมาะสมโดยใช้เทคนิคแอมเพอโรเมทรี ร่วมกับการตรวจวัดด้วยระบบโฟลว์อินเจคชันโดยใช้ขั้วไฟฟ้าฟิล์มบางโบรอน-โดปไดมอนด์ที่ได้ดัดแปรโดยการแอโนไดซ์หรือโดยการฝังด้วยโลหะนิกเกิล เป็นขั้วไฟฟ้าทำงาน จากผลการทดลองที่ได้จากขั้วไฟฟ้าฟิล์มบางโบรอน-โดปไดมอนด์ที่ได้ดัดแปรโดยการแอโนไดซ์ พบว่าศักย์ไฟฟ้าที่เหมาะสมในการตรวจวัดสารในกลุ่มเตตร้าไซคลิน ซึ่งประกอบด้วย ได้แก่ 1.50 โวลต์ สำหรับคลอเตตร้าไซคลิน และ 1.60 โวลต์ สำหรับเตตร้าไซคลิน ออกซีไซคลิน และด๊อกซีไซคลิน ตามลำดับ สำหรับผลที่ได้จากเทคนิคโฟลว์อินเจคชันให้ค่าขีดจำกัดต่ำสุดสำหรับสารทั้งสี่ชนิด ในการตรวจวัดที่ 10 นาโนโมลาร์ (S/N ≈ 3) จากผลการทดลอง เตตร้าไซคลิน ให้ช่วงความเข้มข้นที่เป็นเส้นตรงจาก 0.1 ถึง 50 ไมโครโมลาร์ และสำหรับคลอเตตร้าไซคลิน ออกซีไซคลิน และด๊อกซีไซคลิน ให้ช่วงความเข้มข้นที่เป็นเส้นตรงจาก 0.5 ถึง 50 ไมโครโมลาร์ ผลการทดลองที่ได้จากขั้วไฟฟ้าฟิล์มบางโบรอน-โดปไดมอนด์ที่ได้ดัดแปรโดยการฝังโลหะนิกเกิล เมื่อต่อกับระบบโฟลว์อินเจคชัน พบว่า ศักย์ไฟฟ้าที่เหมาะสมในการตรวจวัดสารเตตร้าไซคลิน คือ 1.55 โวลต์ ค่าขีดจำกัดต่ำสุดในการตรวจวัดเท่ากับ 10 นาโนโมลาร์ (S/N ≈ 3) และให้ช่วงความเข้มข้นที่เป็นเส้นตรงจาก 1 ถึง 100 ไมโครโมลาร์ เมื่อนำขั้วไฟฟ้าฟิล์มบางโบรอน-โดปไดมอนด์ที่ได้ดัดแปรโดยการฝังโลหะนิกเกิล มาใช้เป็นตัวตรวจวัดในระบบไฮเปอร์ฟอร์มานส์ลิควิดโครมาโทกราฟี พบว่า ได้ค่าขีดจำกัดต่ำสุดในการตรวจวัดอยู่ในช่วง 0.01 – 0.05 พีพีเอ็ม (S/N ≈ 3) ช่วงความเข้มข้นที่เป็นเส้นตรงจาก 0.05 ถึง 100 พีพีเอ็ม สำหรับเตตร้าไซคลินและคลอเตตร้าไซคลิน และจาก 0.1 ถึง 100 พีพีเอ็ม สำหรับออกซีไซคลินและด๊อกซีไซคลิน ตามลำดับ
5. นำวิธีที่เหมาะสมมาใช้หาปริมาณเตตร้าไซคลินในสารตัวอย่างยา การทดลองใช้เทคนิคการเติมสารมาตรฐานพบว่า ได้ร้อยละของการคืนกลับอยู่ในช่วง 98.40 -101.50 มีความเที่ยง 1.30-3.0 เปอร์เซ็นต์ กรณีที่ใช้ ขั้วไฟฟ้าฟิล์มบางโบรอน-โดปไดมอนด์ที่ได้ดัดแปรโดยการแอโนไดซ์ และค่าร้อยละของการคืนกลับในช่วง 97.22-102.38 ความเที่ยง 2.82 เปอร์เซ็นต์ สำหรับขั้วไฟฟ้าฟิล์มบางโบรอน-โดปไดมอนด์ที่ได้ดัดแปรโดยการฝังด้วยโลหะนิกเกิล สำหรับการหาปริมาณเตตร้าไซคลินในสารตัวอย่างกุ้ง หลังจากที่แยกด้วยระบบไฮเปอร์ฟอร์มานส์ลิควิดโครมาโทกราฟี พบว่า ได้ร้อยละของการคืนกลับอยู่ในช่วง 97.00 -103.70 สำหรับตัวอย่างกุ้งฟาร์ม และร้อยละ 96.5-99.4 สำหรับตัวอย่างกุ้งทะเล จากผลการทดลองพบว่าการใช้เทคนิคแอมเพอโรเมทรีร่วมกับระบบโฟลว์อินเจชันหรือระบบไฮเปอร์ฟอร์มานส์ลิควิดโครมาโทกราฟี ให้ผลการทดลองที่ถูกต้อง มีความสามารถในการทำซ้ำ และให้ช่วงการทำงานที่เป็นเส้นตรงที่กว้าง จึงสามารถนำไปประยุกต์กับการวิเคราะห์ตัวอย่างได้อย่างมีประสิทธิภาพ

INTRODUCTION

Introduction

Currently, the use of synthetic conductive diamond thin films, a new carbon material, is being increasingly reported [1-10]. Diamond is one of the most insulating of insulators; however, boron can be used as a convenient dopant in diamond, at levels all the way from about 10^{16} up to 10^{21} cm^{-3}, with activation energies down to less than one tenth of an electron volt, so that the conductivity can be fine-tuned for a variety of purposes [11]. Therefore, boron-doped diamond (BDD) is one of the most promising new materials for electroanalytical measurements. It has been reported that the BDD electrode possesses electrochemically attractive properties compared to other electrodes, including low and stable voltammetric background currents. The currents for double layer charging are quite small, due to the low number of carriers and the nearly complete lack of porosity. These attributes make the BDD electrode well suited for current-based electrochemical measurements. Other attractive features include the wide working potential window in aqueous electrolyte solution, low adsorption of polar molecules from aqueous solution, long-term response stability, and good activity without any pretreatment [12-15].

Besides the as-deposited BDD electrode, recently, modified diamond surfaces are becoming more and more extensively used. The modification techniques, which include chemical, electrochemical and photochemical techniques, have been reported; these include ways of attaching anything from terminating atoms, such as oxygen, as well as metal particles and metal oxides. From these modification techniques, chemically pretreated by electrochemical oxidation is the simplest technique. The anodized diamond electrodes retain the excellent properties of the as-deposited diamond electrode even though, the electrode surface of anodized diamond electrode is applied by a high anodic potential. Anodized diamond electrodes are suitable for determination of various analytes such as chlorophenol [16], dopamine and uric acid in the presence of ascorbic acid [17] and homocysteine [18]. These anodized

electrodes have exhibited some attractive properties such as excellent stability and high reproducibility.

While some metals, such as platinum is known to oxidize hydrogen peroxide and methanol, as well as nickel is conventionally used for carbohydrates electrochemical detection in alkali solution [19–21]. BDD electrode is found completely inactive for those kinds of catalytic reactions. However, it has been reported that the dispersion of metallic particles within an organic polymer or an inert surface resulted indrastic increase of the catalytic activity and sensitivity of the electrode because the dispersed particles behave like microelectrode arrays [20]. The chemically modified electrodes (CMEs) which are capable of lowering the operational potential required to oxidize scarcely electroactive organic compounds has caught a great deal of interest. Reduced electrode fouling has also been reported. CMEs based on the modification of glassy carbon or graphite rods with various metals (e.g. copper [22-24], cobalt [25], and nickel [20, 21, 26–28]) have shown catalytic activities towards polyhydroxy compounds. These electrodes have been successfully applied to detect carbohydrate [20–22, 25, 26], amino acids [26, 28], sugars [23] and aliphatic alcohol compounds [27] using amperometric detection. Unfortunately, glassy carbon electrode has a major drawback of yielding high background current. These metalmodified diamond electrodes appear to be well suited to overcome such problems. BDD film would be the best choice for the deposition of metal electrocatalysts. The preparation of some metal-modified BDD electrodes for electrochemical analysis by using chemical precipitation and electrochemical deposition method had been reported [19].

Ion implantation into a material can be used to form near surface composites. The method is used to modify the structure of a target-near-surface by bombardment with heavy ions. This method is popular for the preparation of doping semiconductors, such as silicon and gallium arsenide, so it has been of particular interest for the fabrication of ion-implanted diamond. At present, some applications for electrochemical use by metal-implanted conductive BDD electrodes have been reported [29].

Therefore, we are interested in developing a method for the determination of tetracyclines by using anodized BDD electrode the Ni-implanted diamond electrode

as a working electrode for amperometric determination using flow injection system and HPLC system.

Tetracyclines (Figure1) are board spectrum antibiotics for their high activity against nearly all gram-positive and gram-negative bacteria. Tetracycline, chlortetracycline, oxytetracycline and doxycycline are four members of this antibiotic group that are commonly used in food protection animals (including honeybee), because of their board spectrum activity and low production cost. However, use of these drugs has become the serious problem as regard infectious diseases, as they are substances that residue in milk or meat which can be directly toxic or else cause allergic reactions in some hypersensitive individuals in human. Owing their extensive use in infectious diseases therapy, there are several methods used to determine these compounds in pharmaceutical preparations, biological samples and milk samples. Official methods such as microbiological-based techniques can also provide both qualitative and quantitative analysis for tetracyclines [30-32]. These methods available have their characteristic disadvantages: microbiological tests are not only time consuming laborious and expensive but also poor in term of sensitivity and selectivity. Other methods for quantification the amount of tetracyclines were developed based on batch procedures with spectrophotometry [33-34], chemiluminescence [35-38], spectrofluorimetry [39], and electrochemical method [40]. Flow injection system was incorporated with conventional analytical instrument to improve sample throughput and sensitivity that are the requirement to develop approach in pharmaceutical industry. Many detection methods were coupled to a flow injection system such as spectrophotometry [41-42], chemiluminescence [43-44] and electrochemical method [45-47]. Flow injection based on the spectrophotometric detection is described to determine tetracyclines by the monitoring the color product formed by their reaction with 4-aminophenazone and hexacyanoferrate (III). However, this method has a limitation in a concentration range. Under the optimized conditions, tetracyclines were determined in the ranges 1-20 and 20-250 mg L^{-1}. The lowest limit of detection is 0.2 mg L^{-1} for doxycycline [33]. For chemiluminescence using oxidizing agent such as *N*-Bromosuccinimide, is an alternative method but the oxidizing agent is highly toxic and the methods are expensive. The working range for determining is 0.05-3.00 mg L^{-1} for tetracycline, 0.50-5.00 mg L^{-1} for oxytetracycline and 0.50-7.00 mg L^{-1} for doxycycline and

chlortetracycline. The detection limit is 0.0049, 0.40, 0.23, and 0.22 mg L^{-1} for tetracycline, oxytetracycline, doxycycline, and chlortetracycline respectively [35]. Electrochemical techniques such as amperometric and potentiometric detection are good alternative methods that are widely used in the pharmaceutical application because they are easy to operate, fast and inexpensive. The sensitivity of electrochemical method is also higher than the spectrophotometric method such as the detection limit from HPLC-amperometric detection of 0.1-1 mg L^{-1} for tetracycline family [48]. The calibration graph showed linear relationship between 0.1 and 50 mg L^{-1} for tetracycline, oxytetracycline and doxycycline and relationship between 0.5-50 mg L^{-1} for chlortetracycline. Procedures in electroanalysis strongly depend on working electrode materials. Hence, the searching and synthetic the new electrode material is necessary. Thus, for part I, we described to use of the anodized diamond electrode for the determination of tetracyclines using cyclic voltammetry. Glassy carbon (GC) and as-deposited diamond electrodes were also used for comparison. The anodized diamond electrode was exploited as working electrode for amperometric determination of antibiotic drugs, using flow injection system.

Moreover, today the shrimp farming is an important economic section in south-east asian countries, especially Thailand. The most markets of these countries are Japan, the United States and Europe, which have regulations to control quality of imports. The shrimp farming cannot avoid using antibiotics; however, tetracyclines that are the most important ones of antibiotics are generally used in the shrimp farming. The residues of tetracyclines may be found in shrimps and the levels of tetracycline residues may be unacceptable for the international markets. Therefore, the methods of the detection of tetracyclines at low levels are intensively required.

For detecting the tetracycline residues, the microbiological assays, the official methods, are most usually used, but they are complicated, time-consuming and non-specific. Therefore, sensitive and specific analytical methods for identification and quantitation of tetracyclines are required. High performance liquid chromatography (HPLC) is normally used for this purpose.

HPLC is a common method that separates tetracyclines in the reverse-phase mode with a variety of detection methods, such as spectrophotometry [49-50],

fluorometry [51-52], mass spectrometry [53-54] and electrochemistry [55-56]. Among these, the electrochemical method is distinctly attractive owing to its simplicity, no need for derivatization, fast analysis, low cost and high sensitivity. There are several reports utilizing polarography, potentiometry [57] and amperometry [55-56, 58] for the analysis of tetracycline. In 2005, Charoenraks et al. reported the use of high performance liquid chromatography with pulsed amperometric detection at anodized boron-doped diamond thin film electrode for the detection of tetracyclines.

Therefore, in following part, we report the use of Ni-implanted boron-doped diamond thin film electrodes (Ni-DIA) to study the electrochemical oxidation of tetracyclines using cyclic voltammetry. Focus is placed on comparing the results with as-deposited BDD and glassy carbon electrodes. In addition, the performance of the Ni-DIA electrode for the detection of tetracycline was examined by HPLC with amperometric detection for determination of tetracyclines in shrimp.

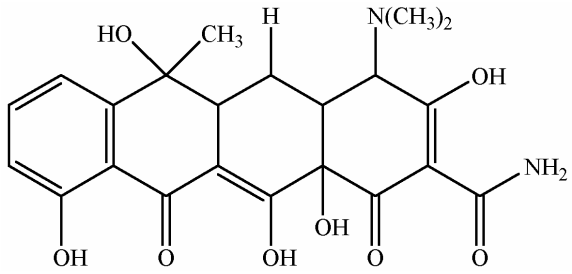

Tetracycline

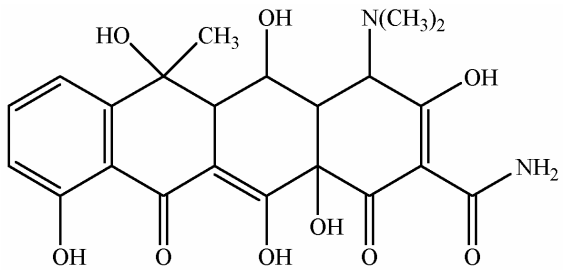

Oxytetracycline

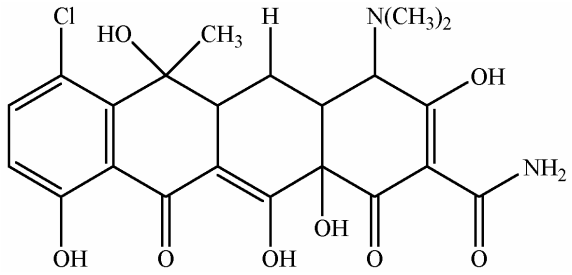

Chlortetracycline

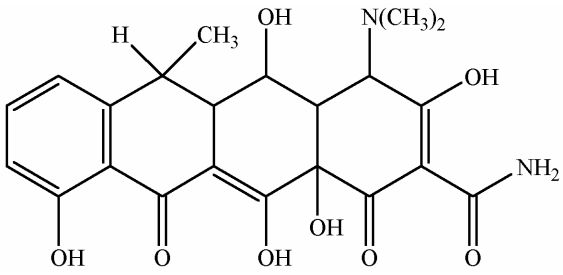

Doxycycline

Figure 1 Structures of 4 tetracyclines

The Objective of Research

The main objective of this research is to develop an analytical method for the determination of tetracyclines at low levels in antibiotic drugs and shrimps. The use of flow injection and high performance liquid chromatography (HPLC) with amperometric detection is proposed.

In the amperometric detection, three electrodes, namely, a BDD electrode, an anodized boron-doped diamond thin film electrode and Ni-implanted boron-doped diamond thin film electrodes (Ni-DIA) are used. In the process of developing the above mentioned method the following specific objectives of the study should therefore be described.

(1) To investigate the oxidation of tetracyclines using cyclic voltammetry at a BDD electrode, an anodized boron-doped diamond thin film electrode and Ni-implanted boron-doped diamond thin film electrodes (Ni-DIA).
(2) To obtain the optimal parameters for ampermetric detection using anodized BDD electrodes under FIA or HPLC system.
(3) To establish the optimal conditions for FIA or HPLC system.
(4) To study the validation of the method.
(5) To compare the developed method to the AOAC Official method.

EXPERIMENTAL

Chemical Reagents

- Tetracycline hydrochloride (Sigma)
- Oxytetracycline hydrochloride (Sigma)
- Chlortetracycline hydrochloride (Sigma)
- Doxycycline hydrochloride (Sigma)
- Potassium dihydrogen orthophosphate (BDH)
- Disodium hydrogen orthophosphate (BDH)
- Phosphoric acid (Merck)
- Diaminetetraacetic acid disodium salt (Fluka)
- Citric acid (J.T.Baker)
- Acetonitrile (HPLC Grade, Merck)
- Methanol (HPLC Grade, Merck))
- 2-Propanol (Analytical Grade, Merck)
- Oxalic acid dihydrate (Merck)

Instruments and Equipments

- An Autolab Potentiostat (PGSTAT 30, Metrohm)
- A Water No. 510 solvent delivery system (Waters Associates Inc, Milford, MA, USA)
- A Rheodyne injection valve, Model 7225 (Altech), with a 20 μl stainless steel injection loop (0.5 mm. i.d.)
- Automated LC system (HP 1100 series from Agilent Technologies, USA.) consisted of auto-sampler, binary pump, on-line degasser, UV-Visible and fluorescence detector
- Milli-Q water system, model Millipore ZMQS5V00Y, (Millipore, USA) (CENTAURA 2, Sanyo)

- Mobile phase filter set included 300 mL glass reservoir, glass membrane holder, 1000 mL flask and metal clip (Millipore, USA)
- Autopipette and tips (Eppendorf, Germany)
- Inertsil-ODS3 C_{18} (5 μm, 4.6 mm × 25 cm, GL Science)
- C18-E cartridges 500 mg, 6 mL, (Phenomenex, USA.).
- A Ag/AgCl electrode (Bioanalytical System Inc.)
- A platinum wire (Bioanalytical System Inc.)
- The as-deposited boron doped-diamond electrode (WD769/1, Purchased from Centre Suisse d' Electronicat de Microtechnique SA (CSEM) and obtained from Associate Prof. Kensuke Honda.
- A polish set of 0.05 and alumina powder slurry (Metrohm)
- A thin layer flow cell (Bioanalytical System Inc.)
- A Teflon cell gasket (Bioanalytical System Inc.)
- Peek tubing (0.25 mm i.d.) and connecting (Upchurch)
- Teflon tubing (1/10 inch i.d., Upchurch)
- A cutting set (Altech)
- A 0.45 μm Nylon membrane filter (Altech)
- A 0.45 μm Nylon membrane syringe filter with polypropylene (Orange Scientific filter)
- A pH meter (Metrohm)
- A sonicator (USA, A006651)
- An analytical balance (Metler, AT 200)
- HPLC vials 2.0 mL with PTFE screw caps (Agilent Technologies, USA)
- Glass containers with Teflon screw cap 25 Ml
- Erlenmeyer flasks 10, 100, and 250 mL
- Separatory funnels 500 mL
- Volumetric flasks 10, 25, 50 and 100 mL
- Beakers 10, 25, 50, 100, 500 and 1,000 mL

Preparation of chemical solutions

❖ Preparation of 0.1 M phosphate buffer solution

13.6 g and 17.6 g of potassium dihydrogen phosphate and disodium hydrogen phosphate dehydrate were dissolved in 1 L of deionized water to make the solution of 0.1 M potassium dihydrogen phosphate buffer and 0.1 M disodium hydrogen phosphate. The recipes of each pH solution were shown in Table 3.1

Table 3.1 Recipes of phosphate buffer preparation.

pH	0.1 M Potassium dihydrogen phosphate (mL)	0.1 M Disodium hydrogen phosphate (mL)
5	99.2	0.8
6	88.9	11.1
7	41.3	58.7
8	3.7	96.3

The 0.1 M of potassium dihydrogen phosphate was adjusted by phosphoric acid to make the range of pH from 2 to 4.

❖ Stock Standard Solutions

Each stock standard solution (1000 μg/mL) of TC, OTC, CTC and DC was prepared daily by weighing 50 mg of each standard into a 50 mL volumetric flask and the volume was adjusted to 50 mL with the mobile phase.

❖ **Working Standard Solutions**

First, the mixture of 4 TCs solutions containing 100 μg/mL was prepared by pipetting 1.0 mL of each standard solution 1000 μg/mL into a 10 mL volumetric flask and the volume was adjusted to 10 mL with mobile phase. Working standard solutions were prepared by diluting the standard mixture solutions 100 μg/mL with mobile phase. All of the solutions were protected from exposure to light and stored in the refrigerator.

❖ **Preparation of Mobile Phase**

The mobile phase for HPLC condition was consisted of acetonitrile and the phosphate buffer solution. The phosphate buffer solution of pH 2.5 was prepared daily by mixing of 0.01 M H_3PO_4 + 0.1 M Na_2HPO_4 (a few drops to adjust the pH). The phosphate buffer was filtered with a 0.45 μm Nylon membrane filter.

❖ **5 Preparation of Na_2EDTA-McIlvaine Buffer**

Na_2EDTA -McIlvaine buffer solution (pH 4) was prepared by dissolving 15 g of disodium hydrogenphosphate dihydrate, 13 g of citric acid monohydrate and 3.72 g of EDTA in deionized water in 1 L volumetric flask.

❖ **Sample Preparation**

- **Drug Analysis**

The pharmaceutical preparations analyzed and the labeled contents (amount present in 1 capsule) were: Tetracycline hydrochloride containing 250 mg tetracycline hydrochloride (TC); Aureomycin containing 250 mg chlortetracycline (CTC); Oxycline containing 250 mg oxytetracycline (OTC); Medomycin containing 100 mg doxycycline (DC). The powder of 20 drug capsules were each weighed so as to obtain the mean capsule weight. An accurately weighed was portion of

homogenized powder corresponding the mean capsule weight was transferred into volumetric flask and dissolved with 0.1 mol l^{-1} phosphate buffer (pH 2), and then shake well. The portion of sample solutions was filtrated through 0.45- μm nylon membrane. The filtrated solutions were further diluted using 0.1 mol L^{-1} phosphate buffer (pH 2) to make the final concentration in the range of 0.96-5.15 μg ml^{-1} within the linear dynamic range. All tetracycline antibiotic solutions were protected form light by covering with aluminum foil and stored at the temperature of 4 ^{0}C in the refrigerator.

- **Shrimp Analysis**

The shells, fins and tails of shrimp were removed and ground in a conventional meat grinder. The ground shrimp were stored at below -10°C until analysis.

2.50±0.05 g of ground shrimp was placed in 25 mL centrifuge tube, 12.5 mL of Na_2EDTA-McIlvaine buffer (pH 4) was added, then the mixture was centrifuged at 3500 rpm for 20 min. The supernatant was loaded into SPE cartridge, previously activated with 10 mL of methanol and 10 mL of Milli-Q water. After sample loading, the SPE cartridge was washed with 10 mL of Milli-Q water and finally tetracyclines were eluted by 10 mL of methanol. The solvent was removed under a nitrogen stream. The residues were diluted in the total volume of 10 mL and the solutions were filtered with a 0.45 μm PTFE filter. Then, 20 μL of aliquot was injected to the HPLC system.

Preparation of Anodized BDD Electrode

An anodized BDD electrode was prepared by treating an as-deposited BDD electrode in 0.1 M KOH solution. The potential was applied between 0 to 2 V versus Ag/AgCl using cyclic voltammetry for 30 min. The anodized BDD electrode was also rinsed with ultrapure water before use.

Preparation of Ni--implanted boron-doped diamond thin film electrodes (Ni-DIA)

The experimental conditions and the apparatus used for the diamond film growth have been described in detail elsewhere. The films were prepared by deposition of the boron-doped polycrystalline diamond than films on highly conductive n-Si (100) substrates by high-pressure microwave plasma-assisted chemical vapor deposition (CVD) system (ASTex Corp., Woburn, MA). The boron source, B2O3, was dissolved in this solvent mixture so that the B/C ratio was approximately 102 ppm. These films were implanted with 750 keV Ni2+ with a dose of 5 x 1014 cm-2 (Tandetron 4117-HC, HVEE). The annealing was performed at 850°C for 10 min in an H2 ambient (80Torr). The nickel-implanted boron-doped diamond electrodes (Ni-DIA) have been prepared in Associate Professor Yasuaki Einaga's laboratory. The presence of Ni particles on BDD surface was con.rmed by XPS and SEM. The experimental conditions and the apparatus used for this characterization have been described in detail elsewhere26. The Ni-DIA electrodes were rinsed with ultra-pure water prior to use.

Cyclic Voltammetric Study

Each of 1 mM of OTC, TC, CTC and DC standard solutions was prepared by weighing 0.0495, 0.0481, 0.0515, and 0.0481 g, respectively and transfering into 100 mL volumetric flask. The phosphate buffer was used for diluting this aliquot to the mask. These solutions were used for the investigation of the oxidation of TCs by cyclic voltammetry at the BDD electrode, the anodized BDD electrode and Ni-implanted boron-doped diamond thin film electrodes (Ni-DIA)

Electrochemical experiment was carried out in the single compartment three-electrode glass cell. The BDD electrode was pressed against a smooth ground joint at the bottom of the cell, isolated by an O-ring vitron (area 0.07 cm^2). Ohmic contact was made by placing the backside of the Si substrate. The GC carbon was used as working electrode for the comparison. The Ag/AgCl with salt bridge and Pt wire were used as reference electrode and counter electrode respectively. The voltammetric measurement was performed with the three types of electrodes using Autolab Potentiostat 100 (Eco-Chemie, The Netherlands).

- **Voltammetric study of TCs**

The 0.5 mM of TCs in 0.1 M potassium dihydrogen phosphate (pH 2) were investigated using BDD electrode by cyclic voltammetry at scan rate 50 mV s^{-1}. Comparison the results using as-deposited BDD and GC electrodes were carried out.

- **The scan rate dependence study**

The 1 mM solution of TCs, experiments were performed at various scan rates including 10, 20, 50, 100, 200 and 300 mV s^{-1} to investigate the adsorption of the analytes on the surface of electrode.

- **pH dependence study**

The 1 mM of the analyte at each pH was measured using anodized BDD electrode by cyclic voltammetry to obtain the optimum pH of the measurement. A scan rate of 50 mV s^{-1} was used. The surface area was 0.28 cm^2. The experiment was carried out in plastic cap cell.

Flow injection with amperometric detection

The flow injection system consisted of a thin layer flow cell (Bioanalytical System, Inc), a 20-µl stainless steel loop of injection port (Rheodyne 7725), a peristaltic pump, and electrochemical detection (Autolab potentiastat 100). The carrier solution (0.1 mol L^{-1} potassium dihydrogen phosphate pH 2) was regulated at the flow rate of 1 ml min^{-1} by measuring the volume of carrier solution in 1 min. The thin layer flow cell consisted of a silicone rubber gasket as a spacer, a Ag/AgCl electrode as the reference electrode and a stainless steel tube as an auxiliary electrode and an outlet of the flow cell. The experiments were performed in a copper faradaic cage to reduce the electronic noise. All experiments were done at room temperature.

HPLC Optimization

A HPLC method equipped with a C_{18} column and phosphate buffer (pH 2.5) and acetonitrile as the mobile phase was used to develop the separation of 4 tetracyclines; i.e. oxyetracycline (OTC), tetracycline (TC), chlortetracycline (CTC) and doxycycline (DC). The injection volume was 20 μL and the detector was Ni-implanted boron-doped diamond thin film electrodes (Ni-DIA). The optimization was determined by vary the mobile phase strength. The separation of tetracyclines was first tested with standard mixture and the condition was later tested with shrimp samples spiked mixed standard.

Calibration and Linearity

Each concentration of the mixed standard TCs solutions at 0.1, 0.5, 1.0, 5.0, 8.0, 10, 25, 50 and 100 mg/L was injected in duplicate. The calibration curves were plotted between the peak areas and the concentrations.

Limit of Detection (LOD) and Limit of Quantitation (LOQ)

The LOD and LOQ were determined by various concentrations under HPLC conditions and optimal PAD parameters. The detection limit (LOD) and quantitation limit (LOQ) are defined as the concentration that provided a current response higher 3 times than the noise ($S/N \geq 3$) and 10 times than the noise ($S/N \geq 10$), respectively.

Precision and Accuracy

For intra-day precision, the repeat of analysis of spiked sample was studied in one day. For inter-day precision, the repeat of analysis of spiked sample was studied on different days. The spiking at level 0.5, 1.0, 5.0 and 10 mg/kg was used in the study and at each level was repeated in triplicate.

Applications

The HPLC-amperometric detection using the Ni-implanted boron-doped diamond thin film electrodes (Ni-DIA) was applied to detect tetracyclines in shrimps. Two types of shrimp that purchased from the local markets were farming-shrimp and sea-shrimp. The developed method was compared to the AOAC Official method (995.09) and Laboratory Center for Food and Agricultural Products Company Limited (LCFA).

AOAC Official Method (995.09)

This method could be used to detect tetracycline, chlortetracycline and oxytetracycline. The column used in this method was the same as in HPLC-EC systems. The HPLC conditions were carried out using the mobile phase of oxalic acid (0.1 M) – methanol – acetonitrile (60:10:30; v/v) on a C_{18} column at a flow rate of 1.0 mL/min at room temperature. The injection volume was 20 μL and the detector was UV-Visible detector at 350 nm.

❖ Preparation of Chemical Solutions

o Preparation of Mobile Phase

First, the oxalic acid solution was prepared by weighing 1.26 g of oxalic acid dihydrate and dissolving into 1 L volumetric flask with Milli-Q water. Then, the mobile phase 600 mL oxalic solution was combined with 300 mL acetonitrile and 100 mL methanol.

o Preparation of McIlvaine buffer-EDTA solution

28.4 g of anhydrous Na_2HPO_4 was dissolved into 1 L volumetric flask and dissolved with deionized water. Then, 21.0 g citric acid was dissolved into another 1 L volumetric flask and dilute to 1 L with deionized water. The mixed solution was the combination of 1 L citric acid solution and 625 mL Na_2HPO_4 solution in 2 L beaker. The mixed solution was adjusted to pH 4.0 by adding 0.1 M

HCl or 0.1 M NaOH. Finally, 60.5 g disodium EDTA dihydrate was dissolved with 1.625 L of mixed solution.

- **Preparation of Methanolic acid**

1.26 g oxalic acid dihydrate was dissolved into 1 L volumetric flask with methanol.

❖ **Sample Preparation**

5.00±0.05 g of sample was placed into 50 mL centrifuge tube, added 20 mL McIlvaine buffer-EDTA solution and blended 30 sec with homogenizer. Then, this tube was centrifuged for 10 min at 2500 rpm and put the supernatant into another 50 mL centrifuge tube. Adding 20 mL McIlvaine buffer-EDTA solution in the first centrifuged tube containing the sample and repeated all steps to obtain the second extraction. Finally, adding 10 mL McIlvaine buffer-EDTA solution in the first centrifuged and repeated all steps. The supernatant from 3 extractions was collected in the second tube, then loaded to the SPE extraction.

SPE cartridges were set, and conditioned with 20 mL methanol and 20 mL Milli-Q water. The supernatant was loaded into SPE cartridge. After sample loading, the SPE cartridge was washed with 10 mL of Milli-Q water and finally tetracyclines were eluted by 6 mL of methanolic oxalic acid. The residues were diluted in the total volume of 10 mL, and the solutions were filtered with a 0.45 μm PTFE filter. Then, 20 μL of aliquot was injected to the HPLC system.

RESULTS AND DISCUSSION

In this chapter, details will be separated into three parts. The first part was the results and discussion from using anodized boron-doped diamond thin film electrode for the determination of tetracycline antibiotic drugs. The results obtained from batch system and flow injection analysis will be presented respectively. For the second part, the working electrode was changed from anodized BDD electrode to Ni-implanted boron-doped diamond thin film electrodes (Ni-DIA) for the analysis of tetracycline using flow injection system and HPLC system. The results obtained were categorized in the same steps as shown in the first part. Additionally, HPLC results will be discussed as well at the end of this part.

Determination of TCs using an anodized BDD electrode

This study focused on the method development of the tetracycline antibiotic determination, based on the electrochemical method using an anodized BDD electrode. The study was separated into 2 parts including cyclic voltammetry and flow injection with amperometric detection. The details of each part were described as the follows.

❖ Investigation of TCs using cyclic voltammetry

o Voltammetric study of TCs

As commonly known, the synthesis of as-deposited BDD electrodes by microwave plasma-assisted chemical vapor deposition is hydrogen-terminated on the diamond surface. The chemical modification can be carried out by anodic polarization or oxygen plasma treatment to change the hydrogen-terminated surface to an oxygen-terminated surface one. In this study, anodic polarization in alkaline solution (0.1 M potassium hydroxide) was used, as described in the experiment chapter. The major type of oxygen functional group is the carbonyl group, which is believed to exist on faces. The highly oriented carbonyl groups

provide a surface dipolar field that could repel a neutral molecule with oxygen-containing functional groups surrounding a central core. On the other hand, the oxygen plasma treatment or thermal oxidation can induce the bridge form of C-O-C on the surface of diamond.

The electrooxidation of four TCs was investigated on as-deposited BDD, GC, and anodized BDD electrodes. Figures 1-4 show cyclic voltammograms of 500 μM of TCs in 0.1 potassium dihydrogen phosphate (pH 2) together with the background voltammograms at the as-deposited BDD, GC, and anodized BDD electrodes. All electrodes provided irreversible cyclic voltammograms. This irreversible behavior suggested that TCs were oxidized, and then reacted rapidly to form a new product. Cyclic voltammetric results of TC, CTC, OTC, and DC at as-deposited BDD, GC, and anodized BDD electrodes are summarized in Table 1. Results showed that the highest current signals were obtained for TC, CTC, OTC, and DC at the anodized BDD electrode and they can be explained in recent work carried out with glutathione on the basis of attractive electrostatic interaction between the negatively charged anodized surface and the positively charged substrates. TCs were fully positively charged in strongly acidic pH, as we used in this experiment. Hence, the positively charged substrates could be attracted to the negative surface of the anodized BDD electrode, which induced the electrooxidation to occur easily. In contrast to as-deposited BDD, the surface is positively charged and non-polar (covered with hydrogen atoms), and the electrostatic interaction was less permitted, which presumably resulted in the ill-defined cyclic voltammagrams.

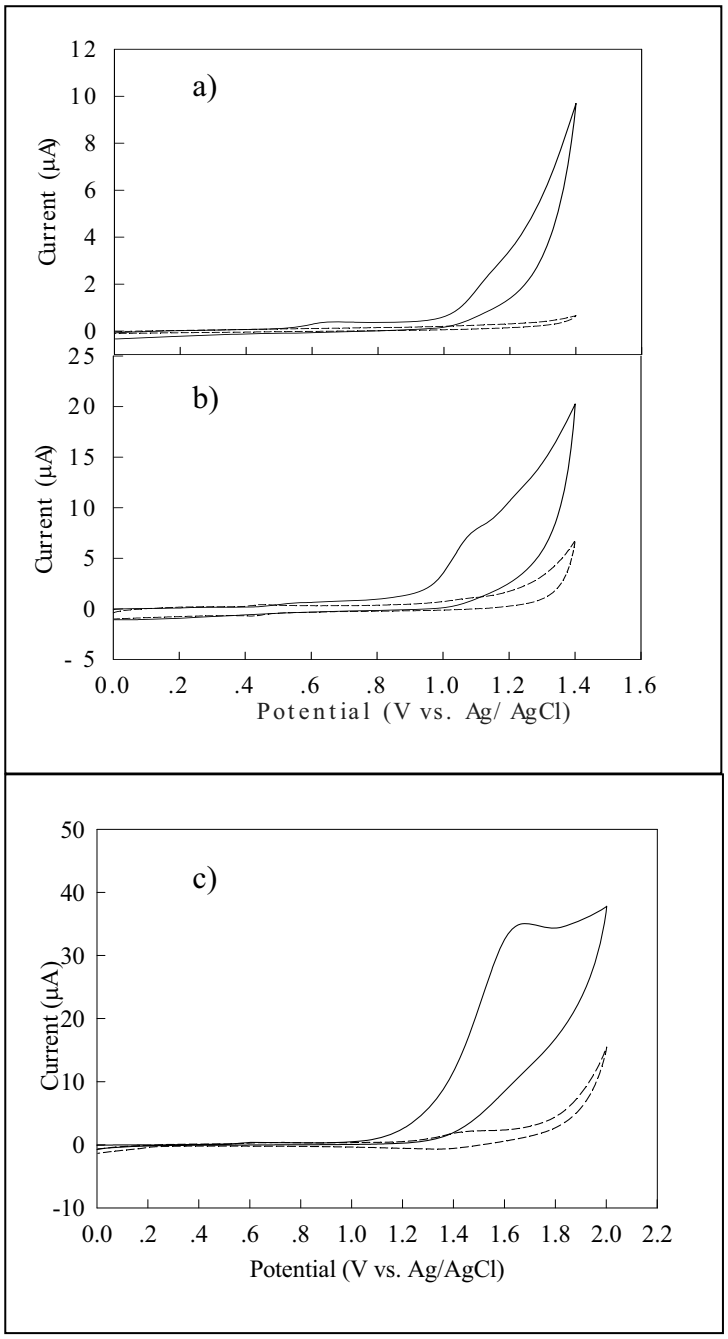

Figure 1 Cyclic voltammograms of 500 μM OTC (solid line) in 0.1 M potassium hydrogen phosphate (pH 2) together with the corresponding background current (dashed line) at a) as-deposited BDD b) GC, and c) anodized BDD electrodes.

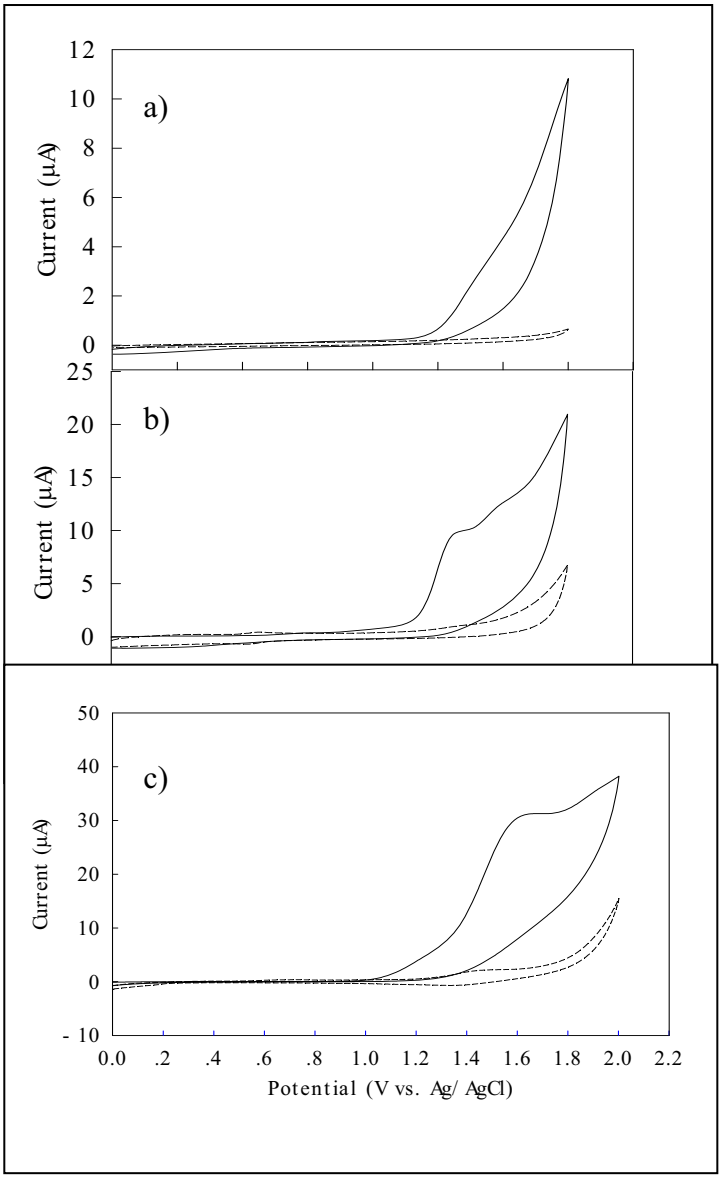

Figure 2 Cyclic voltammograms of 500 μM TC (solid line) in 0.1 M potassium dihydrogen phosphate (pH 2) together with the corresponding background current (dashed line) at a) as-deposited BDD b) GC, and c) anodized BDD electrodes**.**

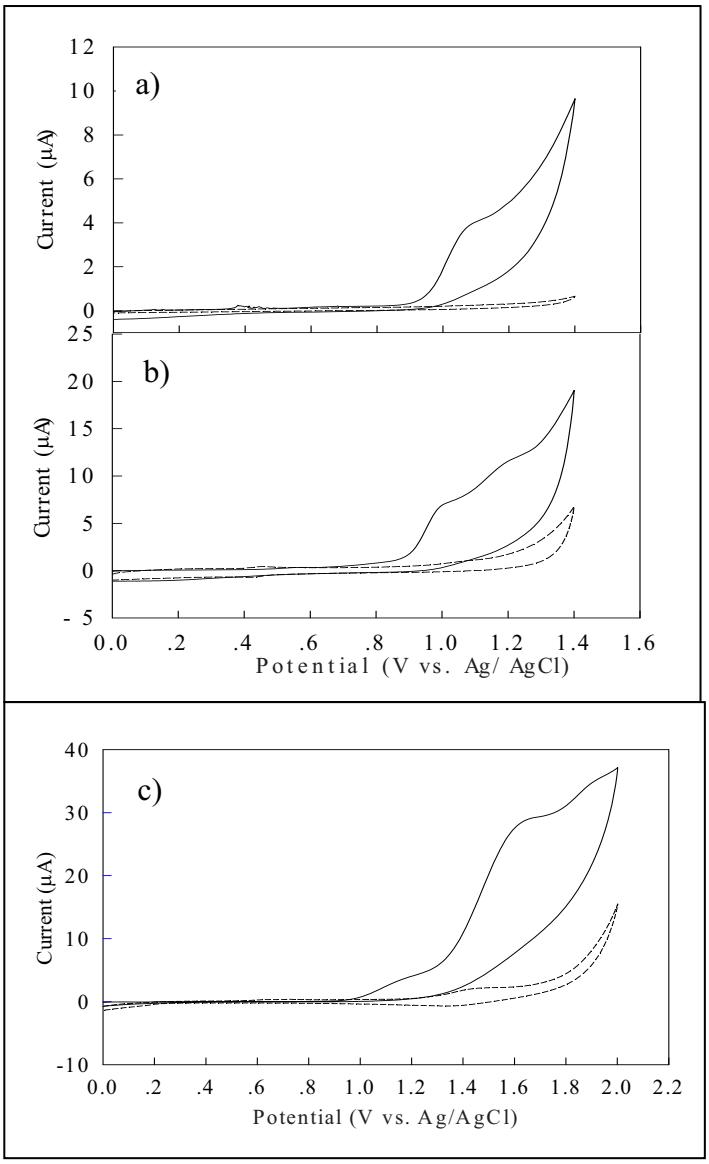

Figure 3 Cyclic voltammograms of 500 µM CTC (solid line) in 0.1 M potassium dihydrogen phosphate (pH 2) together with the corresponding background current (dashed line) at a) as-deposited BDD b) GC, and c) anodized BDD electrodes**.**

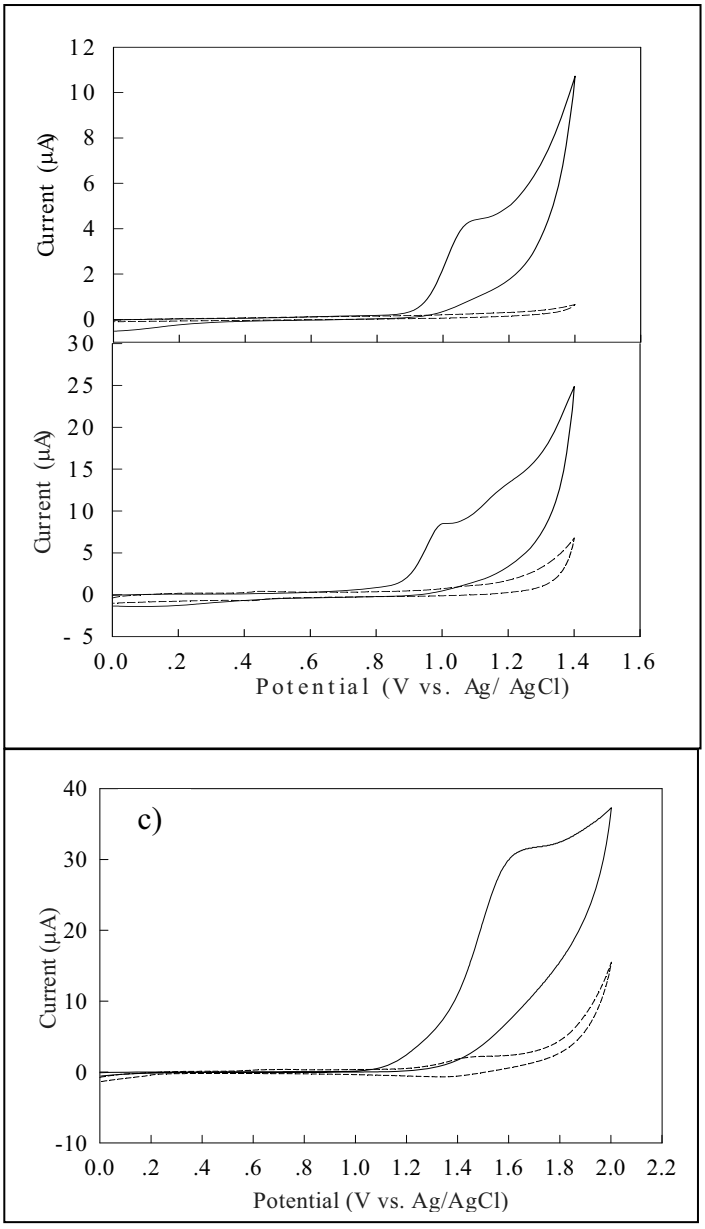

Figure 4 Cyclic voltammograms of 500 μM DC (solid line) in 0.1 M potassium dihydrogen phosphate (pH 2) together with the corresponding background current (dashed line) at a) as-deposited BDD b) GC, and c) anodized BDD electrodes**.**

Table 1 Electrochemical oxidation data obtained from cyclic voltammetry of OTC, TC, CTC, and DC at as-deposited BDD, GC, and anodized BDD electrodes.

Analytes	Concentration (μM)	As-deposited BDD		GC		Anodized BDD	
		E_p (V)	i_p (μA)	E_p (V)	i_p (μA)	E_p (V)	i_p (μA)
OTC	100	1.12	1.21	1.08	2.05	1.59	5.03
	500	1.13	2.02	1.09	6.51	1.69	32.34
TC	100	1.14	1.16	1.08	2.65	1.54	5.20
	500	1.16	3.22	1.06	8.85	1.65	29.88
CTC	100	1.06	1.03	0.99	1.59	1.57	4.67
	500	1.10	3.67	1.02	6.44	1.63	26.10
DC	100	1.04	1.06	0.99	2.95	1.56	4.85
	500	1.07	4.01	1.00	7.77	1.66	28.70

- **pH dependence**

To find the optimum pH for detection of four TCs, the experiments were carried in the pH solution ranged from 2 to 9 at anodized BDD electrode. A plot of pH versus E_p was investigated (Fig. 3.5) with ambiguous results and the expected pK_a was inconsistent with the pK_a value of the dissociation in the literature.

The details concerning the current response and peak potential of TCs at each pH was investigated, as shown in Table 2. In acidic buffer, the well-resolved cyclic voltammograms of tetracyclines were obtained whereas, in neutral and alkaline buffer, ill-defined cyclic voltammograms were obtained. Results for all TCs demonstrated that pH 2 gave the highest current signal.

It can be explained that tetracyclines are derived from a system of four membered rings arranged linearly with characteristic double bonds. They are amphoteric compounds with high polarity and an isoelectric point between 4 and 6. From the reference literature, three portotropic dissociations have been observed for TCs, with pK_1, pK_2, and pK_3 as shown in Table 3.3. In strongly acidic pH, the tetracycline molecules exist as fully protonated from as a singly charged cation. As

proposed in the previous work, the surface of anodized BDD is negatively charged, and the electrostatic interaction between the negatively charged covering of the anodized surface and the positively charged substrates is attractive. Hence, the fully positively charged TCs at pH 2 provided the highest response, and this pH was chosen as the optimum pH for the rest of the experiments.

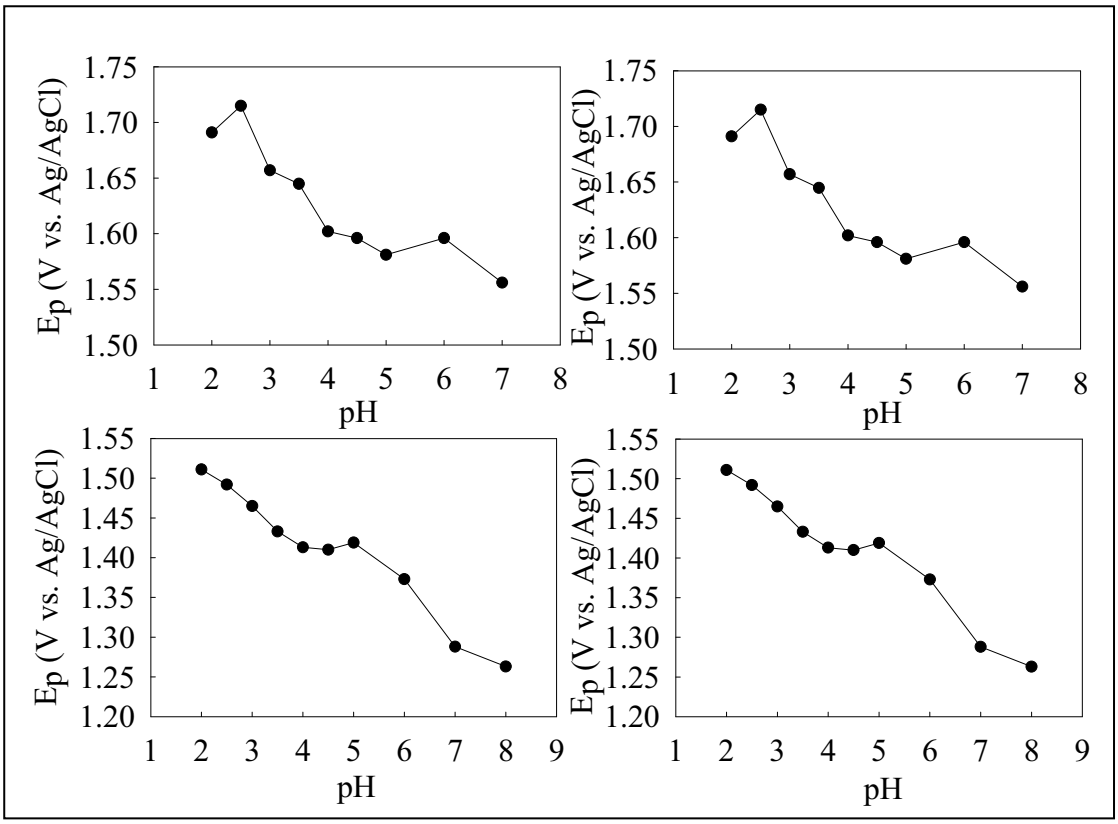

Figure 5 Relationship between the pH and E_p.

Table 2 Electrochemical oxidation data obtained from cyclic voltammetry of 1 mM OTC, TC, CTC, and DC at anodized BDD electrodes.

pH	OTC		TC		CTC		DC	
	E_p (V)	i_p (μA)	E_p (V)	i_p (μA)	E_p (V)	i_p (μA)	E_p (V)	i_p (μA)
2	**1.65**	**170.20**	**1.69**	**161.80**	**1.54**	**242.90**	**1.51**	**191.30**
2.5	1.65	146.60	1.72	130.80	1.57	178.40	1.49	161.50
3	1.61	130.20	1.66	127.80	1.55	173.30	1.47	156.40
3.5	1.60	138.70	1.65	132.50	1.48	154.80	1.43	152.30
4	1.58	142.60	1.60	128.30	1.46	158.70	1.41	155.70
4.5	1.59	138.60	1.60	137.90	1.47	154.10	1.41	149.40
5	1.57	140.80	1.58	137.70	1.46	151.60	1.42	149.00
6	1.58	165.90	1.60	151.60	1.49	178.40	1.37	159.80
7	1.56	163.70	1.56	156.10	1.48	193.50	1.29	169.80
8		-		-	1.38	235.80	1.26	187.60
9		-		-		-		-

Table 3 pK_a values of TCs in aqueous solutions.

Analytes	pK_1	pK_2	pK_3
OTC	3.27	7.32	9.11
TC	3.30	7.68	9.69
CTC	3.30	7.68	9.27
DC	nf*	nf*	nf*

*nf : no reference found

❖ **Determination of TCs using flow injection with amperometric detection**

- **Hydrodynamic voltammetry**

To find the optimum potential, hydrodyanamic voltammetry was carried out. A hydrodynamic voltammogram was obtained from the average of three aliquot injections of the 20 μL of 100 μM TCs solutions in the flow injection system at increasing values of the applied potential from 1.1 to 2.0 V vs. Ag/AgCl in the flow injection system. The carrier solution was 0.1 M potassium dihydrogen phosphate (pH 2). Fig 6a shows the hydrodynamic voltammogram of TCs with the corresponding background current. The hydrodynamic voltammogram of TCs did not exhibit the sigmodial shape of the signal vs. potential probably due to the high oxidation potential of TCs. To obtain the optimum potential, the S/B ratios from Fig 3.6b were calculated at each potential and plot the results versus the potential. The maximum S/B ratio was found at 1.5 V. vs. Ag/AgCl for CTC and 1.6 V vs. Ag/AgCl for TC, OTC, and DC. Hence, this study used these optimum potentials for the quantification experiment in the flow injection system.

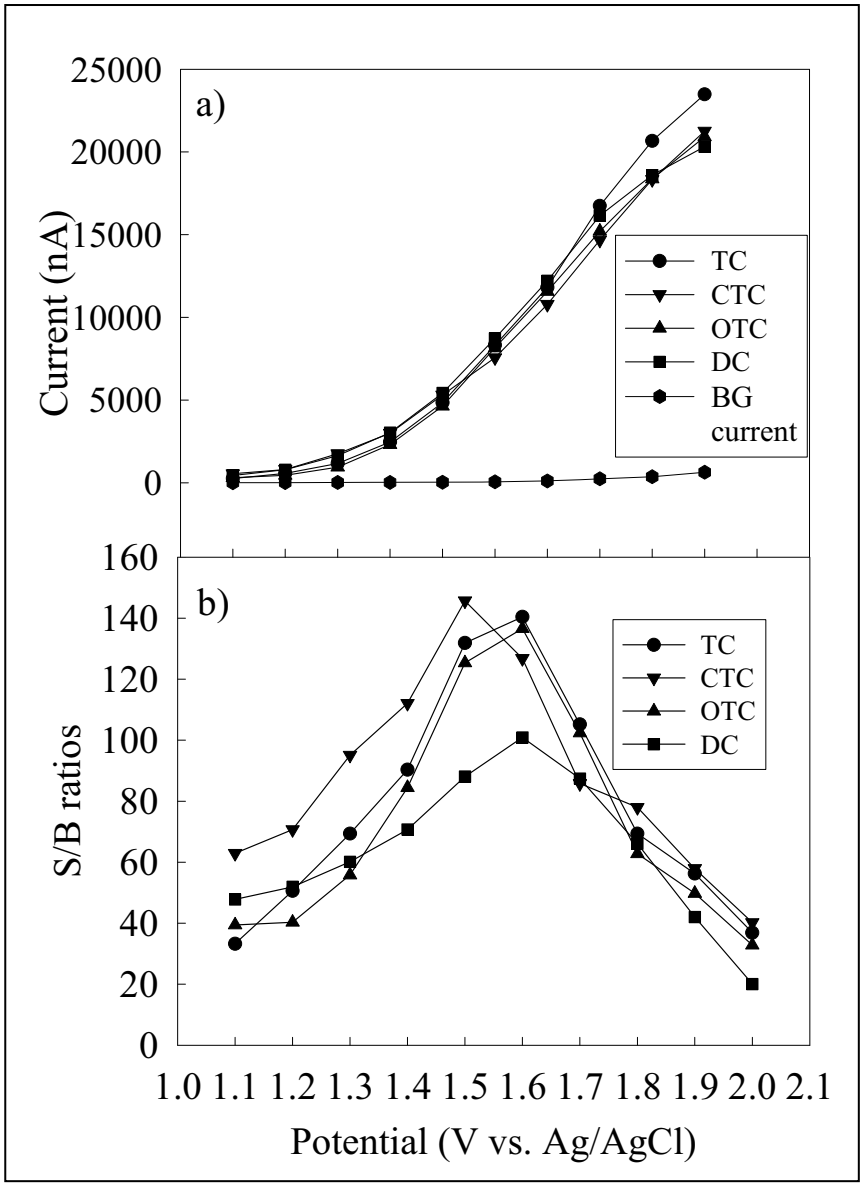

Figure 6 a) Hydrodynamic voltammogram for 100 μM TCs (●) : OTC; (▲):TC; (▼): CTC; and (■):DC in 0.1 M potassium dihydrogen phosphate (pH 2), using 0.1 M potassium dihydrogen phosphate (pH 2) as carrier solution. The flow rate was 1 mL min^{-1}. b) Hydrodynamic voltammogram of signal-to-background ratios.

- **Analytical performance of anodized BDD electrode using the flow injection system**

A series of analytical figures of merit were performed on the proposed method for the quantification of TC, CTC, OTC, and DC.

Linearity and LOD: the calibration curves were constructed separately for each drug in the concentration range of 0.1 to 1000 μM as shown in Fig. 7. Each point of the calibration graph corresponded to the mean value from three replicated injections. The regression analysis parameters for each TC standard solution were summarized such as the linear range and LOD in Table 4. Linear range of the method was about two orders of magnitude range from 0.1-50 for TC and 0.5-50 μM for OTC, CTC, and DC. The LOD defined as the concentration that provided the signal-to-noise ratio of 3 was 10 nM for the four TCs.

Repeatability: to check the repeatability of the proposed method, the experiments were carried out by injecting 10 replicates of the three concentrations (5, 10, 50 μM) of each drug. The peak variability defined as the relative standard deviation (%RSD) was 1.3-1.7, 2.4-3.0, 1.6-3.0, and 1.7-2.7 for TC, CTC, OTC, and DC, respectively.

Stability: the response received from anodized BDD electrodes with amperometric detection was very stable. The flow injection signal obtained by repetitive 100 injections of 50 μM CTC on the anodized diamond provided a peak variation of about 3.4%. Moreover, the anodized BDD electrode could be reactivated in situ by applying a high positive potential (2.6 V vs. Ag/AgCl) during the flow injection measurement. The sample throughput was approximately seventy injections per hour.

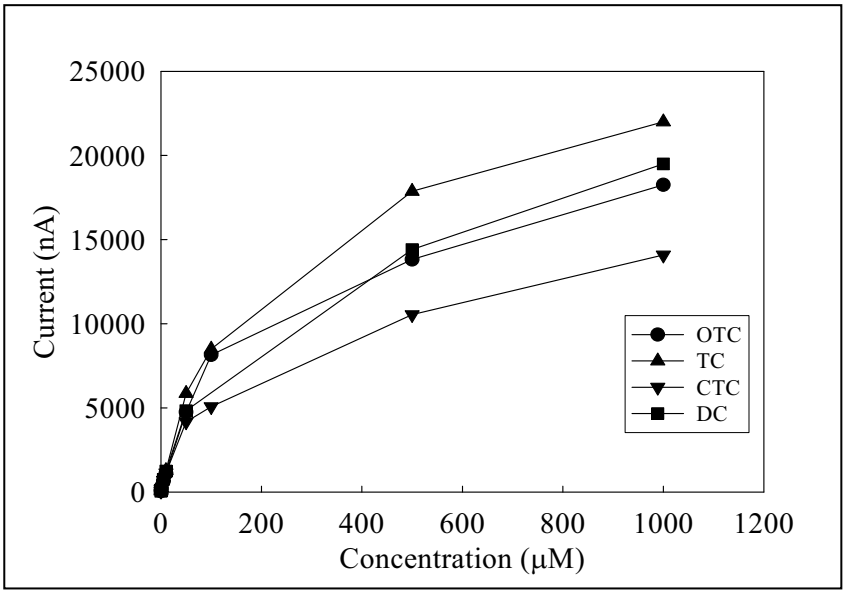

Figure 7 Calibration curves of four TCs (OTC, TC, CTC, and DC) using flow injection system.

Table 4 Regression analysis of parameters, linear range, and LOD for the determination of TCs by FIA with amperometric detection using an anodized BDD electrode (n=2).

Analytes	Linear range (μM)	a	b	r^2	LOD (nM)
TC	0.1-50	110.00±5.96	192.13±4.86	0.9968±0.0006	10
CTC	0.5-50	76.93±3.87	199.72±29.68	0.9969±0.0001	10
OTC	0.5-50	90.23±2.99	165.17±28.86	0.9992±0.0006	10
DC	0.5-50	96.23±3.81	213.73±48.92	0.9966±0.0001	10

[a] $y = ax+b$, where y = current (nA), x = concentration (μM), a = slope (nA μM^{-1})

- **Application**

The proposed method of this study was applied for drug formulations using the standard addition method. The precision of this method was based on the intra-assay and inter-assay. The amounts of each drug were compared with the label contents. The results are summarized in Table 5. There was no significant difference in results between the label contents and those obtained by the proposed method for the intra-assay and inter-assay precision (3 days). To check the accuracy of the method, recoveries of the spiked standard solution were evaluated. The results are summarized in Table 6.

Table 5 Results of TC determination in drug formulations.

Analytes	Intra-assay (n = 2)			Inter-assay (n = 6)		
	Label amount (mg)	Found (mg)	%Found	Label amount (mg)	Found (mg)	%Found
TC	250	249.4±1.7	99.8±0.7	250	246.3±3.2	98.5±1.3
CTC	250	249.7±1.3	99.9±0.5	250	247.3±4.0	98.9±1.6
OTC	250	254.6±2.5	101.9±1.0	250	257.5±3.3	103.0±1.3
DC	100	98.4±1.0	98.4±1.0	100	99.5±1.3	99.5±1.3

Table 6 Recovery studies for the determination of TCs in drug formulations.

Analytes	Intra-assay (n = 2)			Inter-assay (n = 6)		
	Added ($\mu g\ mL^{-1}$)	Found ($\mu g\ mL^{-1}$)	%Recovery	Added ($\mu g\ mL^{-1}$)	Found ($\mu g\ mL^{-1}$)	%Recovery
TC	1.20	1.22±0.01	101.5±0.5	1.20	1.22±0.04	101.5±3.3
	2.40	2.43±0.02	101.4±0.8	2.40	2.41±0.03	100.4±1.3
	3.60	3.56±0.06	98.7±1.6	3.60	3.53±0.09	97.9±2.4
	4.81	4.82±0.05	100.3±1.1	4.81	5.91±0.06	101.0±1.3
CTC	1.29	1.25±0.01	96.9±0.4	1.29	1.26±0.03	97.4±2.7
	2.58	2.55±0.05	98.8±1.9	2.58	2.53±0.04	98.2±1.5
	3.86	3.80±0.00	98.5±0.0	3.86	3.80±0.09	98.6±2.4
	5.15	5.22±0.03	101.4±0.6	5.15	5.22±0.06	101.4±1.2
OTC	1.24	1.19±0.02	95.6±1.2	1.24	1.17±0.06	94.5±4.8
	2.48	2.41±0.07	97.1±2.7	2.48	2.36±0.08	95.1±3.0
	3.73	3.68±0.06	98.7±1.6	3.73	3.73±0.06	100.2±1.6
	4.97	4.98±0.01	100.2±0.2	4.97	5.05±0.08	100.7±1.6
DC	0.96	0.9±0.0	97.5±2.2	0.96	0.92±0.03	94.1±3.7
	1.92	1.86±0.03	96.4±0.0	1.92	1.92±0.06	100.2±2.9
	2.89	2.78±0.08	96.0±2.7	2.89	2.89±0.10	99.9±3.3
	3.85	3.97±0.06	103.2±1.7	3.85	3.87±0.09	100.6±2.3

❖ **Summary**

Anodized BDD electrode has exhibited the attractive feature for the detection of tetracycline antibiotics. Cyclic voltammetric results of tetracycline antibiotics at anodized BDD electrode exhibited a well-resolved peak current response than GC and as-deposited BDD electrode. Flow injection with amperometric detection using anodized BDD electrode also enhanced the sensitivity and improved the detection limit (0.0048 mg L^{-1} for tetracycline and doxycycline, 0.0050 mg L^{-1} for oxycycline and 0.0052 mg L^{-1} for chlortetracycline) of the quantification of tetracycline antibiotics. The remarkably low detection limit obtained from this work showed the superb technique for applying to determine tetracycline antibiotics in biological samples that their common amount was very low. The present method was also overcome the drawback of previous methods based on spectrophotometry and HPLC-amperometry, include simple, fast, low cost, and high sensitivity method. Moreover, the investigated method can be successfully applied to determination tetracyclines in pharmaceutical formulation with the satisfactory results. All tetracycline antibiotics content of the drug were found to be in agreement with the declared amount on the label.

Electroanalysis of Tetracycline Using Nickel-implanted Boron-Doped Diamond Thin Film Electrode Applied to Flow Injection System

❖ **Cyclic voltammetry**

Figures 8 (a) and (b) show cyclic voltammograms for tetracycline oxidation at Ni-DIA and BDD electrodes in 1 mM tetracycline + 0.1 M phosphate buffer (pH 2). The corresponding backgrounds are also shown. The Ni-DIA electrode exhibited a well-defined irreversible oxidation peak at ~1.5 V *versus* Ag/AgCl, whereas the BDD electrode provided a well-defined irreversible oxidation peak at ~1.4 V *versus* Ag/AgCl. Both Ni-DIA and BDD electrodes provided well-defined cyclic voltammograms.

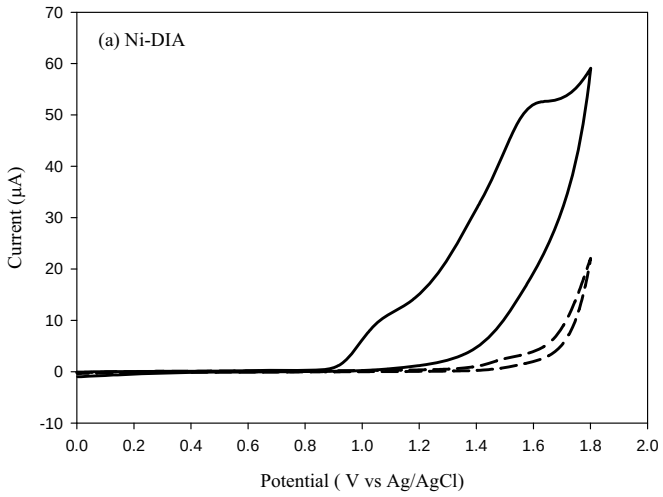

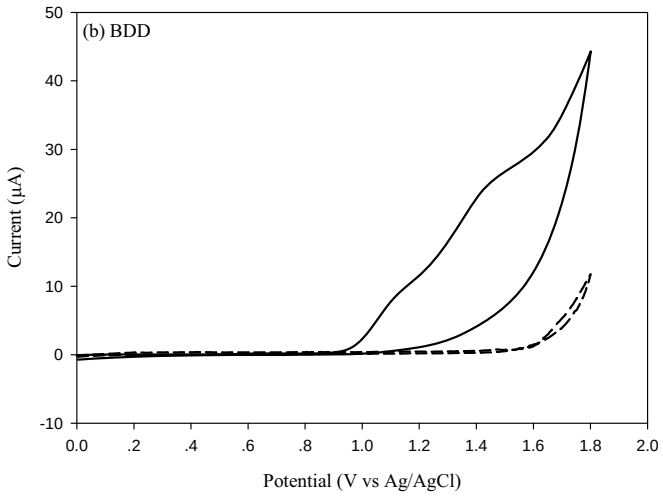

Figure 8 Cyclic voltammograms for 1 mM tetracycline in 0.1 M phosphate buffer (pH 2) at (a) nickel-implanted boron-doped diamond thin film electrode The potential (b) as-deposited boron-doped diamond thin film electrode (solid line). The potential sweep rate was 50 mVs^{-1}. Background voltammograms (0.1 M phosphate buffer, pH 2) are also shown in this Figure (dotted line).

❖ pH dependence study

Table 7 summarizes the electrochemical data obtained from cyclic voltammograms of 1 mM tetracycline hydrochloride oxidation at pH 2, 3, 4, 5, 6, 7, 8, 9, and 10 at the Ni-implanted diamond electrode. The experimental results show that the analyte oxidation peak potential, Ep^{ox} (positive scan) are shifted to more negative values as the pH of the solutions increase. These phenomena may be attributed to the fact that tetracycline hydrochloride was easier to epimerize to the anhydrotetracycline in acidic media or to isotetracycline in basic media. The proposed mechanisms of the epimerization of this compound are shown in Figure 9. In both acidic and alkaline solutions, the epimerization occurred at C-6 hydroxyl group. These occurrences imply that the oxidation process of tetracycline hydrochloride released hydrogen ion into the solution, and the reduction process took up hydrogen ion from the solution. From the electrochemical data displayed in Table 7, the highest oxidation current response at the oxidation peak potential about 1.516 V vs. Ag/AgCl was obtained at the pH 2. Therefore, this pH value was chosen as the optimum pH for the study of tetracycline hydrochloride. The cyclic voltammograms of tetracycline hydrochloride in different pH solutions are shown in Figure 10-12, respectively.

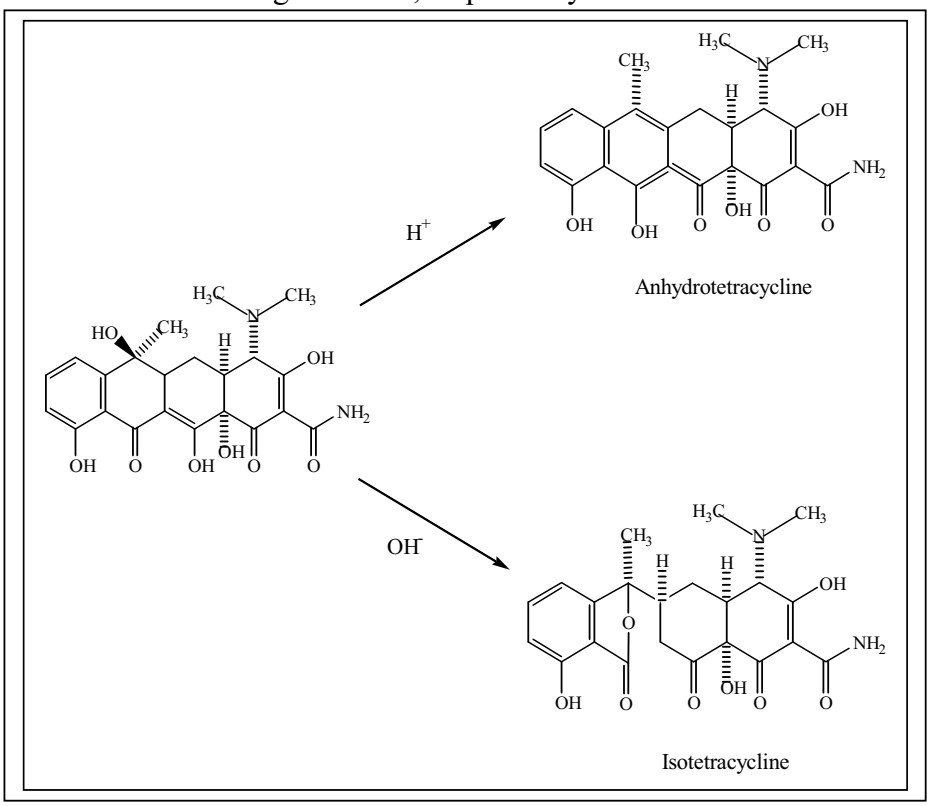

Figure 9 The proposed epimerization mechanism of tetracycline

Table 7 Comparison of electrochemical data obtained from cyclic voltammograms of the 1 mM tetracycline at pH 2, 3, 4, 5, 6, 7, 8, 9, and 10

pH	E_p^{ox} * (V vs. Ag/AgCl)	I_p^{ox} ** (μA)
2	1.516	34.10
3	1.516	28.90
4	1.506	26.30
5	1.511	26.60
6	1.511	30.40
7	1.511	22.30
8	1.516	22.40
9	1.506	19.00
10	1.486	28.80

* Oxidation peak potential of tetracycline

**Oxidation peak current of tetracycline

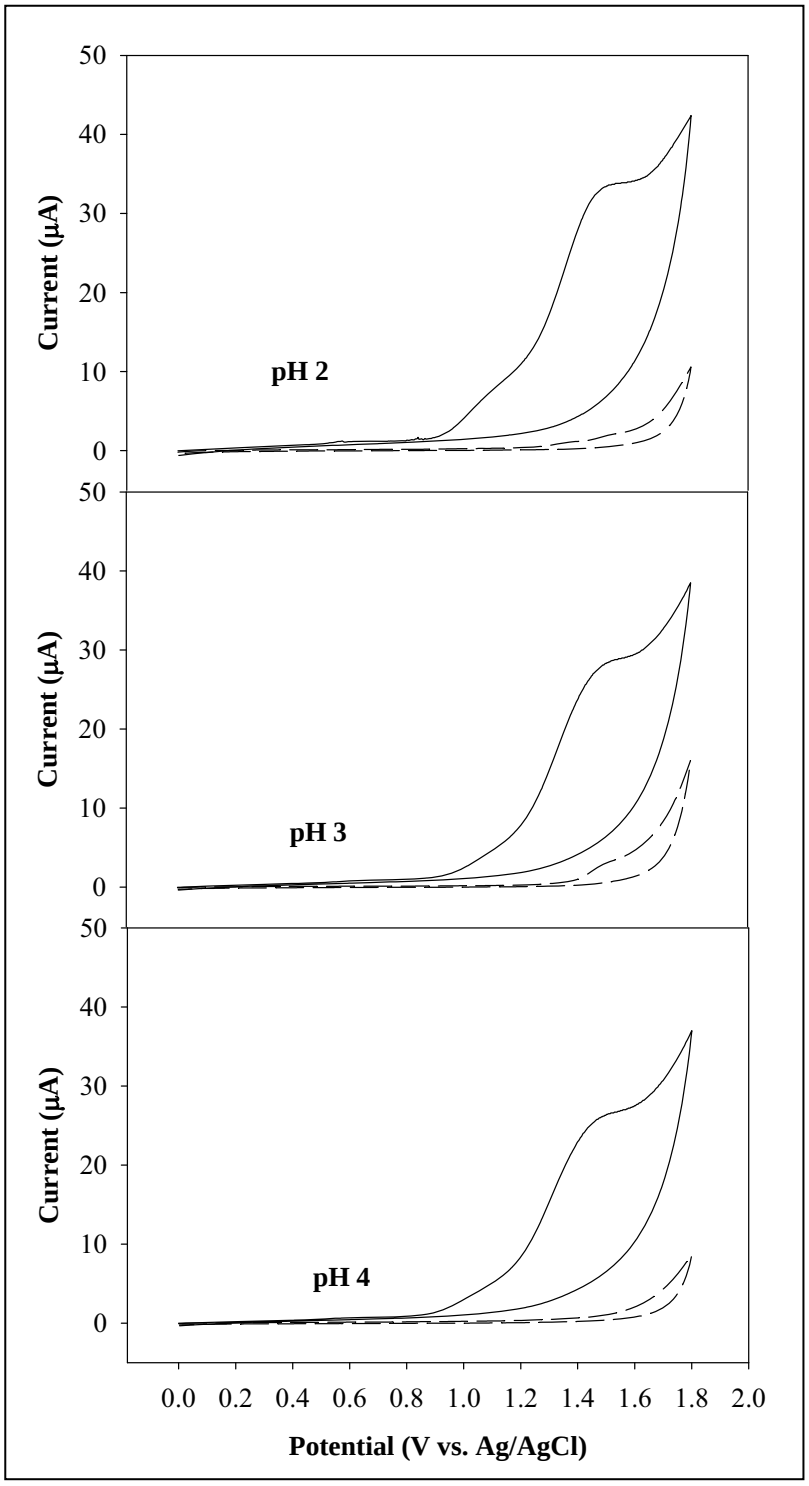

Figure 10 Cyclic voltammogram of 1 mM tetracycline in 0.1 M phosphate buffer (pH 2, 3 and 4) at Ni-implanted diamond electrode (solid line). The scan rate was 50 mV/s^{-1}. Background voltammogram is also shown in this Figure (dash line).

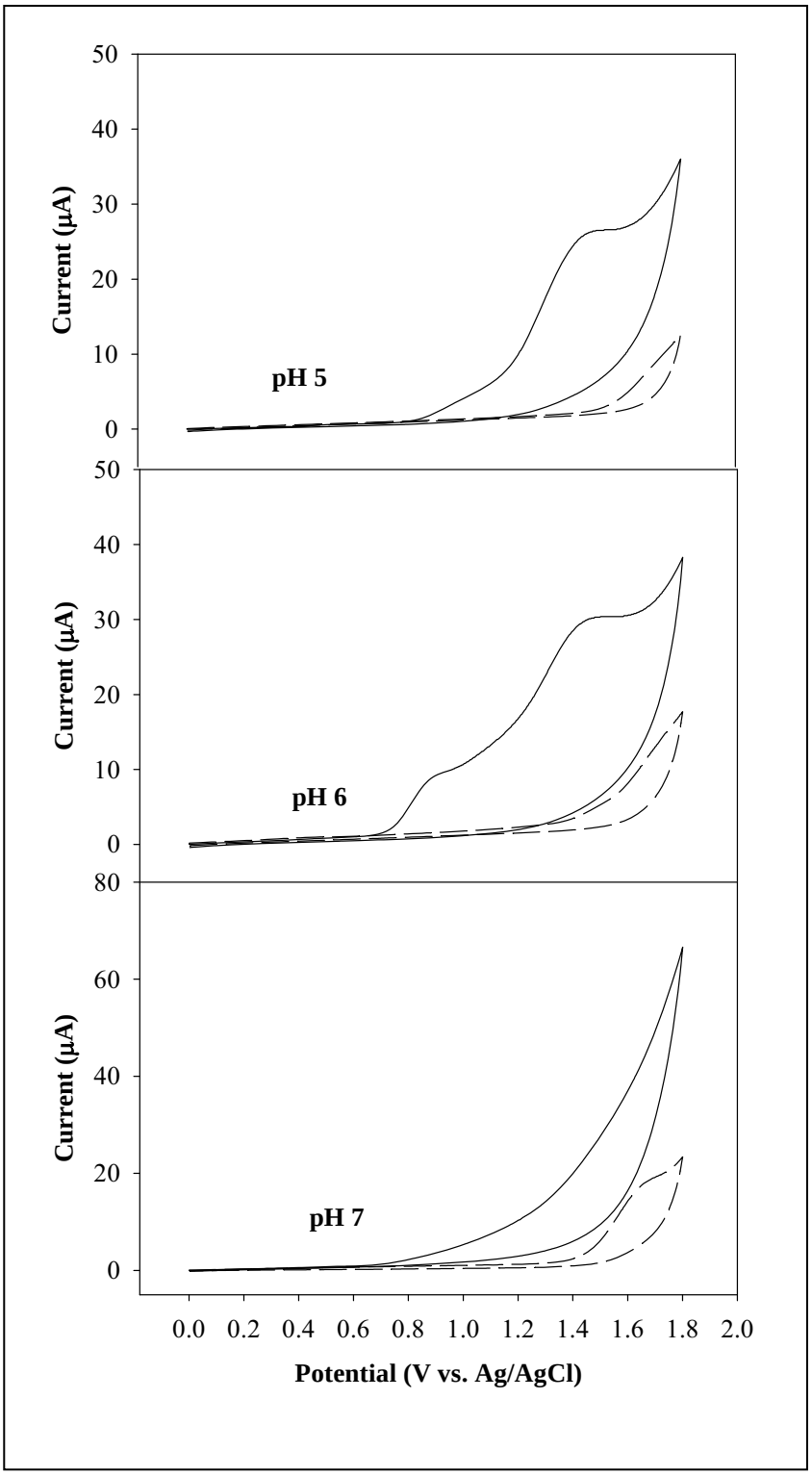

Figure 11 Cyclic voltammogram of 1 mM tetracycline in 0.1 M phosphate buffer (pH 5, 6and 7) at Ni-implanted diamond electrode (solid line). The scan rate was 50 mVs^{-1}. Background voltammogram is also shown in this Figure (dash line).

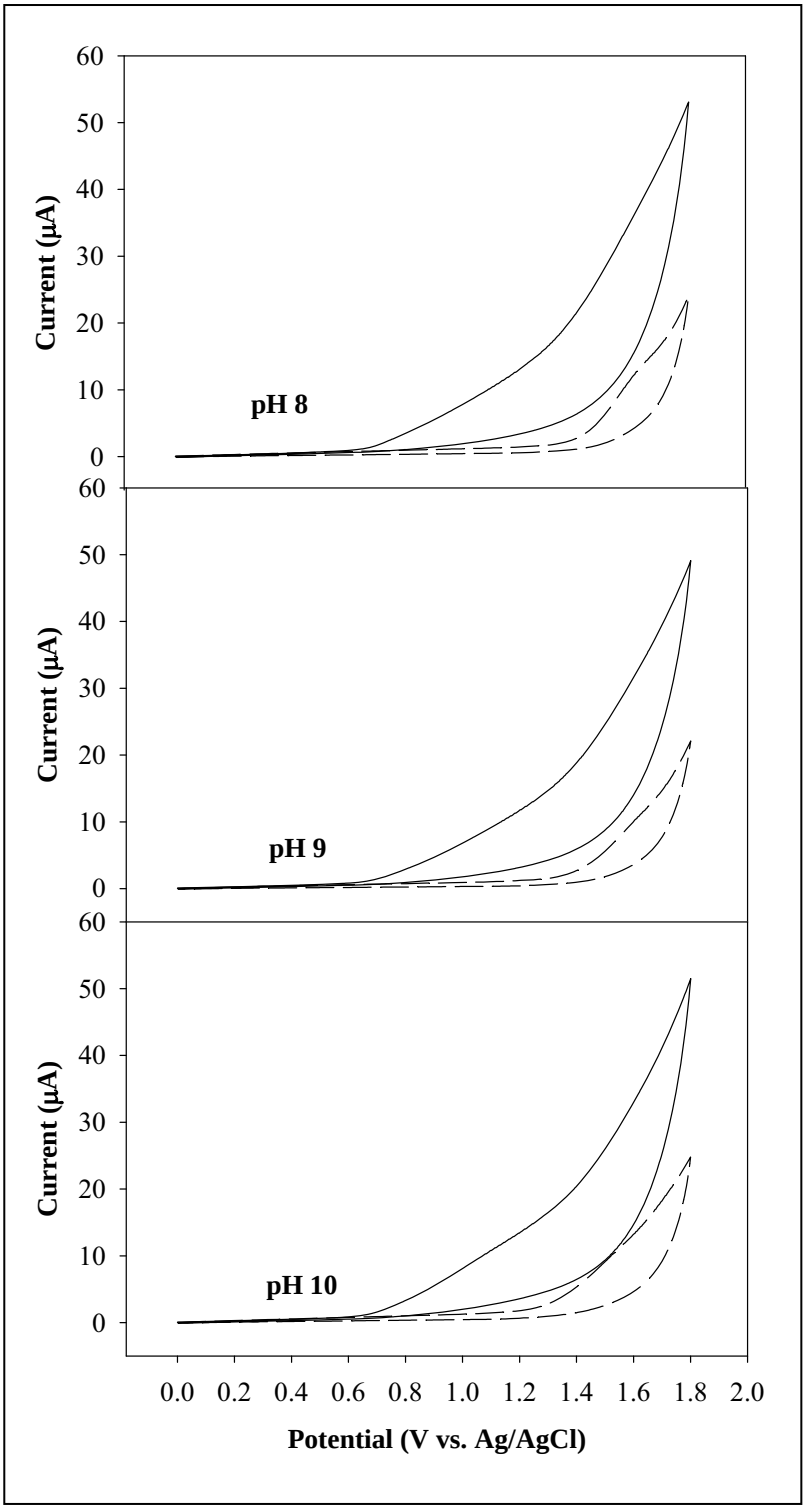

Figure 12 Cyclic voltammogram of 1 mM tetracycline in 0.1 M phosphate buffer (pH 8, 9and 10) at Ni-implanted diamond electrode (solid line). The scan rate was 50 mVs^{-1}. Background voltammogram is also shown in this Figure (dash line).

❖ **Scan rate dependence study**

Figure 13 shows the cyclic voltammetric response of 1 mM tetracycline in 0.1 M phosphate buffer (pH 2) with variation of scan rates from 0.01 to 0.3 Vs^{-1} at the Ni-DIA electrode. The oxidation current varied highly linearly (r^2 > 0.99) with the square root of scan rate ($\upsilon^{0.5}$), as shown in the inset of this figure, indicating semi-infinite linear diffusion of reactant to the electrode surface.

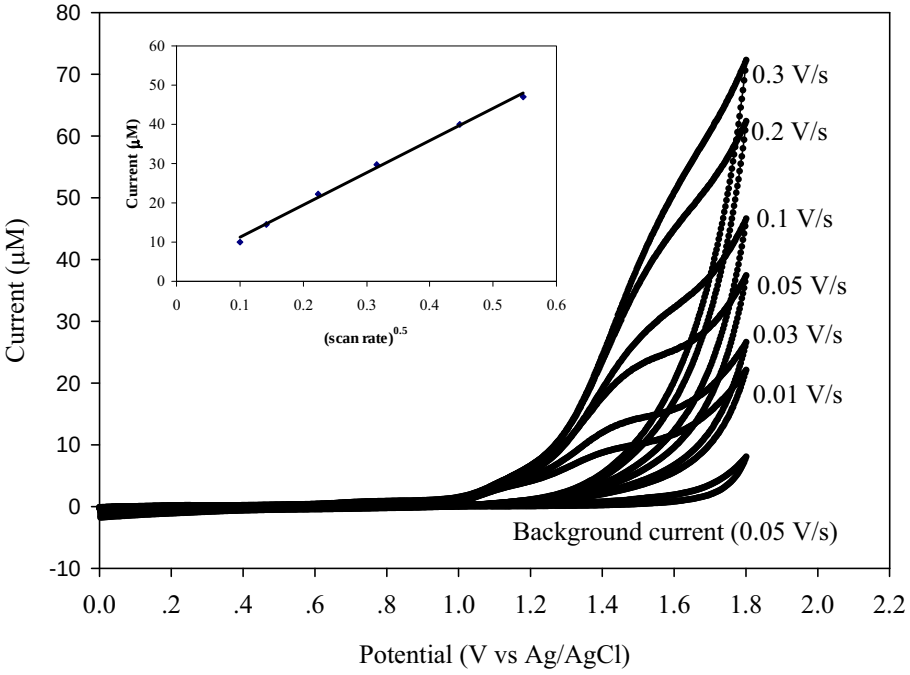

Figure 13 Cyclic voltammograms for 1 mM tetracycline in 0.1 M phosphate buffer (pH 2) at Ni-DIA electrode for a series of sweep rates, area of electrode was 0.07 cm^2. The dependence between peak current (μA) and the square root of the sweep rate appears in the inset.

❖ **Concentration dependence study**

The oxidation peak current was investigated for the concentration range from 0.1 to 3.0 mM of tetracycline at the Ni-DIA. Figure 14 shows the cyclic voltammograms with the concentrations of the tetracycline varied from 0.1 to 3.0

mM. Linear regression analysis of current (μA) *versus* concentration (μM) profile gave a wide linearity from 0.1 to 3.0 mM. (r^2 > 0.99) for the Ni-DIA electrode, as shown in the inset of this Figure.

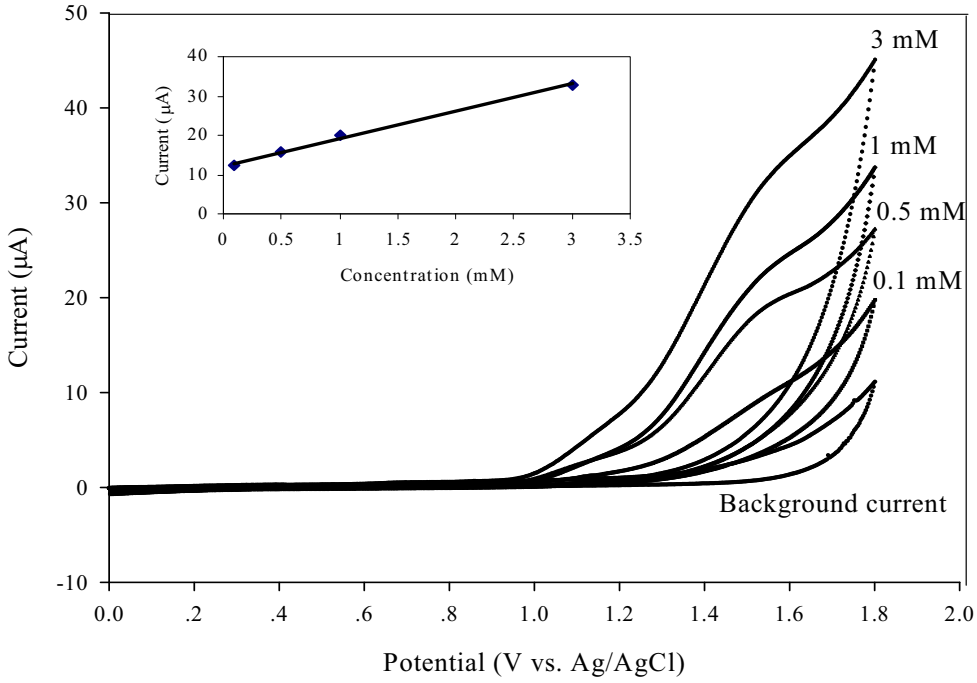

Figure 14 Cyclic Voltammograms for tetracycline in 0.1 M phosphate buffer (pH 2) at Ni-DIA electrode for a series of tetracycline concentrations. The sweep rate was 50 mVs^{-1}; the area of electrode was 0.07 cm^2. The dependence between peak current (μA) and concentrations at the potential of 50 mVs^{-1} appears in the inset.

❖ Flow injection analysis with amperometric detection

o Hydrodynamic voltammetry

Figure 15 (a) shows the hydrodynamic voltammetric *i-E* curves obtained at a Ni-DIA electrode for 20 μL injection of 100 μM of tetracycline in 0.1 M of phosphate buffer (pH 2), using phosphate buffer (pH 2) as the carrier solution. Each datum shows the average of injections. The absolute magnitude of the

background current at each potential is also shown for comparison. Hydrodynamic voltammogram for tetracycline did not produce a sigmodial shape of the signal versus potential. To obtain the maxima potential point, we calculated the S/B ratio from Fig. 3.15 (a) at each potential. Hydrodynamic voltammetric S/B ratio *versus* potential curve was obtained as shown in Fig.15 (b) with the maximum S/B ratio of 1.55 V *versus* Ag/AgCl. Hence, this potential was set as the amperometric potential detection value in flow injection analysis experiments.

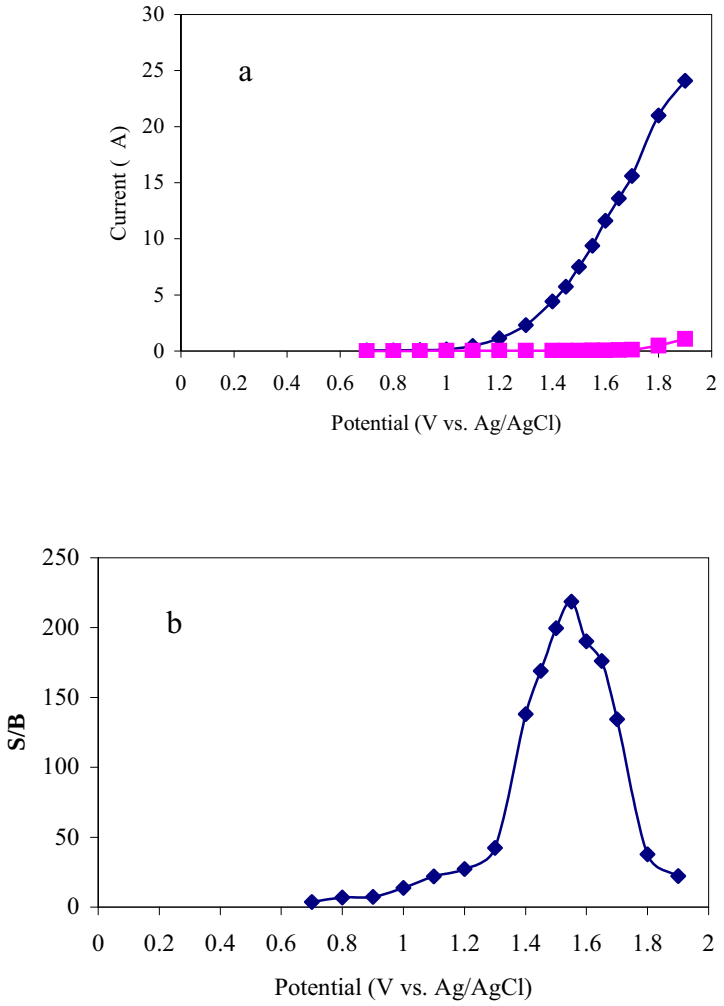

Figure 15 (a) Hydrodynamic voltammograms of (- -) 1 μM of tetracycline in 0.1 M phosphate buffer (pH 2) and (-Δ-) 0.1 M phosphate buffer (pH 2, background current) with four injection of analytes, using 0.1 M phosphate buffer (pH 2) as a carrier solution. (b) Hydrodynamic of signal-to-background ratio. The flow rate was 1 mL min^{-1}.

- **Linear range, detection limit and reproducibility**

A series of repetitive 20 μL injections of tetracycline at a concentration of 1 – 100 μM in 0.1 M phosphate buffer (pH 2) was examined using amperometric potential of 1.55 V *versus* Ag/AgCl. The calibration curve was obtained from three injections of five concentrations of tetracycline (1, 5, 25, 50 and 100 μM). Using a least square-linear regress fit, it was found that slope (sensitivity) was 0.058 μA/mM, intercept was 0.6476 μA and correlation coefficient $r^2 > 0.99$. A linear dynamic range was obtained over two orders of magnitude, from 1 to 100 μM. The limit of detection (LOD) is the concentration of analyte, which provides three times of the ratio of the analyte current to noise signal (S/N ≥ 3). Interestingly, LOD of this proposed method was obtained after five injections of 10 nM tetracycline. The precision of the method was investigated for the standard solution at concentrations of 10 and 25 μg/mL. Ten measurements were made with each concentration on the same day. Results exhibited very good precision with peak variabilites of 2.82%.

- **Drug analysis of tetracycline capsules**

The proposed method for tetracycline was applied to the determination of tetracycline hydrochloride capsules. The precision of the method was obtained on the basis of intra-assay comparisons using standard addition. Recovery results are summarized in Table 8.

The tetracycline content of the drug calculated from this calibration plot (251.03 ± 0.05 mg per tablet, $n = 2$) was found to be in satisfactory agreement with the labeled amount of 250 mg per capsule. There was no significant difference between the labeled contents and those obtained by the proposed method. Recoveries ranged from 97.22 to 102.38%.

Table 8 Recovery of tetracycline capsule sample with amperomatric detection using Ni-DIA electrode applied to flow injection system (n = 2)

Amount of tetracycline tablet sample added/ μg ml^{-1}	Amount of tetracycline tablet sample found/ μg ml^{-1}	Percent of recovery, %
0.36	0.35 ± 0.01	97.22 ± 1.39
0.42	0.43 ± 0.00	102.38 ± 0.00
0.48	0.49 ± 0.01	100.00 ± 1.04
0.54	0.54 ± 0.01	100.00 ± 1.85
0.60	0.61 ± 0.01	101.66 ± 0.83

- **Comparison with other methods**

Table 9 summarizes data obtained from the other methods for determination of tetracycline compared with the proposed method. It was found that using the Ni-DIA electrode with amperometric FIA gave the wide linear dynamic range (two orders of magnitude). Interestingly, the proposed method provided a very low detection limit of 10 nM, because the Ni-DIA electrode exhibited very low background current and noise signals. It also resulted in very high sensitivity. This outstanding performance of the BDD electrode makes it attractive for using as working electrode in FIA system for analysis of tetracycline.

Table 9 Comparison of data for tetracycline determination

Method	Linear dynamic range/μM	Detection limit/ μM	Precision, % RSD	Reference
Flow injection with UV spectrophotometric	1 – 25	0.14	0.7	34
Chemiluminescence	0.2 – 5	0.06	3.2	38
Liquid chromatography with ultraviolet detector	0.104 – 1.350	0.01	1.2	39
Liquid chromatography with coulometric electrode array	0.104 – 2.079	0.04	≤ 4.3	40
Flow injection with pulsed amperometric detection	5 – 600	1.0	3.5	45
Ni-implanted boron-doped diamond thin film electrode applied to flow injection system	1 – 100	0.01	2.8	[a]

[a] This proposed method.

❖ Summary

This is the first use of Ni-DIA electrodes for the electroanalysis of tetracycline. It was found that Ni-DIA electrodes exhibited excellent performance for the oxidative detection of tetracycline. Well-defined voltammograms were obtained

at the Ni-DIA electrode, which exhibited high sensitivity and demonstrated significant advantages over the BDD electrode, because of its superior electrochemical properties. The outstanding capabilities of the Ni-DIA electrode were demonstrated by coupling with FIA. Application of the proposed method for determination of tetracycline in commercially available tablet forms shows that this method is precise, accurate and very sensitive.

Use of nickel implanted boron-doped diamond thin film electrode coupled to HPLC system for the determination of tetracyclines

This part was carried out in the HPLC system. Figure 16 depicts the optimum potential i-E curve obtained at the Ni-implanted diamond electrode for a 20 μl injection of 100 μM of tetracycline mixture standard solution 0.1 M of phosphate buffer (pH 2.5) was used as the carrier solution. Each datum represents the average of two injections. The magnitude of the background current at each potential is also shown in Figure 16. The hydrodynamic voltammogram of tetracycline mixture standard solution at the Ni-implanted diamond electrode exhibited a well-defined sigmodal shape with a half peak potential at about 1.55 V vs. Ag/AgCl. Therefore, this potential was fixed for the amperometric potential detection in HPLC system analysis experiments.

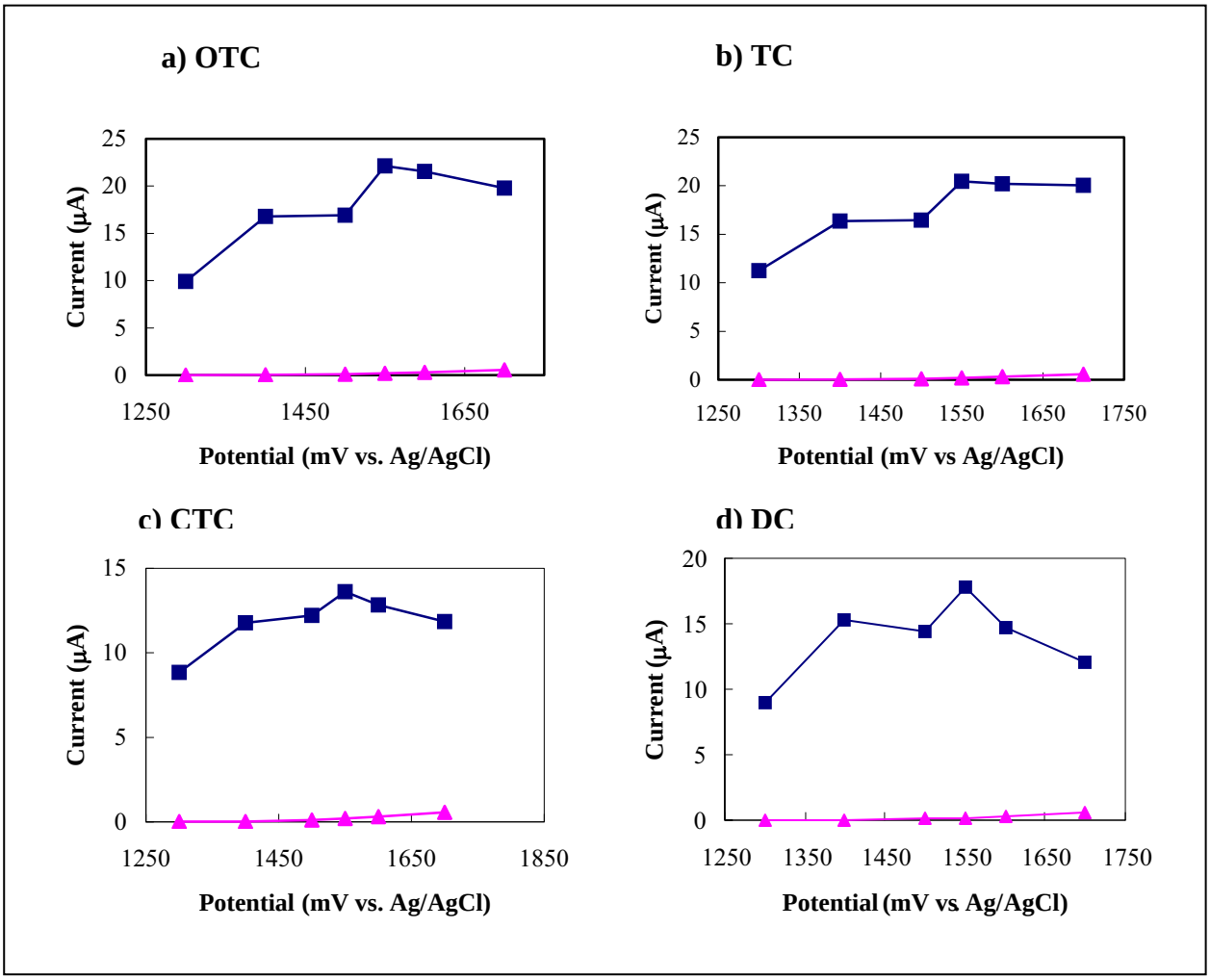

Figure 16 Optimum potential of (- -) 10 ppm of oxytetracycline a), tetracycline b), chlortetracycline c) and doxycycline d) in 0.1 M phosphate buffer (pH 2.5) and (-Δ-) 0.1 M phosphate buffer (pH 2.5, background current) with two injections of analyte. 0.1 M phosphate buffer (pH 2.5) was used as a carrier solution, flow rate 1 ml min^{-1}.

❖ Calibration curve and linear range

The tetracycline mixture standard solutions covering the concentration range of 0.01-100 ppm were analyzed and their peak areas were plotted versus concentration. The regression data are summarized in Table 3.10. Regression plots of the concentration and peak area are shown in Figure 17.

From Table 10, the data of the 10 point calibration curve was acceptable for quantitation because the correlative coefficient (R^2) obtained were between 0.9975 to 0.9996.

Table 10 Linear regression statistics results

Analytes	Linear dynamic range (ppm)	Slope (peak areas units/mg/kg)	Intercept (μA)	R^2
Oxytetracycline	0.05-100	0.0473	0.0562	0.9975
Tetracycline	0.05-100	0.0395	0.0453	0.9977
Chlortetracycline	0.1-100	0.0110	0.0045	0.9990
Doxycycline	0.1-100	0.0111	0.0066	0.9996

The determination of each tetracycline by HPLC can be distinguished by the retention time of 5.97, 7.55, 18.87 and 26.95 min for oxytetracycline hydrochloride, tetracycline, chlortetracycline and doxycycline, respectively.

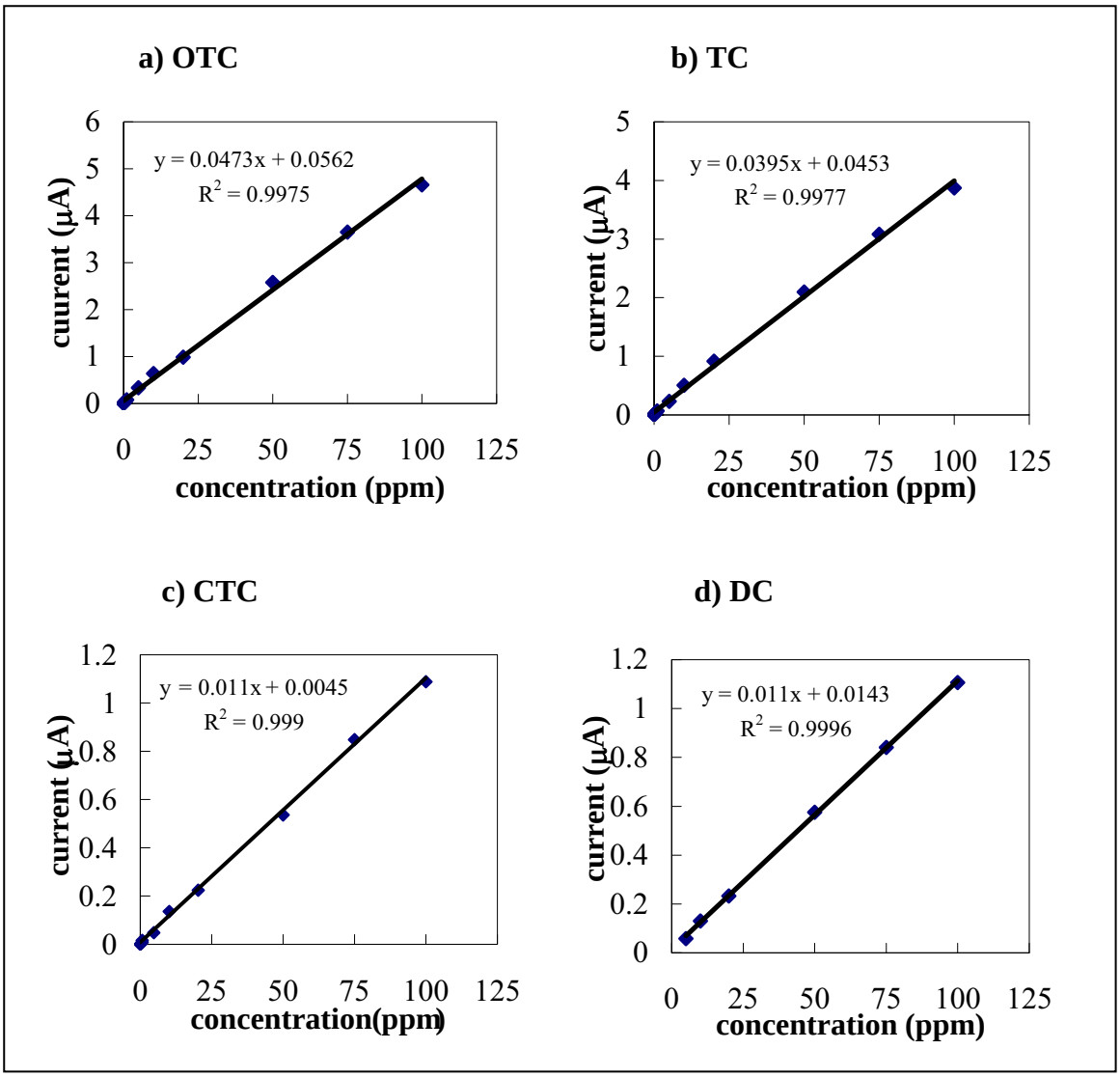

Figure 17 Calibration curve of oxytetracycline a), tetracycline b), chlortetracycline c) and doxycycline d) obtained from HPLC data.

❖ Limit of detection (LOD) and Limit of quantitation (LOQ)

The limit of detection (LOD) and limit of quantitation (LOQ) were defined as the concentration of that yielded the peak area of analyte in matrix standard solutions that signalled significantly different from the peak area of noise equal 3 for LOD and 10 for LOQ of each compound. These are shown in Table 11.

The limit of detection and limit of quantitation of the 4 tetracyclines are in the range of 0.01-0.05 ppm and 0.03-0.17 ppm respectively.

Table 11 The limit of detection and limit of quantitation of analyte in matrix standard solutions.

Analytes	LOD (ppm)	LOQ (ppm)
Oxytetracycline	0.01	0.03
Tetracycline	0.01	0.03
Chlortetracycline	0.05	0.17
Doxycycline	0.05	0.17

- **Precision**

The method for extraction as described in chapter 2 was used to determined %recovery and precision of this method at spiking level of 5 mg/kg for shrimp farming samples and shrimp sea samples.

Table 12-13 displays the intra-day precision of this method at the spiking level of 5 mg/kg for shrimp farming samples and shrimp sea samples respectively.

Table 14-15 illustrates the inter-day precision of the method at the spiking level of 5 mg/kg for shrimp farming samples and shrimp sea samples respectively.

Table 12 Mean of %Recovery of tetracyclines (intra-day precision) at spiking level of 5 mg/kg in Shrimp farming sample (n=3)

Analytes	%Recovery			Mean±SD	%RSD
	1	2	3		
Oxytetracycline	101.4	100.9	100.8	101.1±0.3	0.3
Tetracycline	101.2	101.6	100.5	100.4±1.7	1.7
Chlortetracycline	100.2	99.4	97.0	98.9±1.6	1.6
Doxycycline	101.8	99.9	101.6	101.1±1.0	1.0

Table 13 Mean of %Recovery of tetracyclines (intra-day precision) at spiking level of 5 mg/kg in Shrimp sea sample (n=3)

Analytes	%Recovery			Mean±SD	%RSD
	1	2	3		
Oxytetracycline	107.7	106.4	107.5	107.2±0.7	0.6
Tetracycline	100.9	101.1	101.9	101.3±0.5	0.5
Chlortetracycline	103.0	99.8	98.7	100.5±2.2	2.2
Doxycycline	103.6	99.0	95.9	99.5±3.8	3.8

Table 14 Mean of %Recovery of tetracyclines (inter-day precision) at spiking level of 5 mg/kg in Shrimp farming sample (n=6)

Analytes	%Recovery						Mean±SD	%RSD
	1	2	3	4	5	6		
Oxytetracycline	101.5	101.4	100.9	101.4	100.9	100.8	101.1±0.3	0.3
Tetracycline	101.6	100.5	102.8	101.2	101.6	100.5	101.3±0.8	0.8
Chlortetracycline	100.2	99.4	97.0	99.1	98.2	100.4	99.1±1.2	1.2
Doxycycline	97.2	101.8	99.9	101.6	98.9	101.4	100.1±1.8	1.8

Table 15 Mean of %Recovery of tetracyclines (inter-day precision) at spiking level of 5 mg/kg in Shrimp sea sample (n=6)

Analytes	%Recovery						Mean±SD	%RSD
	1	2	3	4	5	6		
Oxytetracycline	100.3	102.6	101.1	107.7	106.4	107.5	104.3±3.3	3.1
Tetracycline	101.1	100.0	100.9	100.9	101.7	101.9	101.1±0.6	0.6
Chlortetracycline	102.3	99.6	99.6	103.0	99.8	98.7	100.5±1.7	1.7
Doxycycline	93.7	100.3	94.3	103.6	99.0	95.5	97.7±3.8	3.9

3.3.4 Accuracy

From Table 16, %recovery of 4 tetracyclines in Shrimp farming sample at spiking level of 0.5 mg/kg are in the range of 81.6-98.9%, while these of the 1mg/kg, 5 mg/kg and 10 mg/kg spiking levels are in the range of 80.4-99.0%, 87.9-105.0 % and 93.2-109.2%, respectively. And from Table 17, %recovery of 4 tetracyclines in Shrimp sea sample at spiking level of 0.5 mg/kg are in the range of 84.2-109.1%, while these of the 1mg/kg, 5 mg/kg and 10 mg/kg spiking levels are in the range of 72.2-97.4%, 80.3-91.7 % and 93.7-109.1%, respectively. These values agree within the acceptable range set forth by AOAC Regulations of %recovery at 75-125 mg/kg level.

Table 16 Accuracy of extraction method at spiking level of 0.5, 1, 5 and 10 mg/kg for Shrimp farming sample (n=3).

Analytes	Mean of %Recovery			
	Spiking level of 0.5 mg/kg	Spiking level of 1 mg/kg	Spiking level of 5 mg/kg	Spiking level of 10 mg/kg
Oxytetracycline	84.8±3.0	96.8±2.7	102.5±3.4	99.6±1.8
Tetracycline	93.3±5.5	85.9±7.7	96.6±2.4	97.0±5.5
Chlortetracycline	91.48±5.3	94.8±5.9	91.6±5.2	97.9±3.8
Doxycycline	89.2±6.7	88.4±3.0	97.7±5.4	103.7±7.4

Table 17 Accuracy of extraction method at spiking level of 0.5, 1, 5 and 10 mg/kg for Shrimp sea sample.(n=3)

Analytes	Mean of %Recovery			
	Spiking level of 0.5 mg/kg	Spiking level of 1 mg/kg	Spiking level of 5 mg/kg	Spiking level of 10 mg/kg
Oxytetracycline	94.9±1.6	83.3±4.3	86.8±5.0	96.5±2.4
Tetracycline	92.0±1.1	88.4±4.4	89.2±1.2	96.9±4.6
Chlortetracycline	91.8±8.6	91.9±3.0	86.0±8.0	93.3±5.1
Doxycycline	102.0±9.0	96.2±1.7	90.6±0.1	99.4±2.4

3.3.5 AOAC standard method

Standard calibration curve and linear range

The mixed 3 standard tetracyclines solution covering the concentration range of 0.05-10 ppm were measured. The regression data are summarized in Table 18.

From Table 18, the data of the 8 point calibration curve is acceptable for quantitation because the correlative coefficient (R^2) obtained were at 0.9975 to 0.9996.

Table 18 Linear regression statistics results

Analytes	Linear dynamic range (ppm)	Slope(peak areas units/mg/kg)	Intercept	R^2
Oxytetracycline	0.05-10	46.656	3.9474	0.9996
Tetracycline	0.05-10	55.960	4.3590	0.9995
Chlortetracycline	0.10-10	28.108	1.6850	0.9999

- **Limit of detection (LOD) and limit of quantitation (LOQ)**

The limit of detection (LOD) and limit of quantitation (LOQ) were defined as the concentration of that yielded the peak area of analyte in matrix standard solutions that signalled significantly different from the peak area of noise equal 3 for LOD and 10 for LOQ of each compound. These are shown in Table 19

The limit of detection and limit of quantitation of the 3 tetracyclines are in the range of 0.05-0.10 ppm and 0.17-0.33 ppm respectively.

Table 19 The limit of detection and of quantitation of analyte in matrix standard solutions

Analytes	LOD (ppm)	LOQ (ppm)
Oxytetracycline	0.05	0.17
Tetracycline	0.05	0.17
Chlortetracycline	0.10	0.33

- **The result of accuracy**

From Table 20, %recovery of 3 tetracyclines in Shrimp farming sample at spiking level of 0.5 mg/kg are in the range of 72.5-78.6%, while these of the 1mg/kg, 5 mg/kg and 10 mg/kg spiking levels are in the range of 72.6-80.2%, 77.5-82.5% and 80.2-90.2%, respectively. And from Table 3.21, %recovery of 3 tetracyclines in Shrimp sea sample at spiking level of 0.5 mg/kg are in the range of 74.2-80.2%, while these of the 1mg/kg, 5 mg/kg and 10 mg/kg spiking levels are in the range of 76.2-81.2%, 79.3-85.9% and 90.0-92.5%, respectively. This is within the acceptable range set forth by AOAC Regulations %recovery 75-125.

Table 20 Accuracy of extraction method at spiking level of 0.5, 1, 5 and 10 mg/kg for Shrimp farming sample (n=3)

Analytes	Mean of %Recovery			
	Spiking level of 0.5 mg/kg	Spiking level of 1 mg/kg	Spiking level of 5 mg/kg	Spiking level of 10 mg/kg
Oxytetracycline	78.6±6.5	79.0±6.3	82.5±3.2	89.9±3.8
Tetracycline	75.8±8.2	80.2±5.3	80.0±3.5	90.2±2.1
Chlortetracycline	72.56±5.4	72.6±7.7	77.5±4.2	80.2±4.2

Table 21 Accuracy of extraction method at spiking level of 0.5, 1, 5 and 10 mg/kg for Shrimp sea sample.(n=3)

Analytes	Mean of %Recovery			
	Spiking level of 0.5 mg/kg	Spiking level of 1 mg/kg	Spiking level of 5 mg/kg	Spiking level of 10 mg/kg
Oxytetracycline	80.2±5.3	78.4±5.9	85.9±4.5	92.5±3.0
Tetracycline	75.3±7.2	81.2±6.5	82.3±3.7	91.4±2.5
Chlortetracycline	74.2±6.7	76.2±7.0	79.3±4.0	90.0±4.0

Finally results determined tetracyclines in shrimp sample. From Table 3.22-3.23, the comparisons results of 3 methods in 2 shrimp samples at blank sample.

Table 22 Comparisons results of 3 methods in shrimp farming sample

Analyte	Found (mg/kg)		
	HPLC-ECD	AOAC method**	Result for LCFA***
Oxytetracycline	nd*	nd*	nd*
Tetracycline	nd*	nd*	nd*
Chlortetracycline	nd*	nd*	nd*
Doxycycline	nd*	-	-

* Not detected

** AOAC official method 995.09 (Chlortetracycline, Oxytetracycline and Tetracycline in edible animal tissues)

*** Result of Laboratory Center for Food and Agricultural product Co.,Ltd (LCFA)

Table 23 Comparisons results of 3 methods in shrimp sea sample

Analyte	Found (mg/kg)		
	HPLC-ECD	AOAC method**	Result for LCFA***
Oxytetracycline	nd*	nd*	nd*
Tetracycline	nd*	nd*	nd*
Chlortetracycline	nd*	nd*	0.07
Doxycycline	nd*	-	-

* Not detected

** AOAC official method 995.09 (Chlortetracycline, Oxytetracycline and Tetracycline in edible animal tissues)

*** Result of Laboratory Center for Food and Agricultural product Co.,Ltd (LCFA)

❖ Summary

This is the first use of Ni-DIA electrodes for the electroanalysis of tetracyclines. It was found that Ni-DIA electrodes exhibited excellent performance for the oxidative detection of tetracycline.Well-defined voltammograms were obtained at the Ni-DIA electrode, which exhibited high sensitivity and demonstrated significant advantages over the BDD and glassy carbon electrode. The outstanding capabilities of the Ni-DIA electrode were demonstrated by coupling with HPLC. HPLC with amperometry at Ni-DIA electrode has been successfully applied to determine four types of tetracyclines (oxytetracycline, tetracycline, chlortetracycline and doxycycline) in shrimp samples. Experimental detection limit of 0.01–0.05 μg/mL were obtained for four tetracyclines studied. A linear dynamic range from 0.05 to 100 μg/mL was achieved. Application of the proposed method for the determination of tetracycline in shrimp sample shows that this method is precise, accurate and very sensitive.

CONCLUSIONS

In this research, the modified BDD electrodes were used to investigate tetracycline antibiotics. BDD have been widely used as electrode for many electrochemical applications. The superior electrochemical properties were low background current leads to the enhancement of the S/B ratios, wide working potential window in the aqueous solution and slightly adsorption of polar molecules. Moreover, the BDD surfaces covered with hydrogen make this electrode lack of the catalytic property. The modification of BDD surface to change the functional group on the diamond surface can be extended the catalytic capability and enhanced the sensitivity of the electrode. This work was focused on two modification methods (i) anodized BDD electrode and (ii) Ni-implanted diamond electrode for the determination of tetracycline antibiotics in pharmaceutical formulation and shrimp.

The anodized BDD electrode was modified by anodic polarization in the alkaline solution using cyclic voltammetry to make the surface of BDD terminated with oxygen. The obtained anodized BDD electrode was applied to detect tetracycline antibiotics. The electrochemical properties of tetracyclines were investigated using cyclic voltammetry. Comparison results were carried out using glassy carbon and as-deposited BDD electrodes. From the results, all electrodes provided the irreversible cyclic voltammograms. However, the highest current signal was obtained at the anodized BDD electrode. In order to find the optimum pH for the determination of TCs at anodized BDD electrode, the experiments were carried out in the pH solution 2-9. It was found that the pH 2 gave the maximum current signal because the TCs were formed in the fully positive charge that could be attracted to the negatively charged on the anodized BDD surface. The anodized BDD electrode was used as the amperometric detector in the flow injection system. To find the optimum working potential, hydrodynamic voltammetry of TCs were investigated. The results indicated that the optimum potentials were 1.5 V vs. Ag/AgCl for CTC, and 1.6 V vs. Ag/AgCl for TCs, OTC, and DC. The analytical performances of anodized BDD electrode in flow system including the linear range and LOD were investigated. The linear ranges were 0.1–50 μM for TC and 0.5-50 μM for OTC, CTC and DC. The LOD was 10 nM for four TCs. The proposed method was applied to determination TCs in the pharmaceutical formulations. The precision of the method based on the

intra- and inter-day assay were studied. The results were summarized in the Table 3.5 and 3.6.

Ion implantation has been successfully used in doping semiconductors such as silicon and gallium arsenide. In particular, applications of the ion-implanted diamond have recently come to light. In these studies, the electrical conductivity and other physical properties could be controlled by ion-implanting diamond. Flow injection analysis and HPLC electrochemical detection at the Ni-implanted BDD electrode has been accomplish applied to determine TCs in pharmaceutical drugs and shrimps, respectively. The outstanding capabilities of the Ni-DIA electrode were demonstrated by coupling with FIA. Application of the proposed method for determination of tetracycline in commercially available tablet forms shows that this method is precise, accurate and very sensitive.

For the validation of this method, the linear concentration range of TCs was 0.05 to 100 ppm, with correlation coefficient $R^2 > 0.99$. The LOD of this method was in the range of 0.01-0.05 ppm. The recovery of TCs at the spiking level of 0.5 mg/kg, 1.0 mg/kg, 5.0 mg/kg and 10 mg/kg were studied. The recovery was in the range of 83.3-102.0% with RSD < 10%. These results indicated that HPLC electrochemical detection at the Ni-implanted BDD electrode provided high accuracy and precision, respectively.

References

1. Ngamukot, P.; Charoenraks, T.; Chailapakul, O.; Motomizu, S.; Chuanuwatanakul, S. *Analytical Sciences* **2006**, *22*, 111.
2. Treetepvijit, S.; Preechaworapun, A.; Praphairaksit, N.; Chuanuwatanakul, U.; Einaga, Y.; Chailapakul, O. *Talanta* **2006**, *68*, 1329.
3. Lawrence, N. S.; Pagels, M.; Meredith, A.; Jones, T. G. J.; Hall, C. E.; Pickles, C. S. J.; Godfried, H. P.; Banks, C. E.; Compton, R. G.; Jiang, L. *Talanta* **2006**, *69*, 829.
4. Ivandini, T. A.; Rao, T. N.; Fujishima, A.; Einaga, Y. *Analytical Chemistry* **2006**, *78*, 3467.
5. Basu, S.; Kang, W. P.; Davidson, J. L.; Choi, B. K.; Bonds, A. B.; Cliffel, D. E. *Diamond and Related Materials* **2006**, *15*, 269.
6. Peckova, K.; Mocko, V.; Opekar, F.; Swain, G. M.; Zima, J.; Barek, J. *Chemicke Listy* **2006**, *100*, 124.
7. Batchelor-McAuley, C.; Banks, C. E.; Simm, A. O.; Jones, T. G. J.; Compton, R. G. *Analyst* **2006**, *131*, 106.
8. Bouvrette, P.; Hrapovic, S.; Male, K. B.; Luong, J. H. T. *Journal of Chromatography A* **2006**, *1103*, 248.
9. Welch, C. M.; Banks, C. E.; Komorsky-Lovric, S.; Compton, R. G. *Croatica Chemica Acta* **2006**, *79*, 27.
10. Xie, S. T.; Shafer, G.; Wilson, C. G.; Martin, H. B. *Diamond and Related Materials* **2006**, *15*, 225.
11. Xu, J. S.; Granger, M. C.; Chen, Q. Y.; Strojek, J. W.; Lister, T. E.; Swain, G. M. *Analytical Chemistry* **1997**, *69*, A591.

12. Chailapakul, O.; Popa, E.; Tai, H.; Sarada, B. V.; Tryk, D. A.; Fujishima, A. *Electrochemistry Communications* **2000**, *2*, 422.

13. Granger, M. C.; Xu, J. S.; Strojek, J. W.; Swain, G. M. *Analytica Chimica Acta* **1999**, *397*, 145.

14. Wangfuengkanagul, N.; Chailapakul, O. *Talanta* **2002**, *58*, 1213.

15. Swain, G. M.; Anderson, A. B.; Angus, J. C. *MRS Bulletin* **1998**, *23*, 56.

16. C. Terashima, T.N. Rao, B.V. Sarada, D.A. Tryk, A. Fujishima, *Anal. Chem*. **2002**, *74*, 895.

17. E. Popa, Y. Kubota, D.A. Ttyk, A. Fujishima, *Anal. Chem*. **2000**, *72,* 1724.

18. O. Chailapakul, W. Siangproh, B.V. Sarada, C. Terashima, T.N. Rao, D.A. Tyrk, A. Fujishima, *Analyst* **2002**, *127,* 1164.

19. F. Montilla, E. Morallon, I. Duo, C. Comninellis, J.L. Vasquez, *Electrochim. Acta* **2003**, *48*3, 891.

20. I.G. Casella, E. Desimoni, T.R.I. Cataldi, *Anal. Chim. Acta* **1991**, *248*, 117.

21. I.G. Casella, E. Desimoni, A.M. Salvi, *Anal. Chim. Acta* **1991**, 243, 61.

22. S.V. Prabhu, R.P. Baldwin, *Anal. Chem*. **1989**, *61*, 852.

23. S.V. Prabhu, R.P. Baldwin, *Anal. Chem*. **1989**, *61*, 2258.

24. P. Luo, S.V. Prabhu, R.P. Baldwin, *Anal. Chem*. **1990**, *62,* 752.

25. T.R.I. Cataldi, I.G. Casella, E. Desimoni, T. Rotunno, *Anal. Chim. Acta* **1992** , *270* , 161.

26. E. Wang, A. Liu, *J. Electroanal. Chem.* **1991**, *319*, 217.

27. I.G. Casella, T.R.I. Cataldi, A.M. Salvi, E. Desimoni, *Anal. Chem*. **1993**, *65,* 3143.

28. A. Liu, E. Wang, *Anal. Chim. Acta* 1993, *280*, 223.

29. T.A. Ivandini, R. Sato, Y. Makide, A. Fujishima, Y. Einaga, *Diamond Relat.*

Mater. **2004** , *13*, 2003.

30. The United Pharmacopoeia, 21st revision, Easton PA, Mack Printing Company, USP XXI, **1985.**
31. The British Pharmacopeia, HMSO, London **1988**.
32. J. Kurittu, S. Lonnberg, M. Virta, M. Karp, *J. Agri. Food. Chem.* **2000**, *48* 3372.
33. K.M. Emara, H.F. Askal, G.A. Saleh, *Talanta* **1991**, *38*, 1219.
34. U. Saha, A.K. Sen, T.K. Das, S.K. Bhowal, *Talanta* **1990**, *37*, 1193.
35. X.R. Zhang, W.R.G. Baeyens, A. Vandenborre, G. Vanderweken, A.C. Calokerinos, S.G. Schulman, *Analyst* **1995**, *120* , 463.
36. H. Han, Z. He, Y. Zeng, *Anal. Sci.* **1999**, *15,* 467.
37. S. Marczynski, *Biopolymers* **2000**, *57*, 365.
38. A. Pena, L.P. Palilis, C.M. Lino, M.I. Silveira, A.C. Calokerinos, *Anal. Chim. Acta.* **2000**, *405,* 51.
39. S. Croubels, C. V. Peteghem, W. Baeyens, *Analyst* **1994**, *11, 9*2713.
40. S. Sabhawal, K. Kishore, P.N. Moorthy, *J. Pharm. Sci.* **1988**, *77*, 78.
41. R. Karlicek, P. Solich, *Anal. Chim. Acta* **1994**, *285,* 9.
42. S.M. Sultan, F.E.O. Suliman, S. O. Duffuaa, I. I. Abu-Abdoun, *Analyst* **1992**, *117* , 1179.
43. S. A. Halvatzis, M. M. Timotheou-Potamia, A. C. Calokerinos, *Analyst* **1993**, *118* , 633.
44. A. B. Syropoulos, A. C. Calokernos, *Anal. Chim. Acta* **1991**, *255,* 403.
45. C.M. Couta, J.L.F.C. Lima, M. Conceicao, B.S.M. Montenegro, S. Reis, *J. Phram. Biomed. Anal.* **1998**, *18*, 527.
46. H. Ji, E. Wang, *Analyst* **1988,** *113,* 1541.

47. W. Oungpipat, P. Southwellkeely, P.W. Alexander, *Analyst* **1995** , *120* , 1559.

48. A. G. Kazemifard, D. E. Moore, *J. Pharm. Biomed. Anal.* **1997**, *16*, 689.

49. J. Sokol, E. Matisova, *J. Chromatogr. A* **1994**, *669,* 75.

50. J.R. Walsh, L.V. Walker, J.J. Webber, *J. Chromatogr. A* **1992**, *596*, 211.

51. S. Croubels, W. Baeyens, C.V. Peteghem, *Anal. Chim. Acta* **1995** ,*303*,11.

52. D.S. Vienneau, C.G. Kindberg, *J. Pharm. Biomed. Anal.* **1997**, *16*, 111.

53. J. Zhu, D.D. Snow, D.A. Cassada, S.J. Monson, R.F. Spalding, *J. Chromatogr. A* **2001** ,*928*, 177.

54. M. Cherlet, M. Schelkens, S. Croubels, P.D. Backer, *Anal. Chim. Acta* **2003,** *492,* 199.

55. A.G. Kazemifard, D.E. Moore, *J. Pharm. Biomed. Anal.* **1997** ,*16,* 689.

56. S. Palaharn, T. Charoenraks, N. Wangfuengkanagul, K. Grudpan, O. Chailapakul, *Anal. Chim. Acta* **2003**, *499*,191.

57. C.M.C.M. Couto, J.L.F.C. Lima, M. Conceicao, B.S.M. Montenegro, S. Reis, *J. Pharm. Biomed. Anal*. **1998** ,*18*, 527.

58. T. Charoenraks, S. Chuanuwatanakul, K. Honda, Y. Yamaguchi, O. Chailapakul, *Anal. Sci*. **2005**, *212*, 41.

Output

ผลงานวิจัยที่ตีพิมพ์

1. Wangfuengkanagul, N.; Siangproh, W.; Chailapakul, O., Electrochemical analysis of Tetracycline using an Anodized boron-doped diamond thin film electrode. *Talanta* **2004,** 64, (5), 1183-1188.
2. Treetepvijit, S.; Chuanuwatanakul, S.; Einaga Y.; Sato, R and Chailapakul, O Electroanalysis of tetracycline using nickel-implanted boron-doped diamond thin film electrode applied to flow injection system *Analytical Sciences,* **2005**, 21, 531.
3. Kanokporn, B.; Chuanuwatanakul, S.; Wangfuengkanagul, N and Chailapakul, O.; Electroanalysis of lincomycin using boron-doped diamond thin film electrode applied to flow injection system *Sensors and Actuators B: Chemical,* **2005***,108,* 627.
4. Treetepvijit, S.; Preechaworapun, A.; Praphairaksit, N.; Chuanuwatanakul, U.; Einaga Y.; Chailapakul, O Use of nickel implanted boron-doped diamond thin film electrode coupled to HPLC system for the determination of tetracyclines *Talanta* **2006,** 64, (5), 1329-1335.
5. Ngamukot, P.; Charoenraks, T.;Chailapakul, O.; Motomizu, S.; Chuanuwatanakul, S.; Cost-effective flow cell for the determination of malachite green and leucomalachite green at a boron-doped diamond thin-film electrode *Analytical Sciences,* **2006**, *22*, 111.
6. Chailapakul, O.; Siangproh, W.; Tryk, D. A.; Boron-doped diamond-based sensors: A review *Sensor Letters* **2006**, 4 (2), 99-119.

การไปเสนอผลงาน

1. Treetepvijit, S.; Duanchai, W.; Bunnium, R.; Chailapakul, O. “Determination of Hydrogen Peroxide Based on Electrocatalytic Oxidation Using Chrmium(III) Hexacyanoferrate(II) Modified Boron-Doped Diamond Thin Film Electrode” *The 30th Congress on Science and Technology of Thailand,* 19-21 October **2004**, Muang Thong Thani, Bangkok, Thailand

2. Chailapakul, O. ; Treetepvijit, S. “Using Nickel implanted Boron-Doped Diamond Thin Film Electrode Coupled to FIA/HPLC System for the Determination of Tetracyclines” *The 13th International Conference on Flow Injection Analysis,* 24-29 April **2005**. Las Vegas, Nevada US
3. Chailapakul, O. “The use of as-grown and modified boron-doped diamond thin film electrodes for the electroanalysis” *The 11 th Asian Chemical Congress* August, **2005**., Zeoul, Korea
4. Chailapakul, O. “FIA-electrocatalytic determination of hydrogen peroxide at chromium (III) hexacyanoferrate (II) modified boron-doped diamond electrodes” *Pacifichem 2005,* 15 -23 December **2005**, Honolulu, Hawaii, US
5. Chailapakul, O. “Electroanalysis of chloramphenicol at reduction potential using boron-doped diamond thin film electrode applied to a flow injection system” *The 11th International Meeting on Chemical Sensors* , 16-19 July **2006**, University of Brescia, Brescia, Italy.
6. Chailapakul, O. “Boron-Doped Diamond Electrode and its Application to Flow based electroanalysis” 21st Century COE KEIO-LCC International Symposium (*The 9h International Mini-symposium on Diamond Electrochemistry and related Topics*) , 9-10 March **2007**, Keio University Japan.

หนังสือ

1. Chailapakul, O.; Tryk, D. A. and Fujishima, A. In Diamond Electrochemistry Fujishima, A; Einaga. Y.; Rao, T. N. and Tryk, D. A., Ed.; BKC, Tokyo, Japan, 2005, chapter 15, *p 321*
2. Siangproh, W.; Tryk, D. A.; Chailapakul, O. In Recent Advances in Analytical Electrochemistry 2007, Kenneth I. Ozoemena., Ed.; Transworld Research Network: kerala, India, 2007, chapter 6, p.167

Available online at www.sciencedirect.com
SCIENCE DIRECT®
Talanta 64 (2004) 1183–1188
Talanta
www.elsevier.com/locate/talanta

A flow injection method for the analysis of tetracycline antibiotics in pharmaceutical formulations using electrochemical detection at anodized boron-doped diamond thin film electrode

N. Wangfuengkanagul, W. Siangproh, O. Chailapakul*

Department of Chemistry, Faculty of Science, Chulalongkorn University, 254 Phyathai Road, Patumwan, Bangkok 10330, Thailand

Received 1 March 2004; received in revised form 26 April 2004; accepted 26 April 2004
Available online 23 August 2004

Abstract

A method using flow injection (FI) with amperometric detection at anodized boron-doped diamond (BDD) thin films has been developed and applied for the determination of tetracycline antibiotics (tetracycline, chlortetracycline, oxytetracycline and doxycycline). The electrochemical oxidation of the tetracycline antibiotics was studied at various carbon electrodes including glassy carbon (GC), as-deposited BDD and anodized BDD electrodes using cyclic voltammetry. The anodized BDD electrode exhibited well-defined irreversible cyclic voltammograms for the oxidation of tetracycline antibiotics with the highest current signals compared to the as-deposited BDD and glassy carbon electrodes. Low detection limit of 10 nM (signal-to-noise ratio = 3) was achieved for each drug when using flow injection analysis with amperometric detection at anodized BDD electrodes. Linear calibrations were obtained from 0.1 to 50 mM for tetracycline and 0.5–50 mM for chlortetracycline, oxytetracycline and doxycycline. The proposed method has been successfully applied to determine the tetracycline antibiotics in some drug formulations. The results obtained in percent found (99.50–103.01%) were comparable to dose labeled.

Keywords: Tetracycline; Chlortetracycline; Oxytetracycline; Doxycylcine; Flow injection system; Anodized boron-doped diamond thin film electrode

1. Introduction

Tetracyclines are broad spectrum antibiotics for their high activity against nearly all gram-positive and gram-negative bacteria. Tetracycline, chlortetracycline, oxytetracycline and doxycycline are commonly used in food protection animals (including honeybee), because of their board spectrum activity and low production cost. However, tetracycline residues in milk or meat are also toxic and can cause allergic reactions in some hypersensitive individuals in human. Owing to their extensive use in infectious diseases therapy, there have been several analytical methods available for these compounds in pharmaceutical preparations, biological samples and milk samples. Official methods such as microbiological-based techniques can also provide both qualitative and quantitative analysis for tetracyclines [1–3]. These methods have characteristic disadvantages: microbiological tests are not only time consuming, laborious and expensive but also poor in term of sensitivity and selectivity. There are also some batch procedures which employ spectrophotometry [4,5], chemiluminescence [6–9], spectrofluorimetry [10], and electrochemical method [11].

Flow injection (FI) is a well-known tool that offers improvement in most batch methods, especially the high sample throughput. For the tetracyclines, there are some FI methods available with all types of detection such as spectrophotometry [12,13], chemiluminescence [14,15] and electrochemical method [16–18]. The spectrophotometric FI method detections [12,13] for tetracyclines are based on the formation of a color product by their reaction with 4-aminophenazone and hexacyanoferrate(III). However, this method has a limited concentration range. Under the optimized conditions, tetracyclines were determined in the ranges of 1–20 and 20–250 mg L^{-1}. The lowest limit of detection is 0.2 mg L^{-1} for doxycycline [12]. For the chemiluminescence method [14], a highly toxic and expensive agent,

* Corresponding author. Tel.: +66 2 218 7615; fax: +66 2 254 1309.
E-mail address: corawon@chula.ac.th (O. Chailapakul).

0039-9140/$ – see front matter © 2004 Elsevier B.V. All rights reserved.
doi:10.1016/j.talanta.2004.04.032

N-bromosuccinimide is used. The reported working range are 0.05–3.00 mg L^{-1} for tetracycline, 0.50–5.00 mg L^{-1} for oxytetracycline and 0.50–7.00 mg L^{-1} for doxycycline and chlortetracycline.

Electrochemical techniques such as amperometric and potentiometric detection are good alternative methods that are widely used in pharmaceutical applications. The techniques are usually easy to operate, fast and inexpensive. The sensitivity of electrochemical methods is often greater than the spectrophotometric method. For example, the detection limits using HPLC amperometric detection varied from 0.1 to 1 mg L^{-1} for tetracycline family [19].

Procedures in electroanalysis strongly depend on working electrode materials, so the searching and development of new electrode material is necessary. Boron-doped diamond (BDD) thin film electrodes have been emerged as new electrode material in the many fields in electrochemistry, especially in electroanalysis applications [20–29]. The most importance electrochemical properties are: (i) the wide working potential window in aqueous and non-aqueous media; (ii) a stable and low background current, leading to improved signal-to-background and signal-to-noise ratios; (iii) slight adsorption of polar molecules and long term stability of the response, leading to improved resistance to electrode deactivation and fouling. Recently, a diamond electrode has been chemically pretreated by electrochemical oxidation [30–32]. The anodized diamond electrodes retain the excellent properties of the as-deposited diamond electrode even though, the electrode surface of anodized diamond electrode is applied by a high anodic potential. Anodized diamond electrodes are suitable for determination of various analytes such as chlorophenol [30], dopamine and uric acid in the presence of ascorbic acid [31] and homocysteine [32]. These anodized electrodes have exhibited some attractive properties such as excellent stability and high reproducibility. In this present work, the anodized diamond electrode was used for the electrochemical determination of tetracyclines using cyclic voltammetry. Glassy carbon (GC) and as-deposited diamond electrodes were also used for comparison. The anodized diamond electrode was exploited as working electrode for amperometric determination of antibiotic drugs, using flow injection system.

2. Experimental

2.1. Chemicals and reagents

All reagents were analytical reagent grade. All solutions were prepared in ultrapure water. Standards (hydrochloric forms) of tetracycline, chlortetracycline, oxytetracycline and doxycycline were supplied by Sigma Chemical (USA). Potassium dihydrogen phosphate (BDH), disodium hydrogen phosphate, sodium hydroxide (Merck) and phosphoric acid 85% (J.T. Baker) were used to prepare the buffer solution. Phosphate buffer (0.1 M) solutions with pH ranges from 5.0 to 8.0, were prepared by dissolving the appropriate amounts of potassium dihydrogen phosphate and disodium hydrogen phosphate. Phosphoric acid and sodium hydroxide were used to adjust the desired pH that is out of the above range.

The standard tetracycline antibiotics were prepared by dissolving an appropriate amount of the tetracycline antibiotics in the buffer solution. The solutions were prepared daily.

2.2. Electrodes

The as-deposited BDD electrodes used in this work are from Professor Akira Fujishima' s Laboratory. The electrodes were prepared by deposition of the BDD thin films on highly conductive *n*-Si(1 1 1) substrate using the technique of microwave plasma-assisted chemical vapor deposition. Deposition was usually carried out for 10 h to achieve a film thickness of approximately 30 μm. The nominal B/C atomic ratio in the gas phase was 1:100, and the typical boron-doped level in the film was ca. 10^{21} cm^{-3}. The experimental conditions and the apparatus used for the diamond film growth have been described in detail elsewhere [23]. A piece of diamond was rinsed with ultrapure water prior to use for electroanalysis.

Anodized BDD electrode was prepared by treating an as-deposited BDD electrode in 0.1 M KOH solution. The potential was applied between 0 and 2.2 V versus Ag/AgCl using cyclic voltammetry for 30 min. The anodized BDD electrode was also rinsed with ultrapure water before use.

The GC electrode was purchased from Bioanalytical System, Inc. (area 0.07 cm^2). It was pretreated by sequential polishing with 1 and 0.05 μm of alumina/water slurries on felt pads, followed by rinsing with ultrapure water prior to use.

2.3. Cyclic voltammetric investigation

Electrochemical experiments were conducted out in a single compartment three-electrode glass cell. The BDD electrode was pressed against a smooth ground joint at the bottom of the cell, isolated by an *O*-ring vitron (area 0.07 cm^2). Ohmic contact was made by placing the backside of the Si substrate. The GC carbon was used as working electrode for the comparison. The Ag/AgCl with salt bridge and Pt wire were used as reference electrode and counter electrode respectively. The voltammetric measurement was performed with the three types of electrodes using Autolab Potentiostat 100 (Eco-Chemie, The Netherlands).

2.4. Flow injection with amperometric detection

The flow injection system consisted of a thin layer flow cell (Bioanalytical System, Inc), a 20 mL stainless steel loop of injection port (Rheodyne 7725), a peristaltic pump, and

electrochemical detection (Autolab potentiastat 100). The carrier solution (0.1 M potassium dihydrogen phosphate pH 2) was regulated at the flow rate of 1 mL min^{-1} by measuring the volume of carrier solution in 1 min. The thin layer flow cell consisted of a silicone rubber gasket as a spacer, a Ag/AgCl electrode as the reference electrode and a stainless steel tube as an auxiliary electrode and an outlet of the flow cell. The experiments were performed in a copper faradaic cage to reduce the electronic noise. All experiments were done at room temperature.

2.5. Sample preparation

The contents within the pharmaceutical capsule (as described on the label) were: 250 mg tetracycline hydrochloride™ (Tetracycline hydrochloride); 250 mg Aureomycin™ (chlortetracycline); 250 mg Oxycline™ (oxytetracycline); 100 mg Medomycin™ (doxycycline). The powder of twenty capsules of each drug was accurately weighed and homogenized so as to obtain the mean capsule weight. A portion of the homogenized powder corresponding to the mean capsule weight was then transferred into volumetric flask and dissolved in 0.1 M phosphate buffer (pH 2), and then mixed thoroughly. A portion of the sample solutions was filtrated through 0.45 mm nylon membrane. The filtrated solutions were further diluted using 0.1 M phosphate buffer (pH 2) to make the final concentration in the range of 0.96–5.15 mg mL^{-1} within the linear dynamic range. All tetracycline antibiotic solutions were protected from light by covering with aluminum foil and stored at 4 °C.

3. Results and discussion

3.1. Cyclic voltammetry

3.1.1. Voltammetric study

According to Fig. 1, the anodized BDD electrode (Fig. 1c) provided well-resolved irreversible oxidation cyclic voltammogram with the highest current responses in comparison to the as-deposited BDD and the glassy carbon electrodes, Fig. 1a and b respectively. These electrodes produced oxidative waves at +1.0 V versus Ag/AgCl, however the as-deposited BDD electrode produced no voltammetric peak shape in contrast to the results at the anodized BDD electrode. The results obtained from the other antibiotics, i.e., chlortetracycline, oxytetracycline and doxycycline were analogous to the results shown for tetracycline in Fig. 1. These results can be rationalized as follows. The surface of the BDD, after the anodizing treatment, is partly covered with oxygen atoms [30–32]. In acidic condition, all the tetracycline are positively charged. This therefore encourage electrostatic interaction between the negatively charged BDD anodized surface and the analytes. In contrast, the as-deposited BDD, the surface is non-polar (covered with hydrogen atoms), and therefore the electrostatic interaction

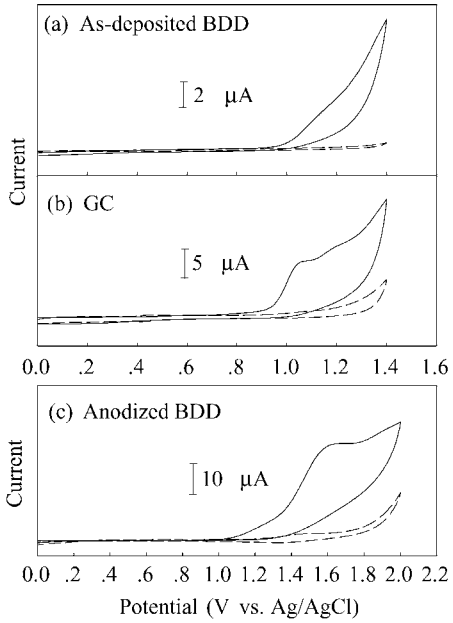

Fig. 1. Cyclic voltammetric results of 500 μM tetracycline (solid line) in 0.1 M potassium dihydrogen phosphate (pH 2) with the corresponding background current (dashed line) at: (a) as-deposited BDD; (b) glassy carbon; and (c) anodized BDD electrodes.

is less permitted. This may be the reason for the ill-defined peak current, in Fig. 1a, for example.

3.1.2. pH dependence

The effect of pH was investigated from pH 2–9 for all four compounds using anodized BDD electrode. A plot of pH versus Ep has been investigated. It was found that results were ambiguous, and the expected pK was inconsistant with the pK value of the dissociation in the literature.

For quantitative purposes, the information concerning about the current response was also investigated. It was found that in acidic buffer, tetracyclines provided the well-defined oxidative responses cyclic voltammograms. However, in neutral and alkaline buffer, ill-defined voltammetric waves were obtained. The current response decreased with increasing the pH. Results for all, the antibiotics demonstrated that pH 2 gave the highest current signal (Fig. 2). Therefore, pH 2 was chosen as the optimal pH for the rest of experiments.

It can be explained that tetracyclines are derived from a system of four membered rings arranged linearly with characteristic double bonds. They are amphoteric compounds with high polarity, and an isoelectric point between 4 and 6. From the literature [33,34], three dissociations have been observed for tetracyclines, with $pK_1 = 3.3$, $pK_2 = 7.5$ and $pK_3 = 9.4$. In strongly acidic pH, the tetracycline molecule exists in its fully protonated form as a singly charged cation. As proposed [30–32], the surface of anodized BDD electrode covered with the negative charge, electrostatically attracts the positive tetracycline. Hence, at pH 2 the positively charged tetracycline provided the highest response.

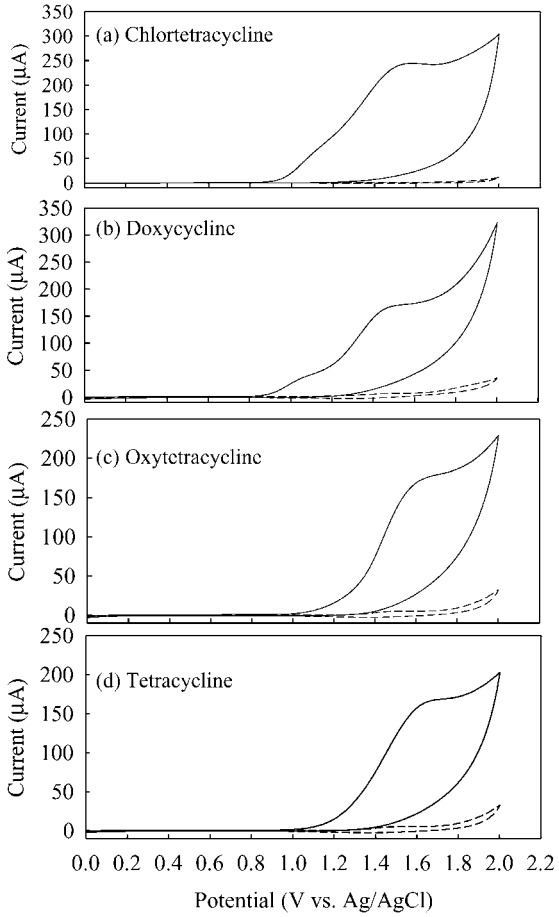

Fig. 2. Cyclic voltammograms at anodized BDD electrode vs. Ag/AgCl in 500 μM chlortetracycline, doxycycline, oxytetracycline, and tetracycline in 0.1 M phosphate buffer pH 2 (solid lines) and 0.1 M phosphate buffer pH 2 (dashed lines). The scan rate was 50 mV s^{-1}; area of electrode, 0.07 cm^2.

Moreover, the anodized diamond surface can be recovered by in situ reactivation (applying a high positive potential 2.6 V versus Ag/AgCl) during the flow injection measurement [30].

3.1.3. Scan rate dependence

The scan rate dependence study was carried out by varying the scan rate ranging from 0.01 to 0.3 V s^{-1}. From the result, we found for all four compounds, that the relationship between current and square root of scan rate was linear with the correlation coefficient of approximately 0.99 (data not shown). The results indicated that the oxidation currents are controlled by the diffusion of tetracyclines in the interfacial reaction zone.

3.2. Flow injection with amperometric detection

3.2.1. Hydrodynamic voltammetry

Hydrodynamic voltammogram was obtained from the average of three injections at aliquot of 20 μL of 100 mM tetracycline antibiotic solutions in the flow injection system. In this case the applied potential was gradually increased from 1.1 to 2.0 V versus Ag/AgCl. The carrier solution was 0.1 M potassium dihydrogen phosphates (pH 2). Fig. 3a shows the hydrodynamic voltammogram of tetracycline antibiotics with the corresponding background currents. The hydrodynamic voltammogram of tetracycline antibiotics did not exhibit the sigmoidal shape of the signal versus potential probably due to the high oxidation potential of tetracycline. To obtain the optimum potential, we calculated the S/B ratios from the results in Fig. 3a at each potential and plotted the ratios versus potentials (Fig. 3b). The maximum S/B ratio was found at 1.5 V (versus Ag/AgCl) for chlortetracycline and at 1.6 V (versus Ag/AgCl) for tetracycline, oxytetracycline and doxycycline. Hence, these optimum potentials were used for the quantification experiments in amperometric flow injection.

3.2.2. Analytical performance of the FI system at anodized BDD electrode

A series of analytical features were performed on the proposed method for the quantification of tetracycline, chlortetracycline, oxytetracycline and doxycycline. Calibration parameters and the linear ranges for all the drugs are summarized in Table 1. The limit of detection (3S/N) was 10 nM for all compounds. To obtain the repeatability, 10 replicates of injections were carried out at three concentrations (5, 10, 50 mM). The peak variability defined as the relative standard deviation (R.S.D. %), were found to be 1.3–1.7 (for tetracycline hydrochloride), 2.4–3.0 for chlortetracycline, 1.6–3.0

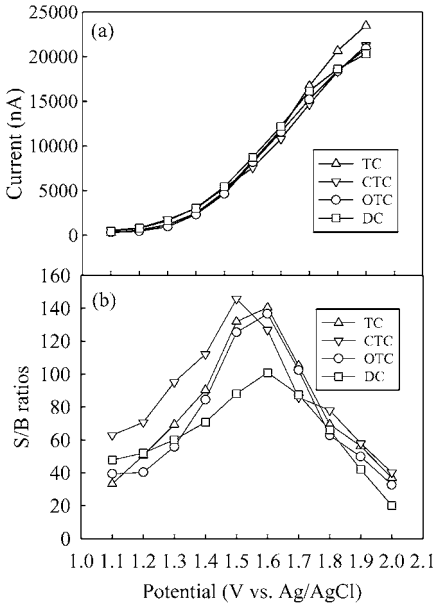

Fig. 3. Hydrodynamic voltammetric results for 100 μM tetracycline antibiotics. (a) (△): tetracycline, TC; (▽): chlortetracycline, CTC; (○): oxytetracycline, OTC; and (□): doxycycline, DC in 0.1 M potassium dihydrogen phosphate (pH 2), using 0.1 M potassium dihydrogen phosphate (pH 2) as carrier solution. The flow rate was 1 mL min^{-1}. (b) Hydrodynamic voltammogram of signal-to-background ratios.

Table 1
Regression parameters and linear range for the determination of tetracycline antibiotics by flow injection with amperometric detection using anodized boron-doped diamond electrode ($n = 2$)

Analytes	Linear range (μM)	a	b	r^2
Tetracycline	0.1–50	110.0 ± 5.9	192.1 ± 5.0	0.997
Chlotetracycine	0.5–50	76.9 ± 3.9	199.7 ± 29.7	0.997
Oxytetracycline	0.5–50	90.2 ± 3.0	165.2 ± 28.9	0.999
Doxytetracycline	0.5–50	96.2 ± 3.8	213.7 ± 48.9	0.997

$ay = ax + b$, where y: current (nA); x: concentration (μM); a: slope (nA/μM); b: intercept (nA).

Table 2
Determination of tetracycline antibiotics in drug formulations ($n = 2$)

Drug formulations	Label amount (mg)	Found (mg)	Found (%)
Tetracycline	250	249.4 ± 1.7	99.8 ± 0.7
Aureomycine	250	249.7 ± 1.3	99.87 ± 0.5
Oxycline	250	254.6 ± 2.5	101.85 ± 1.0
Medeomycin	100	98.4 ± 1.0	98.4 ± 1.0

for oxytetracycline and 1.7–2.7 for doxycycline. The stability of the amperometric response using flow injection at the anodized BDD electrode was obtained by conducting 100 repetitive injections of 50 mM chlortetracycline. It was observed that the peak variation was about 3.4%. The throughput of sample is approximately seventy injections per hour.

3.2.3. Application

Our method was applied for determination of each compound in four drug formulations using the standard addition method. The results are presented in Table 2. The percentages of recovery indicate that the amounts are comparable between the labeled quantity and the value obtained from the proposed method.

4. Conclusion

Anodized treatment has significantly improved the analytical performance of the BDD thin film for the analysis of tetracycline drugs. Current signal of the anodized BDD electrode is greater than the current signal of the glassy carbon electrode. It was observed from the cyclic voltammetric study that pH strongly influenced the current response of the voltammograms with pH 2 being selected for the method development, since the highest current was obtained with a well-defined voltammetric signal.

Amperometric detections of four compounds, i.e., tetracycline, chlortetracycline, oxytetracycline and doxycycline was employed in the method development, using flow injection. The developed method has been successfully applied to determine four types of tetracyclines in various pharmaceutical formulations. The tetracycline antibiotics content of the drug was found to be in excellent agreement with the declared amount on the label.

Acknowledgements

This research was supported by the Thailand Research Fund through the Royal Golden Jubilee Ph.D. Program (Grant No. PHD/0209/2544) and Methee Vijai Grant, the Ratchadaphisek Somphot Endowment Grant and TJTTP-OECF. Special thanks are extended to Professor A. Fujishima (The University of Tokyo) for the BDD electrodes used in this research. The authors also would like to thank Dr. Nathan Lawrence (New Mexico State University) for editing the manuscript.

References

[1] The United Pharmacopoeia, 21st revision, Easton PA, Mack Printing Company, USP XXI, 1985
[2] The British Pharmacopeia, HMSO, London, 1988
[3] J. Kurittu, S. Lonnberg, M. Virta, M. Karp, J. Agric. Food. Chem. 48 (2000) 3372.
[4] K.M. Emara, H.F. Askal, G.A. Saleh, Talanta 38 (1991) 1219.
[5] U. Saha, A.K. Sen, T.K. Das, S.K. Bhowal, Talanta 37 (1990) 1193.
[6] X.R. Zhang, W.R.G. Baeyens, A. Vandenborre, G. Vanderweken, A.C. Calokerinos, S.G. Schulman, Analyst 120 (1995) 463.
[7] H. Han, Z. He, Y. Zeng, Anal. Sci. 15 (1999) 467.
[8] S. Marczynski, Biopolymers 57 (2000) 365.
[9] A. Pena, L.P. Palilis, C.M. Lino, M.I. Silveira, A.C. Calokerinos, Anal. Chim. Acta 405 (2000) 51.
[10] S. Croubels, C.V. Peteghem, W. Baeyens, Analyst 119 (1994) 2713.
[11] S. Sabhawal, K. Kishore, P.N. Moorthy, J. Pharm. Sci. 77 (1988) 78.
[12] R. Karlicek, P. Solich, Anal. Chim. Acta 285 (1994) 9.
[13] S.M. Sultan, F.E.O. Suliman, S.O. Duffuaa, I.I. Abu-Abdoun, Analyst 117 (1992) 1179.
[14] S.A. Halvatzis, M.M. Timotheou-Potamia, A.C. Calokerinos, Analyst 118 (1993) 633.
[15] A.B. Syropoulos, A.C. Calokernos, Anal. Chim. Acta 255 (1991) 403.
[16] C.M.C.M. Couta, J.L.F.C. Lima, M. Conceicao, B.S.M. Montenegro, S. Reis, J. Phram. Biomed. Anal. 18 (1998) 527.
[17] H. Ji, E. Wang, Analyst 113 (1988) 1541.
[18] W. Oungpipat, P. Southwellkeely, P.W. Alexander, Analyst 120 (1995) 1559.
[19] A.G. Kazemifard, D.E. Moore, J. Pharm. Biomed. Anal. 16 (1997) 689.
[20] N. Spataru, B.V. Sarada, E. Popa, D.A. Tryk, A. Fujishima, Anal. Chem. 73 (2001) 514.
[21] J. Xu, G.M. Swain, Anal. Chem. 70 (1998) 1502.
[22] M.D. Koppang, M. Witek, J. Blau, G.M. Swain, Anal. Chem. 71 (1999) 1188.
[23] B.V. Sarada, T.N. Rao, D.A. Tryk, A. Fujishima, Anal. Chem. 72 (2000) 1632.
[24] N. Wangfuengkanagul, O. Chailapakul, J. Pharm. Biomed. Anal. 28 (2002) 841.
[25] N. Wangfuengkanagul, O. Chailapakul, Talanta 58 (2002) 1213.
[26] T.N. Rao, B.V. Sarada, D.A. Tryk, A. Fujishima, J. Electroanal. Chem. 491 (2000) 175.
[27] M.C. Granger, J. Xu, J.W. Strojek, G.M. Swain, Anal. Chim. Acta 397 (1999) 145.
[28] T.A. Ivandini, B.V. Sarada, C. Terashima, T.N. Rao, D.A. Tryk, H. Ishiguro, Y. Kubota, A. Fujishima, J. Electroanal. Chem. 521 (2002) 117.

[29] T.N. Rao, B.H. Loo, B.V. Sarada, C. Terashima, A. Fujishima, Anal.Chem. 74 (2002) 1578.
[30] C. Terashima, T.N. Rao, B.V. Sarada, D.A. Tryk, A. Fujishima, Anal. Chem. 74 (2002) 895.
[31] E. Popa, Y. Kubota, D.A. Ttyk, A. Fujishima, Anal. Chem. 72 (2000) 1724.
[32] O. Chailapakul, W. Siangproh, B.V. Sarada, C. Terashima, T.N. Rao, D.A. Tyrk, A. Fujishima, Analyst 127 (2002) 1164.
[33] X. Ding, S. Mou, J. Chromtogr. A 897 (2000) 205.
[34] J.H. Knox, J. Jurand, J. Chromatogr. 186 (1979) 763.

Available online at www.sciencedirect.com
SCIENCE DIRECT®
Sensors and Actuators B 108 (2005) 627–632
SENSORS AND ACTUATORS B CHEMICAL
www.elsevier.com/locate/snb

Electroanalysis of lincomycin using boron-doped diamond thin film electrode applied to flow injection system

Kanokporn Boonsong, Suchada Chuanuwatanakul, Nattakarn Wangfuengkanagul, Orawon Chailapakul *

Department of Chemistry, Faculty of science, Chulalongkorn University, 254 Phyathai Road, Patumwan, Bangkok 10330, Thailand

Received 12 July 2004; received in revised form 20 December 2004; accepted 23 December 2004
Available online 9 February 2005

Abstract

The electroanalysis of lincomycin was investigated using boron-doped diamond thin film (BDD) electrodes. First, the electrochemistry of lincomycin was studied by cyclic voltammetry as a function of pH of the solution, scan rate and the concentration of lincomycin. Comparison experiments were carried out using glassy carbon electrode. Boron-doped diamond thin film electrode provided well-resolved oxidation irreversible cyclic voltammogram. It was found that the peak position was 1.2 V (versus Ag/AgCl reference electrode). Second, the amperometric detection with BDD electrode was coupled with the flow injection analysis for the determination of lincomycin. The linear range of 0.5–125 μM and the detection limit of 0.02 μM were obtained. The percent recovery was shown in a range of 96–103. This purposed method was also applied to a drug formulation sample. It was found that the results (293 mg mL^{-1}) were comparable to those labeled (300 mg mL^{-1}).

Keywords: Lincomycin; Boron-doped diamond thin film electrode; Cyclic voltammetry; Flow injection with amperometric detection

1. Introduction

Boron-doped diamond thin film electrode is very attractive for many potential applications due to its outstanding properties [1]. The number of researches in electroanalysis is progressively increasing every year. A great deal of properties are very low and stable voltammetric background current [2], wide potential window in aqueous electrolyte solutions (2.5–3 V) [3], slight adsorption of polar organic molecules, high resistance to deactivation and good activity toward some redox analytes without any conventional pretreatment [4].

Lincomycin is a medium spectrum antibiotic produced by *Streptomyces lincolnensis*. Lincomycin inhibits the growth mainly of Gram-positive bacteria. It is used in both human and veterinary medicine. Common impurities in lincomycin bulk drug are lincomycin B and 7-epilincomycin, which are formed during biosynthesis.

Several methods proposed for the determination of lincomycin, including microbiological assay methods [5], which have originally been used, are non-specific and less accurate. Alternative analytical methods were used for lincomycin including chemical assay, thin layer chromatography or paper chromatography, and isotachophoresis [6]. These methods also lack specificity and lincomycin cannot be differentiated from lincomycin B or 7-epilincomycin. Gas chromatographic technique has been introduced [7,8], it requires elaborate extraction and derivatization steps and is not selective for 7-epilincomycin. Liquid chromatography (LC) methods have also been described for quantitative determination of lincomycin [9,10]. One of the important limitations of LC techniques is the fact that lincomycin lacks sufficient UV absorption so a pre- or post-column derivation procedure is normally required. Therefore, these methods increase cost and complication of analysis. Electrochemical techniques are alternative methods for the lincomycin determination because they are simple, fast and low cost. The electrochemical detection of lincomycin has been reported using gold [11,12] as the working electrode. Nevertheless,

* Corresponding author. Tel.: +66 2218 7615; fax: +66 2254 1309.
E-mail address: corawon@chula.ac.th (O. Chailapakul).

0925-4005/$ – see front matter © 2005 Elsevier B.V. All rights reserved.
doi:10.1016/j.snb.2004.12.087

the severe detection conditions can damage the electrode and cause fluctuating background current and the electrode itself can be easily suffered from electrode fouling. Capillary zone electrophoresis with amperometric detection was recently described for the determination of lincomycin and lincomycin B in bulk drug and pharmaceutical formulations using copper disk [13] and copper microparticle-modified carbon fiber microarray electrodes [14]. Boron-doped diamond thin film electrodes can be used to eliminate these problems without any pretreatments because of the stable surface morphologies and the surface carbon atoms terminated by hydrogen. Thus, the BDD surface is relatively non-polar, very stable and suffers less adsorption of polar molecules, as reported by Xu et al. [4]. Because of these attractive properties, boron-doped diamond thin film was used to study several electroanalytical application [15–18].

Alternative automatic procedure based on flow injection technique has been widely suggested, since it enables reduced analysis time. Moreover, it can provide reproducible and accurate results. Flow injection with amperometric detection using a boron-doped diamond thin film electrode has been reported for the determination of some organic compounds such as histamine and serotonin [2], polyamine [19] and sulfa drugs [20].

In this propose, we report the use of the boron-doped diamond thin film electrode to study lincomycin using cyclic voltammetry compared with the glassy electrode. Hydrodynamic voltammetry and flow injection analysis with amperometric detection was also used to determine lincomycin in the standard chemical form and commercial available.

2. Experimental

2.1. Chemical and reagents

All chemicals were analytical grade and used without further purification. All solutions were prepared using deionized water. Phosphate buffers (pH 2.5–9), 0.1 M, were prepared from 0.1 M of potassium dihydrogen phosphate (Merck) and 0.1 M disodium hydrogen phosphate (BDH). Phosphate buffer (pH 2.5) was prepared from 0.1 M potassium dihydrogen phosphate and pH was adjusted with orthophosphoric acid (85%, Carlo Erba). Phosphate buffer (pH 9.0), 0.1 M, was prepared from 0.1 M of potassium dihydrogen phosphate and 0.1 M disodium hydrogen phosphate and the pH was adjusted with 0.1 M sodium hydroxide (Merck) solution.

The standard lincomycin hydrochloride (Fluka) solution was freshly prepared in 0.1 M phosphate buffer.

2.2. Electrode

The BDD electrode was grown on Si(1 0 0) substrate (obtained from Professor A. Fujishima) using microwave assisted chemical vaporization. It was rinsed with ultrapure water prior to use.

The glassy carbon (GC) electrode was purchased from Bioanalytical System, Inc. (area 0.07 cm^2). It was pretreated by sequential polishing with 1 and 0.05 μm of alumina/water slurries on felt pads, followed by rinsing with ultrapure water prior to use.

2.3. Cyclic voltammetry

Electrochemical measurements were recorded using an Autolab Potentiostat 100 (Metrohm, Switzerland) with a standard three-electrode configuration. The BDD electrode was pressed against a smooth ground joint at the bottom of the cell isolated by an O-ring (area 0.07 cm^2) and served as the working electrode. Ohmic contact was made by placing the backside of the Si substrate on a brass plate. A GC electrode was also used as a working electrode in the comparison study with the BDD electrode. A platinum wire and an Ag/AgCl electrode with a salt bridge were used as the counter and reference electrodes, respectively. Cyclic voltammetry was used to probe the electrochemical reaction. The electrochemical measurements were housed in a Faradaic cage to reduce electronic noise. All experiments were done at a room temperature.

2.4. Flow injection analysis with amperometric detection

The FIA system consisted of a thin layer flow cell (Bioanalytical System, Inc.), an injection port (Rheodyne 7725) with a 20 μL injection loop, a peristaltic pump (Ismatec), and an electrochemical detector (PG100). The carrier stream, 0.1 mol L^{-1} phosphate buffer (pH 7), was regulated by a reagent delivery module at a flow rate of 1 mL min^{-1}. A pulse dampener was used in series to reduce the pulsation introducing by the alternation of the roller of the peristaltic pump. The thin layer flow cell consisted of a silicone gasket as a spacer, Ag/AgCl as the reference electrode, stainless steel tube as an auxiliary electrode and outlet. The experiments were performed in a copper Faradaic cage to reduced electrical noise. A hydrodynamic voltammogram was obtained before the amperometric determination was performed. The peak current after each injection was recorded, together with the corresponding background current. These data were plotted as a function of applied potential to obtain hydrodynamic voltammograms. The amperometric measurements were carried out at the potential giving a maximum signal-to-background (S/B) ratio in the hydrodynamic voltammograms.

2.5. Sample preparation

A volume of 2 mL of real sample (LINCON injection) was transferred to a 100 ml volumetric flask and was diluted with 0.1 M of phosphate buffer pH 7. An aliquot of this initial solution was diluted again with appropriated volume of 0.1 M of phosphate buffer pH 7 to yield a final concentration of 6 μg mL^{-1}. In all cases it was assumed that the actual

content of the syrup corresponds to that reported by the manufacturing laboratories.

3. Results and discussion

3.1. Cyclic voltammetry

Fig. 1(a) and (b) shows typical cyclic voltammetric *i–E* curves for 0.1 M of lincomycin with the corresponding background voltammogram of 0.1 M phosphate buffer (pH 7) at BDD and GC electrodes. Both of the BDD and GC electrodes exhibited well-defined peak currents, however the BDD electrode gave well-resolved irreversible peak and higher current signal than the one obtained from using glassy carbon electrode at the same electrode area.

3.1.1. pH effect

The effect of the buffer pH was investigated from pH 2.5 to 9. At buffer between pH 7 and 9 changing of buffer pH effects the oxidation peak potential. It was found that increasing the buffer pH, decrease the oxidation peak potential, probably due to the more facile oxidation of the thiol group of lincomycin in the alkaline medium. In addition the buffer also affected the peak current of the cyclic voltammogram. At the BDD electrode, lincomycin provides the highest S/B in phosphate buffer at pH 7. Therefore, we used this pH for the next experiments.

3.1.2. Scan rate dependence study

Fig. 2 shows the cyclic voltammetric response of 1 mM lincomycin in 0.1 M phosphate buffer pH 7 with variation of the scan rate from 0.02 to 0.3 V s^{-1} at the BDD electrode. The oxidation current varies highly linearity ($r > 0.99$) with the square root of the scan rate, $\nu^{1/2}$, as shown in the inset of this figure. The results indicate that the electrochemical reaction is a diffusion controlled process.

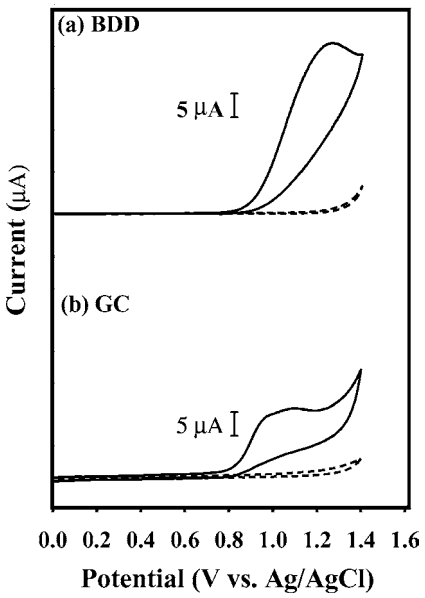

Fig. 1. Cyclic voltammograms for 1 mM lincomycin in 0.1 M phosphate buffer pH 7 (a) at boron-doped diamond thin film and (b) GC electrodes (solid line). Background voltammograms were also shown in this figure (dash line) (scan rate 50 mV s^{-1}).

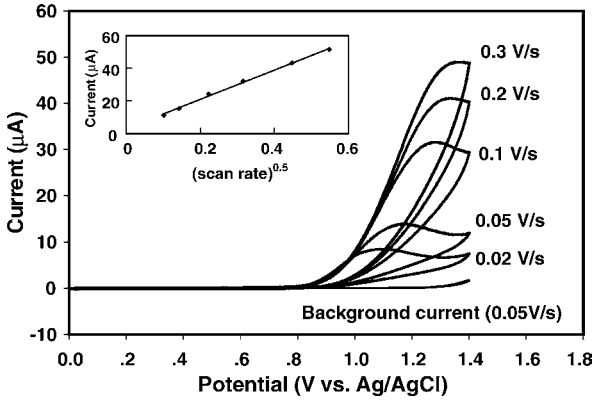

Fig. 2. Cyclic voltammogram for 1 mM lincomycin in 0.1 M phosphate buffer (pH 7) at BDD electrode for a series of sweep rates; area of electrode, 0.07 cm^2. The dependence between peak current (μA) and square root of sweep rate appears in the inset.

3.1.3. Concentration dependence study

The oxidation peak current was measured at the BDD electrode for the lincomycin concentration range from 0.01 to 10 mM in 0.1 M phosphate buffer (pH 7) at sweep rate 50 mV s^{-1}. Based on a series from 0.02 to 0.63 mM, a linear regression statistical analysis of peak current (μA) versus concentration (mM) was obtained, linearly proportional in the range 0.02–0.63 mM ($r > 0.99$, data shown in Fig. 3) The GC electrode provides no linear regression relationship between the oxidation current and the concentration. This may be due to the electrode fouling. At a concentration as low as 0.04 mM and above, a well defined peak with the S/B ratios > 3 was

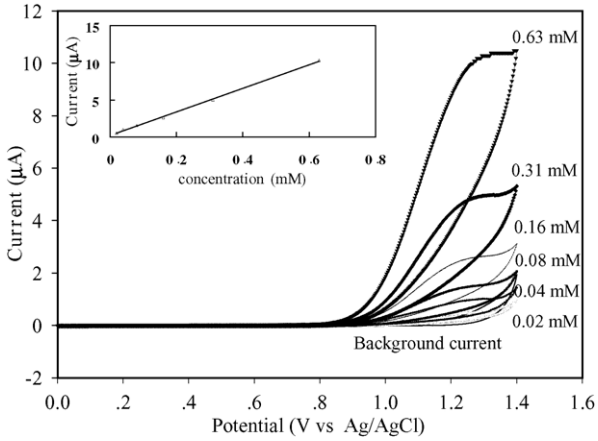

Fig. 3. Cyclic voltammogram for lincomycin in 0.1 M phosphate buffer (pH 7) at BDD electrode for a series of lincomycin concentrations. The sweep rate was 50 mV s^{-1}; area electrode, 0.07 cm^2. The dependence between peak current (μA) and concentration at the sweep rate of 50 mV s^{-1} appears in the inset.

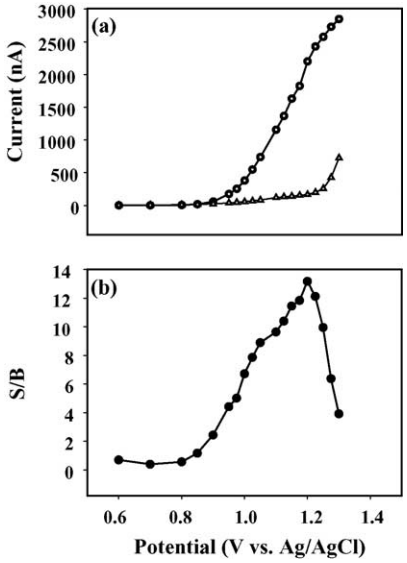

Fig. 4. (a) Hydrodynamic voltammogram of (-△-) 0.1 M phosphate buffer (pH 7, background current) and (-◯-) 0.1 mM of lincomycin in 0.1 M phosphate buffer (pH 7) with four injections of analysis, using 0.1 M phosphate buffer (pH 7) as a carrier solution. (b) Hydrodynamic of signal-to-background ratio. The flow rate was 1 ml min^{-1}.

obtained at the BDD electrode while the GC electrode provided this S/B value at the concentration of 0.5 mM due to its high background current.

3.2. Flow injection with amperometric detection

3.2.1. Hydrodynamic voltammetry

To obtain the optimal potential for amperometric detection in flow injection analysis, the hydrodynamic behavior of lincomycin was studied. Fig. 4 shows a hydrodynamic voltammetric *i–E* curve obtained at the BDD electrode for 20 μL injections of 0.1 mM lincomycin in 0.1 M phosphate buffer (pH 7) as the carrier solutions. Each datum represents the average of four injections. The absolute magnitude of the background current at each potential is also shown for comparison. The S/B ratios were calculated from the Fig. 4(a) at each potential to obtain the maximum potential point. Therefore, the hydrodynamic voltammetric S/B ratios versus potential curve are shown in Fig. 4(b) with the maximum S/B ratio at 1.2 V. Hence, this potential was set as the amperometric potential detection in flow injection analysis experiments. Therefore, this potential was selected for quantitative amperometric detection in flow injection analysis experiments.

3.2.2. Linear range, detection limit and reproducibility

Fig. 5 shows a series of repetitive 20 μL injection of lincomycin in 0.1 M phosphate buffer pH 7 at the detection potential of 1.2 V versus Ag/AgCl. Well-defined signals without peak tailing were obtained at all concentration from 10 nM to 2.5 mM. The current signal increased linearly with the increasing of concentration from 0.5 to 125 μM. The

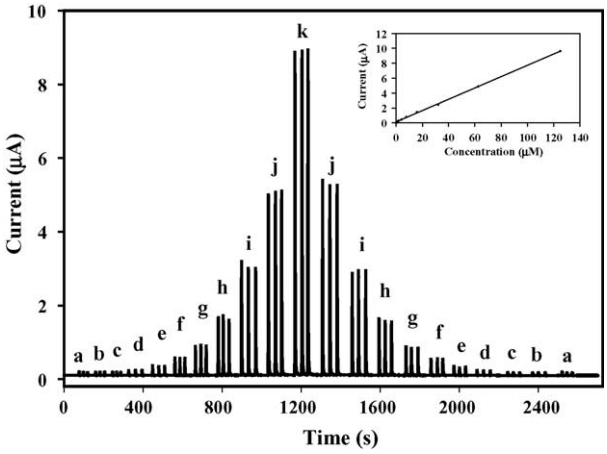

Fig. 5. Flow injection with amperometric detection results for various concentrations of lincomycin in 0.1 M phosphate buffer pH 7 (a) 0.25 μM, (b) 0.5 μM, (c) 1.0 μM, (d) 2.0 μM, (e) 4.0 μM, (f) 8.0 μM, (g) 16 μM, (h) 32 μM, (i) 62.5 μM, (j) 125 μM. Inset is the standard lincomycin calibration graph.

sensitivity of this method, which is the slope of the relation plot between the current and the concentration over the linear range, was 61.1–82.5 nA μM^{-1}. Interesting, the detection limit with S/N > 3 were obtained at the concentration as low as 20 nM of lincomycin. The reproducibility of the response was also examined. A peak variability of 2.04% was found during a course of 50 injections of 100 μM lincomycin, indicating the high stability of the BDD electrode.

3.3. Quantitative determination of lincomycin

Lincomycin in pharmaceuticals sample (LINCON injection) was determined using BDD electrode by the method of the calibration curve. The results were obtained were shown in Fig. 6. Linear least square calibration curve provided a slope of 95.4 nA μM^{-1} (sensitivity) and correlation coefficient of 0.9998. Accuracy and recovery were obtained from using real sample of lincomycin solution and standard addition method. Three concentrations of added solution (0, 1.25, 2.50 μg mL^{-1}) were chosen. Results obtain from 10 injections gave 1.2–2.0% of relative standard deviation (R.S.D.). The recoveries of the added lincomycin are summarized in Table 1. Relative error compared with the claimed amount was lower than 4%.

Table 1
Recovery of lincomycin sample with amperometric detection using diamond electrode applied to flow injection system ($n = 2$)

Amount of lincomycin sample added (mg mL^{-1})	Amount of lincomycin sample found (mg mL^{-1})	Percent of recovery (%)
1.25	1.21 ± 0.02	96.32 ± 2.4
2.50	2.58 ± 0.02	103.1 ± 3.3

Table 2
Comparison of electroanalytical data for determination of lincomycin

Method	Electrode	Linear dynamic range (μmol L^{-1})	Detection limit (μmol L^{-1})	Precision (%R.S.D.)	Ref.
Capillary electrophoresis	Carbon fiber microdisk array electrode	40–2000	6.7	5.9	[14]
Liquid chromatography with pulsed electrochemical detection	Gold electrode	0.3–1.9	–	1.1	[11]
Amperometry applied to flow injection analysis	Diamond thin film electrode	0.5–125	0.02	1.2	[a]

(–) No report.
[a] This proposed method.

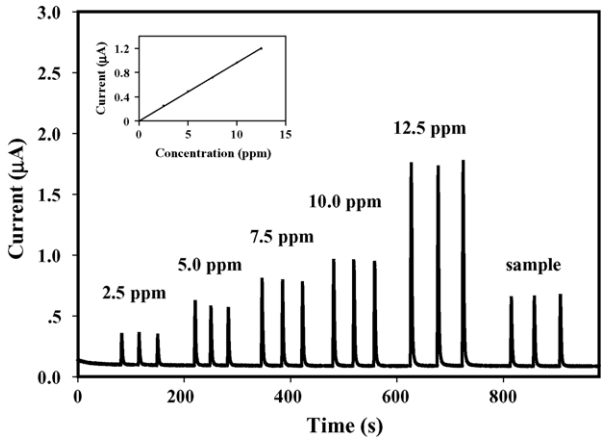

Fig. 6. Flow injection with amperometric detection results for lincomycin hydrochloride standard solution and lincomycin hydrochloride in commercially available solutions and calibration graph at the applied potential of 1.2 V vs. Ag/AgCl in 0.1 M phosphate buffer (pH 7).

3.4. Comparison with other methods

Table 2 summarizes the electroanalytical method for lincomycin from this study compared with other methods. It can be observed that using the BDD electrode with flow injection with amperometric detection provides a significant low detection limit (20 nM), high sensitivity and reproducible response without pretreatment or modification of the electrode, there is no fouling at the BDD electrode and the background current is also very low. Moreover the use of the BDD electrode applied to flow injection with amperometric detection is simple, rapid, and provides high sample throughput.

4. Conclusions

This is the first use of BDD thin film electrodes for the electroanalysis of lincomycin. It was found that the BDD electrodes exhibited excellent performance for the oxidative detection of lincomycin. Well-defined voltammograms were obtained at the BDD electrode, which exhibited high sensitivity, and demonstrated significant advantage over the GC electrode. The use of BDD electrode is simple because no chemical modification is required. Cleaning of the electrode is also not necessary due to the long-term stability of the BDD electrode response. Flow injection analysis with amperometric detection using BDD electrode provides a linear range from 0.25 to 125 μM and remarkably low detection limit (20 nM). The results indicate that lincomycin can be detected amperometrically without derivatization or use of a pulse waveform. BDD electrode is able to achieve a highly stable and sensitive response. Detection of lincomycin in commercially available solution forms shows that this method is precise, accurate, and very sensitive.

Acknowledgements

Acknowledgment is made to the Thailand Research Fund and the Ratchadaphisek Somphot Grant for the financial support.

References

[1] J. Xu, M.C. Granger, Q. Chen, J.W. Strojek, T.E. Lister, G.M. Swain, Boron-doped diamond thin-film electrode, Anal. Chem. 69 (1997) 591A–597A.
[2] B.V. Sarada, T.N. Rao, D.A. Tryk, A. Fujishima, Electrochemical oxidation of histamine and serotonin at highly boron-doped diamond electrodes, Anal. Chem. 72 (2000) 1632–1638.
[3] G.M. Swain, R. Ramesham, The electrochemical activity of boron-doped polycrystalline diamond thin-film electrodes, Anal. Chem. 65 (1993) 345–351.
[4] J. Xu, Q. Chen, G.M. Swain, Anthraquinonedisulfonate electrochemistry: a comparison of glassy carbon, hydrogenated glassy carbon, highly oriented pyrolytic graphite, and diamond electrodes, Anal. Chem. 70 (1998) 3146–3154.
[5] A.R. Barbiers, A.W. Neff, Screening and confirmatory methods for determining lincomycin residues in animal tissues, J. Assoc. Off. Anal. Chem. 59 (1976) 849–854.
[6] H. Klein, R. Teichmann, Isotachophoretic assay of aminoglycosides and lincomycins in pharmaceuticals, J. Chromatogr. 250 (1978) 152–156.
[7] W. Luo, B. Yin, C.Y.W. Ang, L. Rushing, H.C. Thompson Jr., Determination of lincomycin residues in salmon tissues by gas chromtography with nitrogen–phosphorus detection, J. Chromatogr. B 687 (1996) 405–411.
[8] M. Margosis, Analysis of antibiotics by gas chromatography: I. Lincomycin, J. Chromatogr. A 37 (1968) 46–54.
[9] J.A. Orwa, F. Bosmans, S. Depuydt, E. Roets, J. Hoogmartens, Liquid chromatographic method for separation of lincomycin from its related substances, J. Chromatogr. A 829 (1998) 161–166.
[10] P.A. Asmus, J.B. Landis, C.L. Vila, Liquid chromatographic determination of lincomycin in fermentation beers, J. Chromatogr. A 264 (1983) 241–248.

[11] J. Szunyog, E. Adams, K. Liekens, E. Roets, J. Hoogmartens, Analysis of a formulation containing lincomycin and spectinomycin by liquid chromatography with pulsed electrochemical detection, J. Pharm. Biomed. Anal. 29 (2002) 213–220.
[12] W.R. LaCourse, C.O. Dasenbrock, Pulsed electrochemical detection of sulfur- containing antibiotics following high performance liquid chromatography, J. Pharm. Biomed. Anal. 19 (1999) 239–252.
[13] F. Xiaoming, L. Xialfeng, Y. Jiannong, F. Yuzhi, Determination of lincomycin and lincomycin B in bulk drug and pharmaceutical formulations by capillary zone electrophoresis with amperometric detection, Anal. Lett. 29 (1996) 1975–1984.
[14] W.C. Yang, A.M. Yu, H.Y. Chen, Applications of a copper microparticle-modified carbon fiber microdisk array electrode for the simultaneous determination of aminoglycoside antibiotics by capillary electrophoresis, J. Chromatogr. A 905 (2001) 309–318.
[15] O. Chailapakul, E. Popa, H. Tai, B.V. Sarada, D.A. Tryk, A. Fujishima, The electrooxidation of organic acids at boron-doped diamond electrodes, Electrochem. Commun. 2 (2000) 422–426.
[16] O. Chailapakul, P. Aksaharanandana, T. Frelink, Y. Einaga, A. Fujishima, The electrooxidation of sulfur-containing compounds at boron-doped diamond electrode, Sens. Actuat. B 80 (2001) 193–201.
[17] T.N. Rao, I. Yagi, T. Miwa, D.A. Tryk, A. Fujishima, Electrochemical oxidation of NADH at highly boron-doped diamond electrodes, Anal. Chem. 71 (1999) 2506–2511.
[18] T. Yano, D.A. Tryk, K. Hashimoto, A. Fujishima, Electrochemical behavior of highly conductive boron-doped diamond electrodes for oxygen reduction in alkaline solution, J. Electrochem. Soc. 145 (1998) 1870–1876.
[19] M.D. Koppang, M. Witek, J. Blau, G.M. Swain, Electrochemical oxidation of polyamines at diamond thin-film electrodes, Anal. Chem. 71 (1999) 1188–1195.
[20] T.N. Rao, B.V. Sarada, D.A. Tryk, A. Fujishima, Electroanalytical study of sulfa drugs at diamond electrodes and their determination by HPLC with amperometric detection, J. Electroanal. Chem. 491 (2000) 175–181.

Biographies

Kanokporn Boonsong received her BSc in Analytical Chemistry from Rajamangala Institute of Technology in 1999. She has been a Lecturer at Rajamangala Institute of Technology since 1999. Now, she is a doctoral course student of the Department of Chemistry, Chulalongkorn University.

Suchada Chuanuwatanakul received her BSc and MSc degrees in Analytical Chemistry from Chulalongkorn University, Thailand, in 1978 and 1981, respectively. She is currently an Assistant Professor at the Department of Chemistry, Faculty of Science, Chulalongkorn University, Thailand. Her research activity is focused on diamond sensors and food chemistry.

Nattakarn Wangfuengkanagul received her BSc in industrial chemistry in 1999 from King Mongkut ‘s Institute of Technology Ladkrabang and MSc in 2002 from Chulalongkorn University. Presently, she has received the Royal Golden Jubilee scholarship from Thailand Research Fund for her PhD in Analytical Chemistry at Chulalongkorn University since 2002.

Orawon Chailapakul is an Associate Professor at Department of Chemistry, Faculty of Science, Chulalongkorn University. She received her BSc in Chemistry from Mahidol University in 1982, MSc from Chulalongkorn University in 1987, and PhD from The University of New Mexico in 1994. Her research interest includes development of biosensors and diamond sensors. She is now the member of Materials Chemistry and Catalysis Research Unit and Sensor Research Unit.

Available online at www.sciencedirect.com
SCIENCE DIRECT
Talanta 68 (2006) 1329–1335
Talanta
www.elsevier.com/locate/talanta

Use of nickel implanted boron-doped diamond thin film electrode coupled to HPLC system for the determination of tetracyclines☆

Surudee Treetepvijit[a], Anchana Preechaworapun[a], Narong Praphairaksit[a], Suchada Chuanuwatanakul[a], Yasuaki Einaga[b], Orawon Chailapakul[a,*]

[a] *Materials Chemistry and Catalysis Research Unit, Department of Chemistry, Faculty of Science, Chulalongkorn University, Patumwan, Bangkok 10330, Thailand*
[b] *Department of Chemistry, Faculty of Science and Technology, Keio University, 3-14-1 Hiyoshi, Yokohama, Kanagawa 223-8522, Japan*

Received 24 May 2005; received in revised form 24 July 2005; accepted 24 July 2005
Available online 25 August 2005

Abstract

The electrochemical analysis of tetracyclines was investigated using nickel-implanted boron-doped diamond thin film electrode (Ni-DIA) by cyclic voltammetry and high performance liquid chromatographic with amperometry. Cyclic voltammetry was used to study the electrochemical oxidation of tetracyclines. Comparison experiments were carried out utilizing as-deposited BDD and glassy carbon electrodes. Ni-DIA electrode provided well-resolved oxidative irreversible cyclic voltammograms and the highest current signals among the electrode studied. High performance liquid chromatography (HPLC) with amperometric detection was also studied. The chromatography was performed using a commercially available Inertsil C18 column, with the mobile phase being: 80% phosphate buffer (pH 2.5)–20% acetonitrile and detected at 1.55 V. The methods were validated over the concentration range 0.05–100 ppm with the overall average recoveries from 83.3 to 102.5% and R.S.D. of less than 10%. The proposed method was further applied to analyse shrimp samples.

Keywords: Tetracyclines; Nickel-implanted boron-doped diamond; Cyclic voltammetry; Flow injection system; HPLC; Amperometric detection

1. Introduction

Conductive boron-doped diamond electrodes (BDD) have attracted tremendous interest for various electrochemical applications, including electroanalysis [1], electrosynthesis [2] and electrochemical treatment of wastewater [3]. BDD electrodes have recently attracted a great deal of attention due to their superior properties, which are significantly different from those of other conventional electrodes, e.g. glassy carbon or platinum electrode materials [4,5]. The growing popularity of this boron-doped diamond electrode in analytical applications over its conventional counterparts lies mainly on its various attractive features, such as very low and stable voltammetric background currents, wide working potential window in aqueous solutions, high resistance to deactivation via fouling, insensitivity to dissolved oxygen and long-term response stability [6–8].

While some metals, such as platinum is known to oxidize hydrogen peroxide and methanol, as well as nickel is conventionally used for carbohydrates electrochemical detection in alkali solution [9–11]. BDD electrode is found completely inactive for those kinds of catalytic reactions. However, it has been reported that the dispersion of metallic particles within an organic polymer or an inert surface resulted in drastic increase of the catalytic activity and sensitivity of the electrode because the dispersed particles behave like microelectrode arrays [10]. The chemically modified electrodes (CMEs) which are capable of lowering the operational potential required to oxidize scarcely electroactive organic compounds has caught a great deal of interest. Reduced electrode fouling has also been reported. CMEs based on the modification of glassy carbon or graphite rods with various metals (e.g.

☆ Presented at the 13th International Conference on Flow Injection Analysis, April 24–29, 2005, Las Vegas, Nevada, and erroneously omitted from Talanta 62(2) 2005.

* Corresponding author. Tel.: +662 2187615; fax: +662 2541309.
E-mail address: corawon@chula.ac.th (O. Chailapakul).

0039-9140/$ – see front matter © 2005 Elsevier B.V. All rights reserved.
doi:10.1016/j.talanta.2005.07.047

copper [12–14], cobalt [15], and nickel [10,11,16–18]) have shown catalytic activities towards polyhydroxy compounds. These electrodes have been successfully applied to detect carbohydrate [10–12,15,16], amino acids [16,18], sugars [13] and aliphatic alcohol compounds [17] using amperometric detection. Unfortunately, glassy carbon electrode has a major drawback of yielding high background current. These metal-modified diamond electrodes appear to be well suited to overcome such problems. BDD film would be the best choice for the deposition of metal electrocatalysts.

The preparation of some metal-modified BDD electrodes for electrochemical analysis by using chemical precipitation and electrochemical deposition method had been reported [9].

Ion implantation into a material can be used to form near surface composites. The method is used to modify the structure of a target-near-surface by bombardment with heavy ions. This method is popular for the preparation of doping semiconductors, such as silicon and gallium arsenide, so it has been of particular interest for the fabrication of ion-implanted diamond. At present, some applications for electrochemical use by metal-implanted conductive BDD electrodes have been reported [19]. Therefore, we are interested in developing a method for the determination of tetracyclines by using the Ni-implanted diamond electrode.

Many antibiotics are widely used in veterinary for preventing and treating diseases as well as for promoting growth in food producing animals. These antibiotics are, for example, aminoglycosides, β-lactams, chloramphenicol, tetracyclines, macrolides, sulphonamides, quinolines, and nitrofurans. Tetracycline is one of the most important antibiotics utilizing in the industry and thus it is of particular interested. Tetracycline is a broad-spectrum antibiotic, such as tetracycline (TC), chlortetracycline (CTC), doxycycline (DC) and oxytetracycline (OTC). These compounds are commonly used in human pathologies as well as in veterinary medicine, animal nutrition and feed additives for cattle growth. It is used to treat many different infections, such as respiratory tract infections, urethritis and severe acne. It also plays a major role in the treatment of multidrug resistant malaria. Adverse effects in these subtances include gastrointestinal disturbances, renal dysfunction, hepatotoxicity, raised intracranial pressure and skin infections, such as rosacea and perioral dermatitis. Tetracyclines are widely used in diary cattle, poultry and shrimp.

The percentage of total worldwide shrimp consumption produced by farming increased from less than 2% in 1980 to more than 26% in 1989 [20]. In recognition of the steadily increasing amount of shrimp produced by aquaculture (rising from∼100 million lbs worldwide in 1979 to 1600 million lbs in 1999), oxytetracycline (OTC) is widely known to be one of the most common antibiotics used in shrimp aquaculture, particularly in countries other than the US. Therefore, shrimps were chosen as the test subject in this study.

Numerous methods have been reported for the determination of tetracyclines in various samples, such as milk [21], shrimp [22], animal feed [23,24], animal tissues [25,26] and pharmaceutical formulations [27,28] based on thin-layer chromatography, capillary electrophoresis [29], and high performance liquid chromatography (HPLC). HPLC is a common method that separates tetracyclines in the reverse-phase mode with a variety of detection methods, such as spectrophotometry [25,26], fluorometry [30,31], mass spectrometry [32,33] and electrochemistry [27,28].

Among these, the electrochemical method is distinctly attractive owing to its simplicity, no need for derivatization, fast analysis, low cost and high sensitivity. There are several reports utilizing polarography, potentiometry [34] and amperometry [27,28,35] for the analysis of tetracycline. In 2005, Charoenraks et al. reported the use of high performance liquid chromatography with pulsed amperometric detection at anodized boron-doped diamond thin film electrode for the detection of tetracyclines.

In this present work, we report the use of Ni-implanted boron-doped diamond thin film electrodes (Ni-DIA) to study the electrochemical oxidation of tetracyclines using cyclic voltammetry. Focus is placed on comparing the results with as-deposited BDD and glassy carbon electrodes. In addition, the performance of the Ni-DIA electrode for the detection of tetracycline was examined by HPLC with amperometric detection for determination of tetracyclines in shrimp.

2. Experimental

2.1. Chemicals and reagents

Tetracycline-HCl (TC), oxytetracycline-HCl (OTC), chlorteteacycline-HCl (CTC), and doxycycline-HCl (DTC) were available from Sigma–Aldrich. Acetonitrile and methanol (Merck) were of HPLC grade. Disodium hydrogenphosphate (BDH), citric acid monohydrate (J.T. Baker), ethylenediaminetetraacetic acid disodium salt dehydrate (Fluka), and phosphoric acid (Merck) were of analytical grade. Distilled water was purified in a Milli-Q system (Millipore, Bedford, MA, USA). Soild-phase extraction (SPE) C-18E cartridges (500 mg, 6 mL) were obtained from Phenomenex (USA).

Phosphate buffer solution of pH 2.5 were prepared from 0.01 M H_3PO_4 and adjusted to 2.5 by adding drop-wise 0.1 M Na_2HPO_4. The mobile phase for the HPLC condition consisted of 20% acetonitrile in 0.01 M phosphate buffer (pH 2.5).

Na_2EDTA–McIlvaine buffer solution (pH 4) was prepared by dissolving 15 g of disodium hydrogen phosphate dihydrate, 13 g of citric acid monohydrate and 3.72 g of EDTA in water and diluting to 1 L.

Stock standard solutions of tetracycline, oxytetracycline, chlortetracycline, and doxycycline were prepared by dissolving 10 mg of each compound in 10 mL of mobile phase to obtain a final concentration of 1000 μg/mL. Working standard solutions were prepared by diluting the stock solution

with the mobile phase. All of the solutions were protected from exposure to light and stored in a refrigerator.

2.2. Sample preparation procedure

Sea and farming shrimp were purchased locally. The shells and tails of shrimp were removed and ground in a conventional meat grinder. The homogenate was degassed overnight and kept in frozen until use. A 2.50 g shrimp samples were placed in 15 mL capped centrifuge tubes, 12.5 mL of Na_2EDTA–McIlvaine buffer (pH 4) was added to each tube portion and blended for 30 s with a homogenizer. The resulting homogenates were shaken for 10 min on a flatbed shaker at high speed. The tube was removed from the shaker and centrifuged for 30 min at 3500 radian per second. The supernatant was loaded into a SPE cartridge, previously activated with 10 mL of methanol and 10 mL of Milli-Q water. After sample loading, the SPE cartridge was washed with 10 mL of Milli-Q water, and finally tetracyclines were eluted by 10 mL of methanol. The solvent was removed under room temperature. The residues were filtered with a 0.45 μm PTFE filter. The solutions were analysed by HPLC.

2.3. Electrode

Highly boron-doped diamond electrode was deposited on Si (100) wafers in microwave plasma-assisted chemical vapor deposition (MPCVD) system (ASTeX Corp., Woburn, MA). A mixture of acetone and methanol in the ratio of 9:1 (v/v) was used as the carbon source. B_2O_3, used as the boron source, was dissolved in the acetone–methanol solution at B/C atomic ratio of 1:100. These films were implanted with 750 keV Ni^{2+} with a dose of 5×10^{14} cm^{-2} (Tandetron 4117-HC, HVEE). Annealing process was performed at 850 °C for 10 min in an H_2 ambient (80 Torr). It was reported that surface morphology and color change after implantation were not observed, a SEM image of the BDD surface after implantation showed the presence of small holes [19]. The presence of metal particles could not be seen, because the particle size is very small as well as the metal position is deeply inside the holes due to the high energy of the bombardment in implantation process.

The nickel-implanted boron-doped diamond electrodes have been prepared in Associate Professor Yasuaki Einaga's laboratory. The Ni-DIA electrodes were rinsed with ultrapure water prior to use.

2.4. Voltammetry

Electrochemical measurements were recorded using an Autolab Potentiostat 30 (Metrohm, Switzerland) with a standard three-electrode configuration. The planar working Ni-DIA or BDD electrode was pressed against a smooth ground joint at the bottom of the cell, isolated by an o-ring (area 0.07 cm^2). Placing the backside of the Si substrate on a brass plate made ohmic contact. For comparison, the as-deposited BDD electrode was used. A platinum wire was used as the auxiliary electrode and Ag/AgCl in KCl (sat'd) was used as the reference. Cyclic voltammetry was used to study the electrochemical reaction. The electrochemical measurements were housed in a Faradaic cage to reduce electronic noise. All experiments were performed at room temperature.

2.5. LC system and conditions

The LC system consisted of a thin layer flow cell (GL Science), an injection port (Rheodyne No. 7125) with a 20 μL injection loop and a pump (Water Model 510 solvent delivery system, Waters Associates Inc., Milford, MA, USA). The column was ODS-3 Inertsil C18, 5 μM 4.6 mm × 250 mm i.d. (GL Science Inc.). The electrochemical detector was applied using a computer controlled potentiostat (Autolab PGSTAT 30, Metrohm, Switzerland). Separations were carried out under isocratic conditions using a mobile phase of 0.01 M phosphate buffer (pH 2.5)–acetonitrile (80:20, v/v). The flow rate was 1 mL/min. The thin layer flow cell consisted of a silicone gasket as a spacer, the Ag/AgCl in 3 M in NaCl as the reference electrode, and a stainless steel tube as the auxiliary electrode and outlet. The experiments were performed in a copper faradaic cage to reduce electrical noise.

3. Results and discussion

3.1. Cyclic voltammetry

Fig. 1(a–d) shows the cyclic voltammograms obtained for 1 mM tetracycline hydrochloride, 1 mM chlortetracycline, 1 mM doxycycline and 1 mM oxytetracycline + 0.1 M phosphate buffer (pH 2) at Ni-DIA electrode, as-deposited diamond electrode and glassy carbon electrode. The corresponding backgrounds are also shown. A well-defined irreversible cyclic voltammograms were obtained at the Ni-DIA electrode and diamond electrode while an ill-defined irreversible cyclic voltammograms was obtained at the glassy carbon electrode for all analytes. The electrochemical data obtained from cyclic voltammograms of these solutions at the mentioned electrodes is shown in Table 1. It was found that the Ni-DIA electrode provided the highest S/B ratios for tetracycline, chlortetracycline, doxycycline and oxytetracycline among the three electrodes studied. We have also carried out the experiments using pure nickel electrode for the comparison with the Ni-DIA electrode. It was found that no any response obtained for the determination of tetracycline antibiotics when using pure nickel electrode.

3.2. Liquid chromatography with amperometric detection

In general, because tetracyclines are analyzed by reversed phase HPLC, the seperation in this experiment was then per-

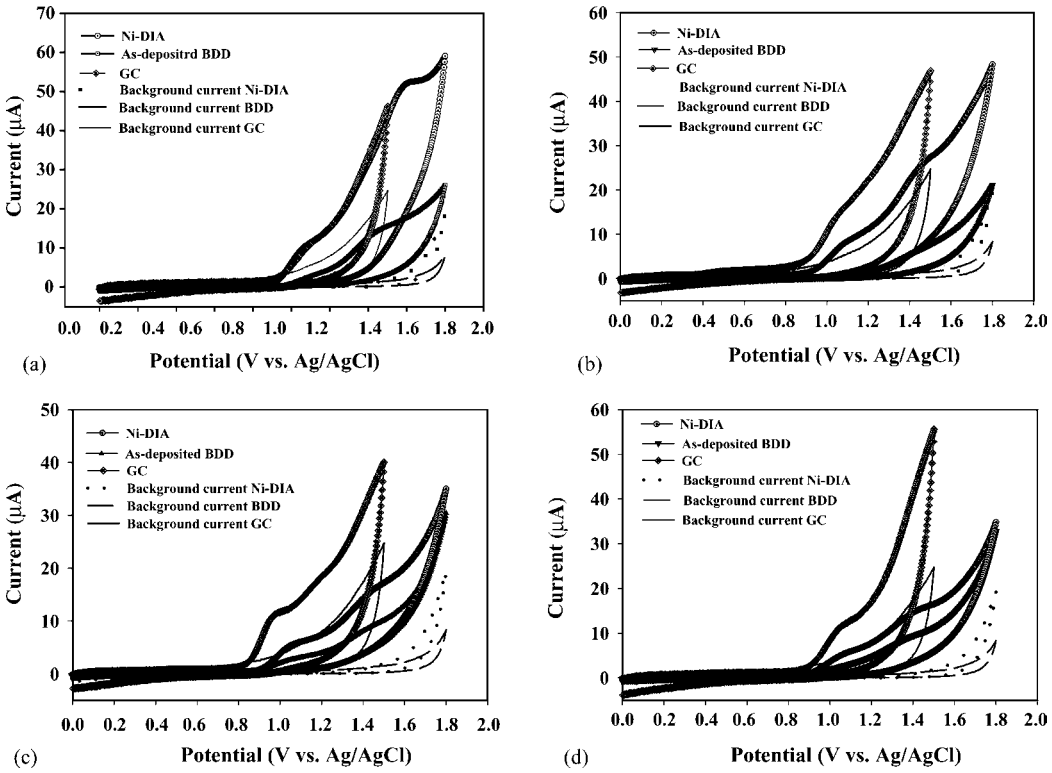

Fig. 1. Cyclic voltammograms for (a) tetracycline, (b) oxytetracycline, (c) chlortetracycline, and (d) doxycycline in 0.1 M phosphate buffer (pH 2) at Ni-DIA, as-deposited diamond and glassy carbon electrodes. The scan rate was 50 mVs^{-1}. Background voltammogram (0.1 M phosphate buffer, pH 2) is also shown in this figure.

formed using a C-18 column. The pH of the mobile phase was selected to be 2.5 so as to reduce the formation of isometric analogues. This pH also gave a well-defined and high signal of cyclic voltammograms of tetracycline oxidation. In this experiment, the phosphate buffer was chosen because it provided low background currents. No reaction between buffer and tetracyclines was observed over the potential range of interest. Therefore, phosphate buffer (0.01 M, pH 2.5) was used to separate tetracyclines, and significantly prolonged the retention time in the presence of 20% acetonitrile. The chromatograms of a standard solution of tetracyclines are presented in Fig. 2. The orders of elution were oxytetracycline,

Table 1
The electrochemical data of 1 mM tetracycline, 1 mM chlortetracycline, 1 mM doxycycline and 1 mM oxytetracycline at Ni-DIA electrode, as-deposited diamond electrode and glassy carbon electrode

Analytes	Electrode	E_p^{oxa}(V)	I_p^{oxb}(μA)	S/B^c
Tetracycline	Ni-DIA	1.501	20.90	12.06
	BDD	1.501	17.00	11.56
	GC	1.178	7.10	1.42
Chlortetracycline	Ni-DIA	1.501	17.30	9.61
	BDD	1.438	9.00	6.12
	GC	0.975	7.80	1.56
Doxycycline	Ni-DIA	1.501	16.60	9.22
	BDD	1.477	10.60	7.21
	GC	1.059	7.00	1.40
Oxytetracycline	Ni-DIA	1.511	27.90	15.50
	BDD	1.506	7.80	5.31
	GC	1.064	9.90	1.98

[a] Oxidation peak potential.
[b] Oxidation peak current.
[c] calculated from I_p^{ox}/background current.

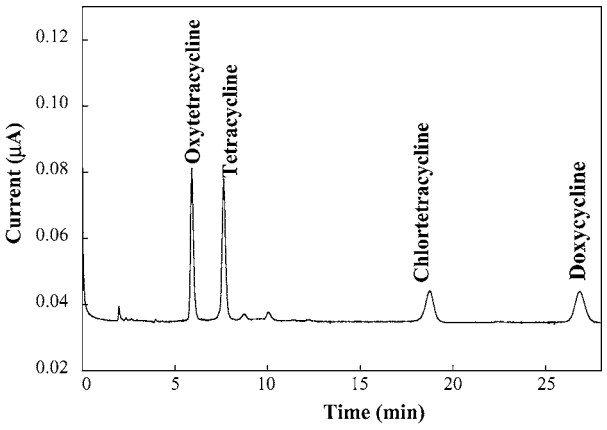

Fig. 2. Chromatogram of 1 ppm a standard mixture seperated on ODS Inertsil C18 column (5 μM 4.6 × 250 mm i.d.) using a mobile phase of phosphate buffer (0.01 M, pH 2.5)–acetonitrile (80:20). The injection volume was 20 μL, and the flow rate was 1 mL/min.

Table 2
Calibration characteristics of oxyteracycline, tetracycline, chlortetracycline and doxycycline for the proposed method at the Ni-DIA electrode

Analytes	Linear dynamic range ($\mu g\,mL^{-1}$)	Slope (peak areas units/mg/kg)	Intercept (μA)	R^2	Limit of detection ($\mu g\,mL^{-1}$)
Oxytetracycline	0.05–100	0.0473	0.0562	0.9975	0.01
Tetracycline	0.05–100	0.0395	0.0453	0.9977	0.01
Chlortetracycline	0.1–100	0.0110	0.0045	0.9990	0.05
Doxycycline	0.1–100	0.0111	0.0066	0.9996	0.05

Table 3
Recoveries of tetracyclines in shrimp farming samples using the HPLC with amperometry method at the Ni-implanted electrode ($n = 3$)

Analyte	Mean of %recovery ($x \pm$ S.D.)			
	Spiking level of 0.5 mg kg^{-1}	Spiking level of 1 mg kg^{-1}	Spiking level of 5 mg kg^{-1}	Spiking level of 10 mg kg^{-1}
Oxytetracycline	84.8 ± 3.0	96.8 ± 2.7	102.5 ± 3.4	99.6 ± 1.8
Tetracycline	93.3 ± 5.5	85.9 ± 7.7	96.6 ± 2.4	97.0 ± 5.5
Chlortetracycline	91.48 ± 5.3	94.8 ± 5.9	91.6 ± 5.2	97.9 ± 3.8
Doxycycline	89.2 ± 6.7	88.4 ± 3.0	97.7 ± 5.4	103.7 ± 7.4

Table 4
Recoveries of tetracyclines in shrimp sea samples using the HPLC with amperometry method at the Ni-DIA electrode ($n = 3$)

Analyte	Mean of %recovery ($x \pm$ SD)			
	Spiking level of 0.5 mg/kg	Spiking level of 1 mg/kg	Spiking level of 5 mg/kg	Spiking level of 10 mg/kg
Oxytetracycline	94.9 ± 1.6	83.3 ± 4.3	86.8 ± 5.0	96.5 ± 2.4
Tetracycline	92.0 ± 1.1	88.4 ± 4.4	89.2 ± 1.2	96.9 ± 4.6
Chlortetracycline	91.8 ± 8.6	91.9 ± 3.0	86.0 ± 8.0	93.3 ± 5.1
Doxycycline	102.0 ± 9.0	96.2 ± 1.7	90.6 ± 0.1	99.4 ± 2.4

tetracycline, chlortetracycline and doxycycline, respectively. To complete the separation of tetracyclines, approximately 27 min are required.

3.3. Optimum potential for HPLC

Fig. 3 depicts the optimum potential *i–E* curve obtained at the Ni-DIA electrode for a 20 μl injection of 100 μM of tetracyclines mixture standard solution. 0.01 M of phosphate buffer (pH 2.5) was used as the carrier solution. Each datum represents an average of two injections. The magnitude of the background current at each potential is also shown for comparison. The optimum potential of tetracyclines mixture standard solution at the Ni-DIA electrode exhibited a well-defined sigmodal shape with a half peak potential at about 1.55 V versus Ag/AgCl. Therefore, this potential was fixed for the amperometric potential detection in HPLC system analysis experiments.

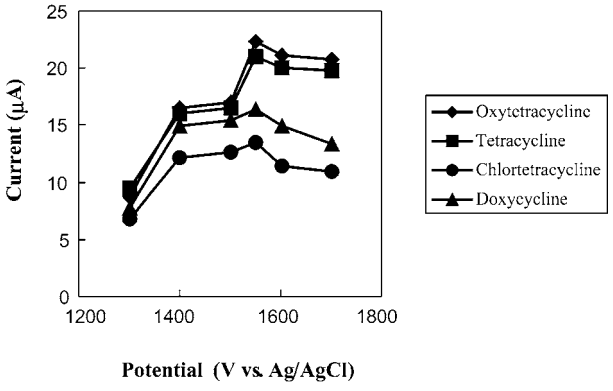

Fig. 3. Optimum potential of 10 ppm of tetracyclines in 0.01 M phosphate buffer (pH 2.5). 0.1 M phosphate buffer (pH 2.5) was used as a carrier solution, flow rate 1 ml min^{-1}.

3.4. Linearity and detection limit

The tetracycline mixture standard solutions covering the concentration range of 0.01–100 $\mu g\,mL^{-1}$ were analyzed and their peak areas were plotted versus concentration. The calibration characteristics of oxytetracycline, tetracycline, chlortetracycline and doxycycline at the Ni-DIA electrode are given in Table 2.

3.5. Recoveries

The average recoveries of tetracyclines from shrimp farming and shrimp sea sample at four different spiking levels (0.5, 1, 5 and 10 μg/mL each compound) are summarized in Tables 3 and 4. It can be observed from the chromatogram

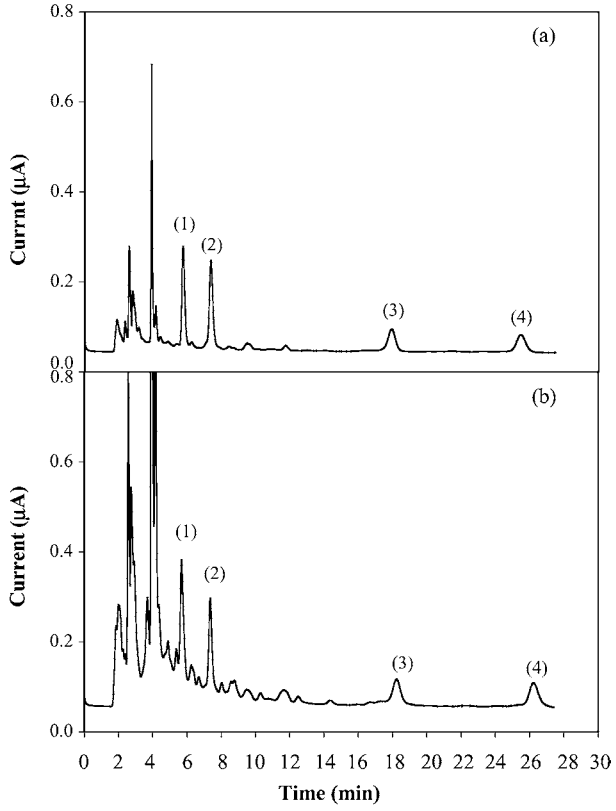

Fig. 4. HPLC chromatograms of (a) shrimp farming sample and (b) shrimp sea sample spiking with 5 μg/mL each of (1) oxytetracycline, (2) tetracycline, (3) chlortetracycline, and (4) doxycycline at the Ni-implanted diamond electrode. The other conditions are the same as in Fig. 2.

(Fig. 4) that the peaks due to the other components did not interfere with those of tetracyclines.

4. Conclusions

This is the first use of Ni-DIA electrodes for the electroanalysis of tetracyclines. It was found that Ni-DIA electrodes exhibited excellent performance for the oxidative detection of tetracycline. Well-defined voltammograms were obtained at the Ni-DIA electrode, which exhibited high sensitivity and demonstrated significant advantages over the BDD and glassy carbon electrode. The outstanding capabilities of the Ni-DIA electrode were demonstrated by coupling with HPLC. HPLC with amperometry at Ni-DIA electrode has been successfully applied to determine four types of tetracyclines (oxytetracycline, tetracycline, chlortetracycline and doxycycline) in shrimp samples. Experimental detection limit of 0.01–0.05 μg/mL were obtained for four tetracyclines studied. A linear dynamic range from 0.05 to 100 μg/mL was achieved. Application of the proposed method for the determination of tetracycline in shrimp sample shows that this method is precise, accurate and very sensitive.

Acknowledgements

The authors would like to thank The Thailand Research Fund, Ratchadaphisek Somphot Grant and Chulalongkorn University. Special thanks are extended to Associate Professor Yasuki Einaga (Keio University) for providing the Ni-DIA electrodes used in this research

References

[1] M.C. Granger, G.M. Swain, J. Electrochem. Soc. 146 (1999) 12.
[2] F. Okino, H. Shibata, S. Kawasaki, Electrochem. Solid-State Lett. 2 (1999) 382.
[3] M. Fryda, D. Herrmann, L. Schater, et al., New Diamond Frontier Carbon Technol. 9 (1999) 229.
[4] D. Sopchak, B. Miller, Y. Avyigal, R. Kalish, J. Electroanal. Chem. 538–539 (2002) 39.
[5] T.A. Ivandini, B.V. Sarada, C. Terashima, T.N. Rao, D.A. Tryk, H. Ishiguro, Y. Kubota, A. Fujishima, J. Chromatogr. B 791 (2003) 63.
[6] O. Chailapakul, P. Aksharanandana, T. Frelink, Y. Einaga, A. Fujishima, Sens. Actuators B 80 (2001) 193.
[7] N. Wangfuengkanagul, O. Chailapakul, J. Pharm. Biomed. Anal. 28 (2002) 841.
[8] M.C. Granger, J. Xu, J.W. Strojek, G.M. Swain, Anal. Chim. Acta 397 (1999) 145.
[9] F. Montilla, E. Morallon, I. Duo, C. Comninellis, J.L. Vasquez, Electrochim. Acta 48 (2003) 3891.
[10] I.G. Casella, E. Desimoni, T.R.I. Cataldi, Anal. Chim. Acta 248 (1991) 117.
[11] I.G. Casella, E. Desimoni, A.M. Salvi, Anal. Chim. Acta 243 (1991) 61.
[12] S.V. Prabhu, R.P. Baldwin, Anal. Chem. 61 (1989) 852.
[13] S.V. Prabhu, R.P. Baldwin, Anal. Chem. 61 (1989) 2258.
[14] P. Luo, S.V. Prabhu, R.P. Baldwin, Anal. Chem. 62 (1990) 752.
[15] T.R.I. Cataldi, I.G. Casella, E. Desimoni, T. Rotunno, Anal. Chim. Acta 270 (1992) 161.
[16] E. Wang, A. Liu, J. Electroanal. Chem. 319 (1991) 217.
[17] I.G. Casella, T.R.I. Cataldi, A.M. Salvi, E. Desimoni, Anal. Chem. 65 (1993) 3143.
[18] A. Liu, E. Wang, Anal. Chim. Acta 280 (1993) 223.
[19] T.A. Ivandini, R. Sato, Y. Makide, A. Fujishima, Y. Einaga, Diamond Relat. Mater. 13 (2004) 2003.
[20] A.W. Fast, Marine Shrimp Aquaculture: Principles and Practices, Elsevier, New York, 1992.
[21] F.J. Schenck, P.S. Callery, J. Chromatogr. A 812 (1998) 99.
[22] M.C. Carson, M.A. Ngoh, S.W. Hadley, J. Chromatogr. B 712 (1998) 113.
[23] A.D. Cooper, G.W.F. Stubbings, M. Kelly, J.A. Tarbin, W.H.H. Farrington, G. Shearer, J. Chromatogr. A 812 (1998) 321.
[24] W. Naidong, S. Hua, E. Roets, J. Hoogmartens, J. Pharm. Biomed. Anal. 33 (2003) 85.
[25] J. Sokol, E. Matisova, J. Chromatogr. A 669 (1994) 75.
[26] J.R. Walsh, L.V. Walker, J.J. Webber, J. Chromatogr. A 596 (1992) 211.
[27] A.G. Kazemifard, D.E. Moore, J. Pharm. Biomed. Anal. 16 (1997) 689.
[28] S. Palaharn, T. Charoenraks, N. Wangfuengkanagul, K. Grudpan, O. Chailapakul, Anal. Chim. Acta 499 (2003) 191.
[29] J. Tjornelund, S.H. Hansen, J. Chromatogr. A 779 (1997) 235.
[30] S. Croubels, W. Baeyens, C.V. Peteghem, Anal. Chim. Acta 303 (1995) 11.

[31] D.S. Vienneau, C.G. Kindberg, J. Pharm. Biomed. Anal. 16 (1997) 111.
[32] J. Zhu, D.D. Snow, D.A. Cassada, S.J. Monson, R.F. Spalding, J. Chromatogr. A 928 (2001) 177.
[33] M. Cherlet, M. Schelkens, S. Croubels, P.D. Backer, Anal. Chim. Acta 492 (2003) 199.
[34] C.M.C.M. Couto, J.L.F.C. Lima, M. Conceicao, B.S.M. Montenegro, S. Reis, J. Pharm. Biomed. Anal. 18 (1998) 527.
[35] T. Charoenraks, S. Chuanuwatanakul, K. Honda, Y. Yamaguchi, O. Chailapakul, Anal. Sci. 21 (2005) 241.

SENSOR LETTERS

www.aspbs.com/sensorlett

VOLUME 4
NUMBER 2
JUNE 2006

53–213 (2006)
ISSN 1546-198X
EISSN 1546-1971

Manuscript Submission

Submit your manuscript electronically as a PDF or MS Word file to the Editor-in-Chief, Professor Craig A. Grimes, or one of the Regional Editors.

SENSOR LETTERS

www.aspbs.com/sensorlett

VOLUME 4
NUMBER 2
JUNE 2006

53–213 (2006)
ISSN 1546-198X
EISSN 1546-1971

ON THE COVER: The cover image shows the fluorescence spectra of PBA and myristic acid layers chemisorbed onto nanoporous alumina, from "Fluorescence Behavior of Pyrene-1-Butylic Acid Chemisorption Layer onto Nano-Porous Anodic Oxidized Aluminum with Myristic Acid Layer for Optical Oxygen Sensing," *Yuki Fujiwara and Yutaka Amao*, pp. 139–143 of this issue.

REVIEWS

GENERAL RESEARCH ARTICLES

FOREWORD

RESEARCH ARTICLES

SENSOR LETTERS

www.aspbs.com/sensorlett

Editor-in-Chief:

Professor Craig A. Grimes
Department of Electrical Engineering
The Pennsylvania State University
University Park, PA 16802, USA
Tel.: (814) 865-9142
Fax: (814) 865-2326
E-mail: cgrimes@engr.psu.edu

FOR SUBSCRIPTION

SENSOR LETTERS
American Scientific Publishers
25650 North Lewis Way
Stevenson Ranch, CA 91381-1439, USA
Tel.: (661) 254-0807
Fax: (661) 254-1207
E-mail: order@aspbs.com

Aims and Scope:

The growing interest and activity in the field of sensor technologies requires a forum for rapid dissemination of important results: *Sensor Letters* is that forum. *Sensor Letters* offers scientists, engineers and medical experts timely, peer-reviewed research on sensor science and technology of the highest quality. *Sensor Letters* publishes original rapid communications, full papers and timely state-of-the-art reviews encompassing the fundamental and applied research on sensor science and technology in all fields of science, engineering, and medicine. Highest priority will be given to short communications reporting important new scientific and technological findings. Authors receive these benefits:

Research Topics Covered:

Innovative sensing concepts, Cell and tissue-based sensors, Chemical, biological and physical sensors, Sensor networks and systems, Sensor system integration, Advanced sensing materials, Sensor architectures, Self-cleaning sensors, One-shot disposable sensors, Biotoxin sensors, Data fusion of sensor arrays, Sensor fabrication, packaging, testing and reliability, Sensor instrumentation, Electronic interfaces and data processing, Sensor signal processing electronics, Sensor applications and uses, Optical, acoustic, mechanical, thermal, electromagnetic, electrochemical and radiation sensors, Environmental sensors, Fiber optic sensors, Sonar sensors, Flow sensors, Analytical μ-systems, lab-on-a-chip, Sensor neural networks, Sensor telemetry, Measurement compensation and calibration, Electronic-nose sensors, Nanosensors, Computational and theoretical aspects of sensors, Fabrication techniques, Characterization, Spectroscopy, and much more.

Instructions for Authors:

Please visit the journal Web site (http://www.aspbs.com/sensorlett) or see the instructions in each issue of the journal. Authors should follow the instructions when submitting their manuscripts.

Manuscript Submission:

Submit your manuscript electronically. Send an electronic file in a PDF or Word format to Editor-in-Chief Professor Craig A. Grimes at the above address. Please see "Instructions for Authors" for submitting manuscripts.

Books for Review:

Publications should be sent to the Editorial Office: Sensor Letters, American Scientific Publishers, 25650 North Lewis Way, Stevenson Ranch, CA 91381-1439, USA; Tel.: (661) 254-0807; Fax: (661) 254-1207; Email: sensor@aspbs.com. Readers are encouraged to send books that may be of interest to other readers of *Sensor Letters*.

Referee's Report:

Please submit Reviewer's Reports on the *Sensor Letters* home page.

Annual Subscription Rates (Print Edition) for 2006:

Volume 4, 2006, 4 issues
Personal: US$ 200 (USA)/US$ 300 (Foreign)
Institutional: US$ 690 (USA)/US$ 790 (Foreign)
Postage and handling charges add $50 for USA, $100 for foreign.
The publisher reserves the right to refuse nonqualified subscriptions.

Web Edition:

Sensor Letters is available to subscribers via the internet. For institutional subscriptions to the Web Edition or site licensing, please contact publisher.

Subscription Orders, Advertising, Renewals and Reprints:

For quotes, and other details, contact: American Scientific Publishers
Tel.: (661) 254-0807 Fax: (661) 254-1207
E-mail: order@aspbs.com, sensor@aspbs.com

Honorable Claim Period:

Claims for issues not received will be honored only if submitted within 90 days of the issue date for subscribers in North America or 180 days for all other subscribers. Send your written request to American Scientific Publishers.

Digital Object Identifier (DOI):

The DOI identification system for digital media has been designed to provide persistent and reliable identification of digital objects. Information on the DOI and its governing body, the International DOI Foundation, can be found at http://www.doi.org. The DOI appears in the lower right of the first page of each article.

SENSOR LETTERS
Vol. 4, 53–98, 2006

REVIEW

Carbon Materials for Chemical Sensors: A Review

Jerzy P. Łukaszewicz

Faculty of Chemistry, Nicholas Copernicus University ul. Gagarina 7, 87-100 Torun, Poland

(Received: 2 October 2004. Accepted: 6 February 2006)

This paper reviews application of different carbon materials, including graphite, polycrystalline carbon, carbon black, and carbon nanotubes, to the construction of chemical sensors. Basic chemical properties of carbons are presented as well as selected synthesis methods. Different ways of carbon surface functionalization are considered in relation to chemical sensing properties.

Keywords: Carbon, Chemical Functionalization, Carbon Black, Nanotubes, Fullerenes, Sensor, Sensing.

CONTENTS

1. INTRODUCTION

Chemical sensors have become one of the most important branches of contemporary science and technology. Recently there is growing interest in application of fullerenes and carbon nanotubes in chemical sensors. However, the term "carbon" or "carbonaceous material" is not limited to fullerenes and nanotubes but also applicable to carbon black, glassy carbon, or active carbon. The aim of this paper is to review the basic types of carbon-based materials, selected methods of carbon preparation, and the most recent announcements on application of carbon to chemical sensing. We intend to show how the chemical properties of the carbon surface can be controlled, and how the properties influence possible application of carbons to the construction of chemical sensors.

*Corresponding author; E-mail: lukaszju@chem.uni.torun.pl

Carbon is an element mostly known as a basic component of organic molecules. However, elemental carbon may also be found in the nature, e.g., graphite and diamond. The term carbon is often extended to numerous synthetic materials that are characteristic because of their high carbon content. The synthetic materials usually called "carbon" should be rather named "carbonaceous materials" because:
(1) Often they are not pure, i.e., they contain considerable amounts of other elements such as oxygen, nitrogen, metal ions, etc.
(2) Their chemical and crystallographic structure differs from elemental carbon, e.g., diamond and graphite; very often so called "carbons" are amorphous materials with minor traces of graphite.

However, the term "carbon" is traditionally used in science since it is convenient in use. Therefore the general term "carbon" will be in use in this review keeping in mind the above mentioned qualifications.

Carbons are often artificially synthesized in a laboratory or on an industrial scale, with the fabrication route influencing their chemical and physical properties which in turn determine their field of application. One may propose a rough classification of carbonaceous materials with reference to the most common applications:
(1) Carbon as a construction material: Carbon fibres as reinforcement in composites, mechanically, and thermally stable bearings, artificial joints and other elements implanted in human bodies, chemically resistant laboratory ware, etc.
(2) Carbon for electrochemical applications (electrodes for industrial application, electrodes in the sources of electric power: Metal-gas batteries, lithium batteries, fuel cells etc.).

(3) Carbon as a material with chemically active surface: Carbon adsorbents for the removal of impurities form gases and liquids in military, industry and at home.
(4) Carbon as an absorber for storage of gases like hydrogen and methane.
(5) Carbon as a catalyst or support for a catalyst.

The above listed major fields of carbon application rely to the specific mechanical, electrical, and chemical properties. One may find in the literature many different materials of various properties all referred to as carbons; the broad terminology prevents definition of materials with well-defined and stable chemical and physical properties.

1.1. Basic Types of Carbon and the Methods of Their Preparation

1.1.1. Polycrystalline Carbons

The much differentiated properties and applications of carbons result from the selection of raw materials and methods of carbon production. Many of the technically applicable carbons are obtained by a thermal decomposition of carbon-rich organic substances. There are many possibilities in selecting a raw material but it is quite rare that one obtains the same carbon material from different precursors. Usually the raw material significantly influences the final properties of the carbon. Raw materials for carbon fabrication can be divided in to two general categories, natural carbon-rich substances, and synthetic organic materials. To the first group of materials one may account: Different types of wood, nut shell (coconut), fruit stones (plums, olives, apricot), black coal, brown coal, peat, cellulose-rich substances, sugar, and other carbohydrates, selected hydrocarbons (sucrose), selected proteins (e.g., animal blood). The second group of precursors consists of temperature degradable synthetic polymers: Polyvinyl chloride, poly(vinilydene chloride), poly(styrene), poly(acrylonitrile), etc., Some of them are thermosetting polymers and resins (poly(furfuryl alcohol), epoxy resins, rubber, bakelite, phenol based resins), which easily can be carbonised to active carbon. Any successful transformation of commonly used polymers (polyethylene, polypropylene, polyesters etc.,) into technically applicable carbons may help to solve ecological problems by the partial elimination of poorly degradable polymers from the environment. However, these polymers usually transform into volatile products upon heat-treatment at elevated temperatures. Brown coal often yields macroporous and mesoporous active carbons while from black coal and anthracite one often obtains microporous active carbon. Commercially available active carbons from brown coal are not stable from a mechanical point of view. Anthracite is an attractive raw material used in the production of molecular sieves.

The mentioned carbon-rich raw materials undergo thermal decomposition during the necessary heat-treatment (carbonisation). In the first step, the chemical structure of the organic raw material decomposes, i.e., the original system of chemical bonds vanishes. This process is usually accompanied by more or less intensive evolution of volatile products such as H_2O, HCl, NH_3, HCOH, CO_2, CO, aliphatic, and aromatic hydrocarbons, etc. Usually, the most dramatic changes occur between 150–400 °C. The nature of volatile products depends on the chemical nature of the raw material. In some cases (polyethylene, some polyesters), the carbonised substance yields almost only volatile products. It happens despite the very high carbon content in such materials. The raw solid obtained just after the completion of the most spectacular stage of thermal decomposition (temperature range 150–400 °C) is often called coke or raw coke. At this stage, the obtained solid mainly consists of carbon atoms randomly bonded to each other and some residual foreign atoms (e.g., oxygen, nitrogen, sulphur, phosphor). There are many unsaturated bonds and defects in the material. Coke is a chaotic mixture of carbon atoms that may form bonds using sp, sp^2, and sp^3 hybrid orbitals.

The second stage in the thermal decomposition of organic solids occurs above 400–500 °C. At this stage one observes the re-arrangement of the chaotic system of carbon–carbon and carbon–hetero atom bonds and the formation of regions of specifically oriented carbon atoms, i.e., small graphite layers that later can be stuck one over another. Thus, small domains of graphite start to grow in the amorphous carbon phase. The changes in the structure of a heat-treated carbon-rich organic material may be summarized in Figure 1.[1]

Dr. Jerzy P. Lukaszewicz has been working in the field of chemistry since 1977 when he was employed at Nicholas Copernicus University. His attention is currently focused on the synthesis of new materials for different purposes: adsorbents, catalysts, chemically sensitive materials. His expertise covers in particular fabrication of semiconductor carbon films, carbon-based molecular sieves and carbon-based electrode materials containing nano-sized particles of metals and metal oxides. He pays special attention to the characterization of carbon surfaces by instrumental methods. SEM, AFM, FT-IR, UV-VIS, HREELS, XPS, DTA-DTG-TG, TPD-TPR, and gas adsorption. He has got Ph.D. in chemistry in 1983. Since that time he was mainly employed as a post-doc fellow.

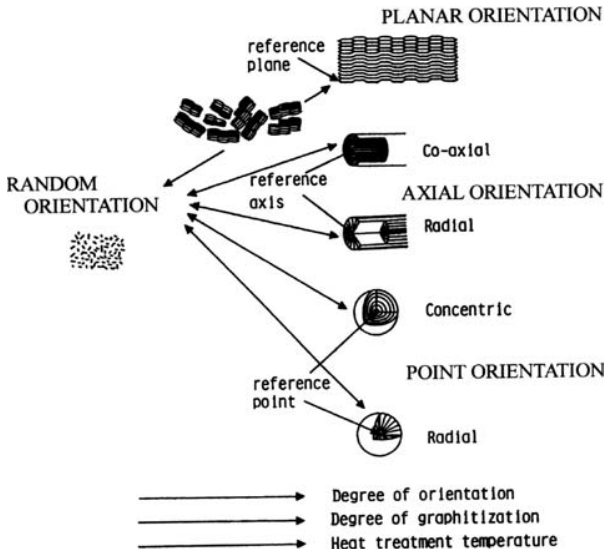

Fig. 1. Changes of the degree of orientation and the degree of graphitisation of heat-treated carbons. Reprinted with permission from [1], M. Inagaki, New carbons. *Control of structure and functions* **(2000)**, p. 11. © 2000, Elsevier.

The structure of most carbons obtained by thermal decomposition of organic species is described as turbostratic[2] (Fig. 2). The turbostratic structure consists of numerous small and randomly oriented graphite domains (crystallites) suspended in amorphous carbon phase. Carbons of turbostratic structure are mainly obtained at relatively low temperatures up to 1000–1300 °C.

There is a possibility to transform carbons of turbostratic structure into pure graphite. The longer the carbonisation duration and the higher the temperature the bigger are the graphite crystallites. Their growth upon increasing temperature and heat-treatment duration often leads to the formation of pure graphite. In such a case, the whole process is called graphitisation. The process of graphite formation from disordered carbon atoms is accompanied by the elimination of foreign atoms from the heat-treated carbon material. Finally, at elevated temperatures of ca. 3000 °C one may obtain pure carbon in graphitic form. The mentioned process of carbon structure re-arrangement and purification usually negatively affects specific surface properties of carbons since defects and foreign atoms are usually active in adsorption and catalysis over the surface of carbons obtained by pyrolysis.

Chemical changes occurring upon heat-treatment have been widely investigated for different raw materials. Thermal degradation of polyvinyl alcohol (PVAl)[3] may be used to illustrate typical processes associated to the transformation from the polymer to coke and carbon. It also means the transformation from a liner polymer (non-conducting) to an aromatic structure (conducting graphene sheets). Figure 3 shows that degradation of PVAl begins with elimination of water along linear polymeric chains. The process is intensive up to 300 °C when it

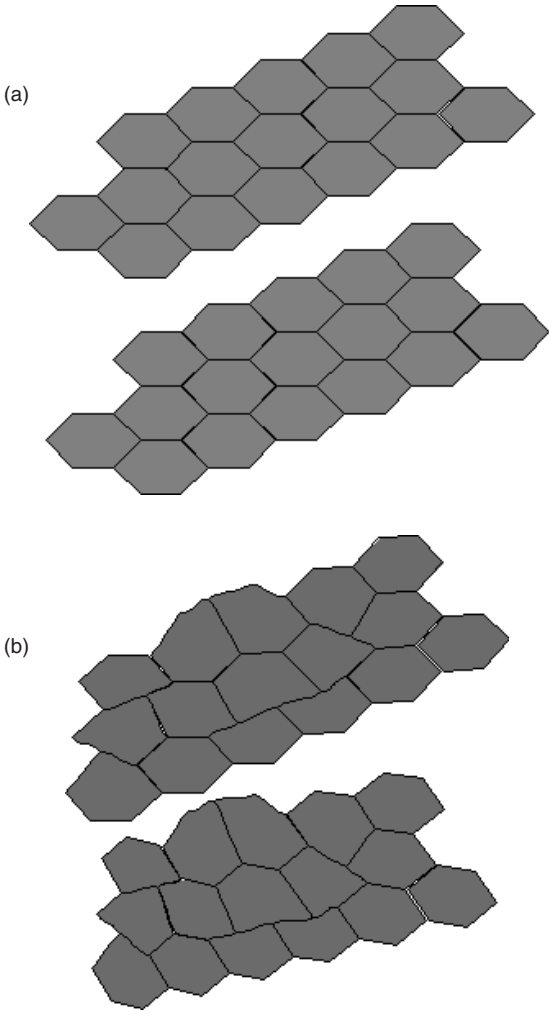

Fig. 2. Graphitic an turbostratic structure of graphene layers in graphite (a) and polycrystalline carbon (b).

seems to stop. At this stage, the material consists of polymer chains with numerous double bonds. Further heating above 300 °C leads to cyclisation (Deals-Alder mechanism or intermolecular mechanism) and aromatisation (elimination of H_2). This is a spectacular example illustrating how linear polymer chains transform into aromatic structures and finally into graphite layers. The variety of carbon materials that may be obtained as a terminate stage of various organic compounds is presented in Figure 4.[4]

Carbonisation of organic matter also yields turbostratic carbons. It means that despite a completely different chemical structure of the raw material (comparing to PVAl), the thermal decomposition leads finally to aromatisation, i.e., a system of condensed aromatic rings. On the way to the final stage, (carbon) the basic components of wood (cellulose, chemicelluloses, and lignin) undergo several processes like depolymerization, dehydratation, hydrolysis, oxidation, decarboxylation, and transglycosylation. In the case of wood, one observes the evolution of acetic acid

REVIEW

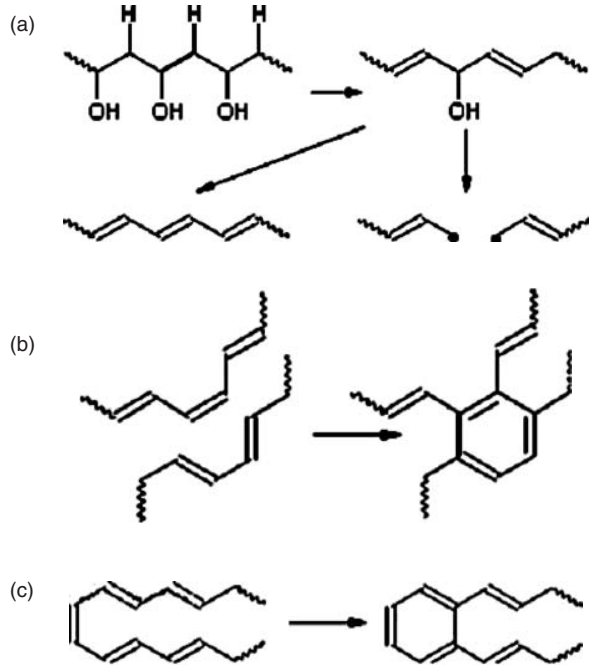

Fig. 3. Thermal degradation of poly(vinyl alcohol). (a) Chain-stripping—elimination of H_2O, (b) Intermolecular cyclisation (Diels-Alder reaction), and (c) Intermolecular cyclisation.

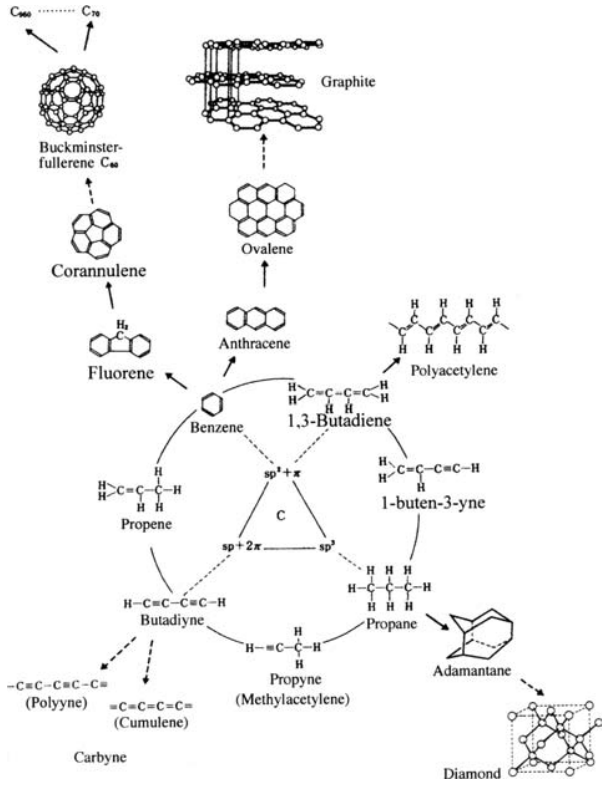

Fig. 4. Enormous organic compounds based on carbon-carbon bonds using sp^3, sp^2, and sp hybrid orbitals and inorganic materials as their extension. Reprinted with permission from [4], M. Inagaki, New carbons. *Control of Structure and Functions*, Elsevier, Amsterdam **(2000)**, p. 9. © 2000, Elsevier.

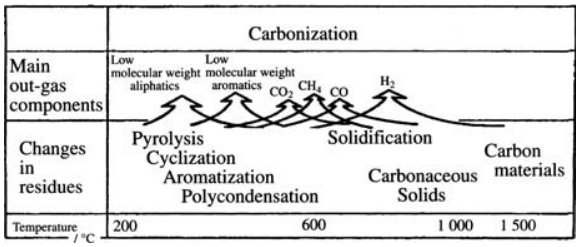

Fig. 5. General scheme of out-gas components and changes in residues with carbonisation. Reprinted with permission from [5], M. Inagaki, New carbons. *Control of Structure and Functions*, Elsevier, Amsterdam **(2000)**, p. 124. © 2000, Elsevier.

(decomposition of cellulose and chemicelluloses) and phenols (degradation of lignin) beside the usual volatiles: Water, carbon monoxide, carbon dioxide, and aliphatic hydrocarbons. All possible processes occurring during heat treatment of organic solids are summarized[5] in Figure 5 where they are placed on a temperature scale.

Spray pyrolysis is a method that may be very useful in the preparation of carbons needing only liquid precursors. This requirement results from the merit of the method: The substance must be transformed into the form of small drops. The drops of precursor move (powered by a stream of gas applied in atomizer) towards a hot solid substrate (or to a hot environment). The temperature of the substrate is usually kept at the level enabling thermal decomposition of the substance. The liquid drops, in contact with hot substrate, may undergo a variety of processes at a given temperature. The result is that preparation of carbon requires rapid solidification of the liquid precursor. Solidification may result from different phenomena depending on the nature of the raw material used. In the case of some monomers, one observes polycondensation, or polymerisation of the monomer being sprayed in pure or diluted form. Furfuryl alcohol is a typical example; the monomer polycondensates yielding a solid thermosetting resin. The resin is not stable at elevated temperatures (above 300 °C) and decomposes giving a black coke. A similar effect can be achieved by the application of polymer solutions or dispersions. A typical example is a solution of polystyrene (in organic solvents), water solution of polyvinyl alcohol (PVAl) or water dispersion of polyvinyl acetate (PVAc). In the case of the mentioned polymers, solvent or dispersing liquid evaporates from the drops of precursor. After the removal of liquid, one gets a layer of polymer on a hot substrate. Sometimes due to polymer transformation into volatile products (PVAc and PVAl) the raw coke phase grows very slowly on the substrate.

At this stage, the deposited film cannot be treated as a film of carbon. It is only a film of partially decomposed polymer or any other raw material due to the low substrate temperature, usually 200–300 °C. Such a temperature is high enough to decompose the raw material but much to low to initiate aromatisation. On the other had, it is not

possible to lift the temperature of substrate considerably above 300 °C if spray pyrolysis is performed at room conditions, i.e., when oxygen from air has an access to the film. Coke is a burnable solid that easily ignites itself in contact with air provided the temperature is high enough. Therefore, spray pyrolysis does not yield carbon materials directly. Usually, the raw product of pyrolysis (a film of coke) needs an additional heat-treatment to become a carbon material containing microcrystallites of graphite. This means heating of raw coke in a furnace without oxygen. The temperature of carbonisation and its duration depend on the desired properties (electric and surface), which the final product should exhibit. The presence of a solid substrate is inevitable when one intends to prepare a coke or carbon film. It is possible to spray liquid precursor to a wide chamber where temperature is high enough to cause the rapid evaporation of dispersing liquid and/or begin solidification (polymerisation, crystallization, etc.) of the dispersed matter. In such a case, one gets the solid in form of fine powder.

Another chemical method to carbon fabrication is the thermal decomposition of carbon-rich gaseous substances in conditions required by the method called Chemical Vapour Deposition (CVD). The standard CVD method is sometimes combined with physical techniques like radio frequency sputtering. One can obtain carbons by other methods that are more physical in character, for example evaporation of carbon particles from a solid sample of carbon (or graphite) in vacuum. Evaporation of carbon phase may result from the application of high temperature or the formation of plasma by means of an applied electromagnetic field. Evaporated carbon particles condense (on a substrate) in form of a thin carbon film.

Pyrolysis of carbon-rich substances uses combustible gases (methane, propane, acetylene), a gaseous oxidant (oxygen pure or from air) and a burner to ignite the flame. Such a flame has two different zones called: Oxidizing zone and reductive zone. In the reductive zone, combustion of the applied burnable gas is incomplete. This part of the flame contains products of partially oxidized gaseous fuel. A sudden insertion of a cool solid object can additionally reduce the temperature of the reductive zone. In these conditions, combustion of some hydrocarbons yields element carbon as one of the products. The gases flowing through the burner can be saturated with vapours of organic liquids (aliphatic hydrocarbons, aromatic hydrocarbons, and their derivatives with hetero atoms, etc.) or inorganic ones (gases, vapours, atomised solutions). In such a case, the formed carbon particles contain residuals of the substances added to the flame. It is well known that the flame over benzene may be the source of carbon black. It is enough to put a cold object into the flame to get its surface covered with a carbon black film. It consists of small particles and part of it is easily removable by rubbing. Therefore, the mechanical stability of such obtained carbon films is unsatisfactory regarding the requirements usually expected from the materials applied in chemical sensors.

In some cases, the carbon material applied for the construction of a chemical sensor is in fact a kind of carbon black. The reports dealing with carbon black usually pay little attention to the surface properties of carbon black. Frequently carbon black is treated like a chemical reagent of known formula and properties that always behave in the same manner. However carbon black properties, in common with other types of carbon materials, is sensitive to surface chemical treatment, as will be discussed.

1.1.2. Glassy Carbon, Carbon Black, Fullerenes, Nanotubes

Relatively new members of the "carbon family" such as nanotubes, fullerenes, and glassy carbon are currently the focus of considerable investigation. Glassy carbon can be obtained by the thermal decomposition of resins as phenol-formaldehyde and poly(furfuryl alcohol). The resins should be thermosetting providing the specific form of carbon called 'glassy,' with properties that include high hardness, low gas transparency, high chemical, and thermal stability. In chemical sensing glassy carbon usually is employed for fabrication of sensing electrodes.

The family of carbon nanotubes (CNTs) consist of two basic types of the tubes: Single-walled (SWCNTs) and multi-walled (MWCNTs). There are three methods of CNT fabrication: Arc-discharge (gas or liquid environment), decomposition of hydrocarbons over a metal/metal oxide catalyst, and laser ablation. The synthesis of nanotubes is a separate branch of carbon science and technology and more detailed information may be found in extended reviews.[6] The report of Rao and co-workers, as well as other reviews, present the conditions favourable for the synthesis of SWCNTs or MWCNTs. CNTs are of a great interest for sensor applications. The current report devotes a large part of the text to chemical sensing applications of CNTs.

1.2. Chemical Functionalisation of Carbon Surfaces

1.2.1. Oxygen-, Nitrogen-, Sulphur-Containing Functionalities

Carbonised organic matter (coke, char) mostly consists of carbon atoms bonded to each other by hybridised orbitals (sp^3, sp^2, or sp). Non-carbon atoms, i.e., heteroatoms, are usually implanted in the system of carbon–carbon bonds. It is probable that heteroatoms are not uniformly distributed between the surface and the bulk since the carbon matrix retains some heteroatoms from the raw material. The adsorbed molecules often react with carbon atoms at the surface yielding so called surface functional groups. The process is particularly important in the case of oxygen. Therefore, one has to expect the presence of O-containing

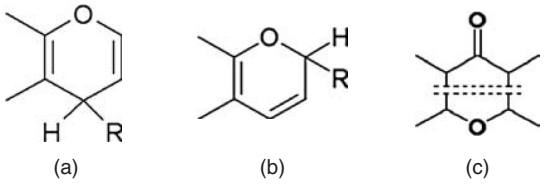

Fig. 6. The structure of oxygen functional groups of base properties. Reprinted with permission from [7], V. A. Garten and D. E. Weiss, *Australian J. Chem.* 10, 309 **(1957)**. © 1957, CSIRO Publ.

surface functional groups in most samples of carbon if it was stored for long in air. Heteroatoms in bulk carbon trace the chemical nature of the precursor while heteroatoms at the surface may be regarded as the witness of the carbon sample history. The process of carbon self-oxidation (low temperature) has been investigated extensively; see Figure 6.[7] The most reactive spots in the carbon matrix are: Broken bonds at carbon atoms, edge carbon atoms in aromatic rings and triple bonds between carbon atoms.

The mechanism of basic self-oxidation is valid for relatively low temperatures, up to 150 °C. Carbons with such groups on the surface adsorb acids from solution. Basic properties of the groups may differ from case to case since the groups are strongly influenced by π-electrons from the system of aromatic (graphitic) rings to which the groups are bonded or incorporated. The proposed growth mechanism assumes the evolution of CO_2. It means in practice a slow, low temperature burning of carbon. This statement may be confirmed by the well-known phenomenon of self-ignition of some carbon-rich substances like black coal. Basic groups can be also created at elevated temperatures (usually above 800–900 °C) if carbon is in contact with limited amounts of oxygen.

Carbon surfaces are oxidized when in contact with oxygen at intermediate temperatures (150–800 °C). Thus, simple heating of a carbon sample in air above 300 °C may dramatically change the chemical structure of its surface. Moreover, oxygen atoms may react with carbon atoms when they are subjected to the action of other oxidising agents in gas (ozone) or in liquid phase (wet chemistry oxidants like $Cr_2O_7^{2-}$, ClO_4^-, ClO^-, H_2O_2, HNO_3, NO_3^-). Wet oxidation is limited by the boiling point of water, which is the major component of the oxidising mixtures. To be effective, wet oxidation should be performed at 50–90 °C. Both treatments i.e., oxidation by O_2 at intermediate temperatures and wet oxidation in a warm solution create so-called acidic O-containing surface functional groups. Researchers have investigated a number of structures including: Carbonyl (quinone type), carboxyl, phenolic hydroxyl, carboxylic anhydride, and lactone (normal and fluoresceine type, see Fig. 7).[8]

The acidic nature of the various structures may be experimentally tested in simple reactions with basic solutions. Boehm and other researches[9] established a set of standard base solutions to determine the acidity of a sample. These

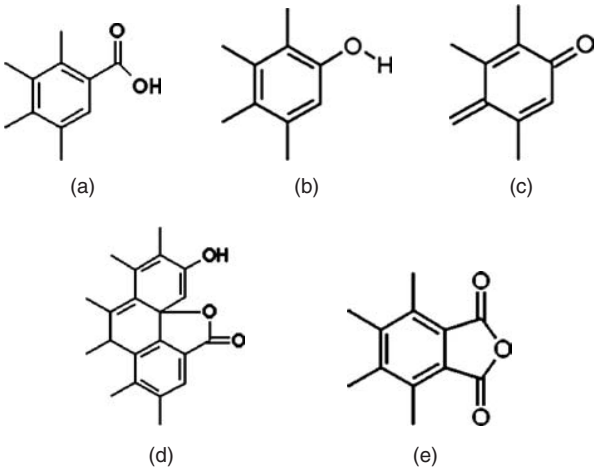

Fig. 7. The structure of acidic oxygen-based functionalities on carbon surface. Reprinted with permission from [8], J. S. Mattson and H. B. Mark, Jr., *Activated Carbon*, M. Dekker, New York **(1971)**.

are solutions of $NaHCO_3$, Na_2CO_3, NaOH, and C_2H_5ONa. The reagents neutralize surface functional groups of different acidity in a relatively selective way: $NaHCO_3$—carboxylic, Na_2CO_3—carboxylic, and lactone, NaOH—carboxylic, lactone, and phenolic, C_2H_5ONa—carboxylic, lactone, phenolic, and carbonyl. The results of acid-base titration enable determination of surface functional groups of a certain type. Beside that simple chemical method, a large number of advanced instrumental methods (FT-IR, XPS, NMR, EPR, TPD, thermogravimetry, electrochemical methods etc.,) can be applied for carbon surface characterization. One can also use additional reagents designed to react exclusively with a certain type of surface functional groups. Acetilation, methylation, reaction with hydroxylamine, $LiAlH_4$, diazomethane are in common use for this purpose. The reaction of surface groups with the reagents transforms the groups into new organic structures, which are detectable by means of chemical and instrumental methods. Regarding the differentiated electron structure of particular carbon atoms at the surface (radicals, broken bonds, interaction with π-electrons etc.,) and oxidising conditions (type of oxidant, phase of reaction, temperature etc.,) one may expect a variety of surface structures called as O-containing surface functional groups. Laszlo et al.[10] elaborated a diagram (Fig. 8) that additionally includes possible positions of radicals and electron pairs.

Oxygen is not the only element that is present in the bulk and surface carbon. Nitrogen is often responsible for specific (basic) surface properties of carbons due to the presence of N-containing surface functional groups. Nitrogen can be introduced to carbon matrix in two ways: As a residual element from a nitrogen-rich precursor or due to the secondary treatment of carbon with a nitrogen containing reagent like NH_3 at elevated temperatures above 1000 K. As mentioned above, oxygen

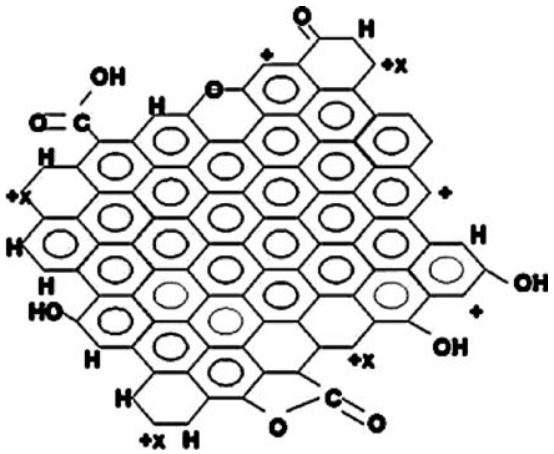

Fig. 8. Graphene bonded to different oxygen containing functional groups. Unpaired σ and localized π electrons marked as x+ and +, respectively. The graph follows the idea of Ref. [10], K. Laszlo et al., *Anal. Sci.* 17, i1741 **(2001)**. © 2001.

from air reacts with carbon atoms at the surface even at room temperature. Atmospheric nitrogen is an inert gas if brought to contact with the bare carbon surface at low temperatures. However, an oxidized carbon surface reacts with NH_3 even at room temperature yielding mainly ammonium salts—ONH_4 (reaction with hydroxyl—OH groups) and less amide—$CONH_2$ and imide—CO-NH-CO- derivatives. Carbonyl C=O groups react as shown in Figure 9.[11] Biniak et al.[12] investigated NH_3-modified carbons by means of several instrumental (XPS, FTIR, TPD-MS, mercury porosimetry) and chemical (acid-base titration) methods. The results are consistent with the above statements.

Nitrogen due to its electron structure is able to enter aromatic (graphitic) rings being built in the carbon matrix. That can happen if one treats a carbon surface (even not oxidized) with NH_3 at temperatures above 600 °C. The action of NH_3 changes also physical properties of carbons like developing their pore structure.

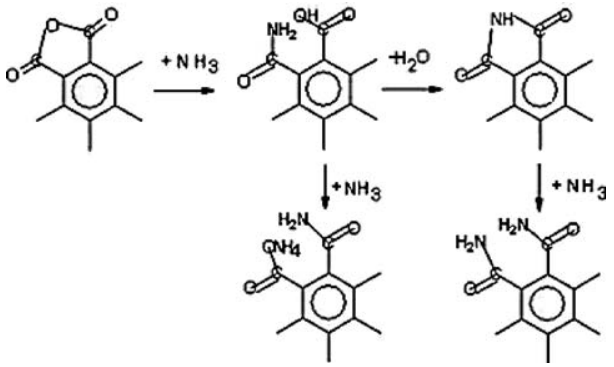

Fig. 9. The reaction pathway for the oxygen functional groups and ammonia according to the concept presented in Ref. [11], H. Jankowska et al., Adsorpcja jonów na weglu aktywnym (in Polish), PWN, Warsaw **(1991)**, p. 88.

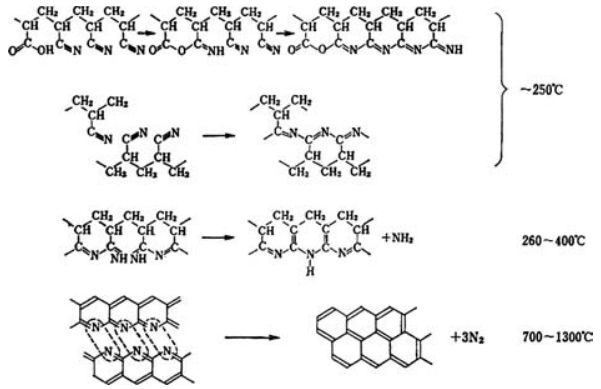

Fig. 10. Changes in the molecular structure of PAN at high temperatures. Reprinted with permission from [13], M. Inagaki, New Carbons. *Control of Structure and Functions*, Elsevier, Amsterdam **(2000)**, p. 88. © 2000, Elsevier.

Carbonisation of N-rich substances like some polymers poly(acrylonitryle—PAN and poly(imide)) yields carbons containing aromatic rings like in the case of poly(vinyl alcohol) or cellulose. Figure 10 presents the idealized mechanism of chain-to-ring transformation emphasizing the presence of nitrogen atoms.[13] Nitrogen atoms contained in the nitrogen surface functional groups exhibit nucleophilic properties that influence some catalytic reactions.

Contrary to O-containing and N-containing functional groups on the carbon surface, there are few papers published on S-containing functional groups. S-containing surface species are thermally stable and hardly decompose below 500 °C. Element sulphur cannot be extracted from S-containing carbons by means of aniline or CS_2. Beside residual sulphur atoms from carbonised precursor S-atoms can be introduced to carbons by heating of mixed carbon and sulphur particles above 100 °C or by reaction with vapour of sulphur. Moreover, one observed the transfer of sulphur from CS_2 vapours to carbon surface when the substances were in contact at elevated temperature. The action of strong oxidants in liquid phase removes sulphur as H_2SO_4 however some residual (oxidized) forms of sulphur remain on the carbon surface. Sulphur can be present on the carbon surface as sulfonic functional groups, SO_3H. The groups are polar and hydrophilic exhibiting strong acidic properties. One may also find papers describing methods for immobilisation of fluorine, chlorine, bromine, and iodine atoms on the carbon surface. The methods are usually based on the high chemical reactivity of these elements. Direct contact with the elements (gases or vapours) at elevated temperatures almost always causes direct reaction with carbon.

1.2.2. Ion Exchange

Some carbons exhibit a unique ability for the adsorption and durable bonding of ions (particularly cations). This

property may be utilized in two general ways:
(1) Application of carbons for purification of liquids from dangerous impurities like heavy metal cations.
(2) Controlled deposition of metal cations on the carbon surface to prepare chemically active materials, where implanted metal atoms (ionised or not) play the role of catalytic centres.

Accumulation of ions on a carbon surface may result from its exchange properties that are similar to the exchange properties of minerals (clays, zeolites) and polymer ion exchangers: The ions being exchanged must have the same type of electric charge, and the total electric charge taken by ions leaving the exchanger must be equal to the total electric charge brought by ions adsorbed from solution.

In the case of carbons, one has to specify sulfonic, carboxylic, and phenolic surface functional groups as possible centres of ion exchange. The groups are polar, easily dissociate in water and release proton H^+. In this way, cations from solution can take the empty places. One can prepare a carbon having such polar functional groups following some methods previously described. The content of metal in carbons subjected to ion exchange may be very different. Szymański et al.[14] prepared carbons modified by ion exchange of Zn^{2+}, Ni^{2+}, and Na^+ containing from 0.0278 mol/kg C to 0.654‘mol/kg C of these cations. In another paper,[15] one reported the introduction of metal cations like Mn^{2+}, Pb^{2+}, Cu^{2+}, Al^{2+}, Cr^{3+}, K^+ but the metal content was similar to that of Szymanski and co-workers.[14] One report specifies Fe^{3+} ion exchange on oxidised carbons with 9.2% atomic content of iron on the carbon surface.[16] The concentration of the ion exchange groups on carbons is often similar to the resin-based ion exchangers. Metal cations bearing more than a single positive elementary charge should interact with 2, 3, or 4 polar groups on carbon surface to keep electric neutrality of the adsorbent. It is not possible if the number of polar groups is too small within certain regions. In such a case the electric neutrality of the system is provided by the immobilisation of anions from solution in the adsorbed layer. Therefore, one should expect the presence of anions (sometimes undesired) when one tries to immobilize metal cations on the carbon surface.

In the case of carbons an additional bonding effect may appear due to mobile π-electrons that are present in the partly graphitised carbon matrix. Metal cations are bonded directly at carbon surface (without any assistance of functional groups) by the formation of coordination complexes where π-electrons from graphite rings play the role of ligands. The capability for such non-ionic immobilisation of metal cations is a specific property of carbons and does not occur in the case of mineral, polymer, and bio exchangers.

Since the adsorption of metal cations on carbons is a complex phenomenon, the affinity of the carbon surface to a particular cation depends on many factors. These factors may be divided into two basic categories: factors related to cation properties (electronic configuration, polarizability), and factors resulting from the conditions of ion exchange (concentration of metal cations, pH of the solution, advancement of ion exchange). Jankowska et al.[11] summarized the known experimental data and suggested that the affinity of metal cations to the oxidised carbon surface increases in the following order: $NH_4^+ < Na^+ < Rb^+ < Cs^+ < Mg^{2+} < Ca^{2+} < Ba^{2+} < Mn^{2+} < Co^{2+} < Sr^{2+} < Zn^{2+} < Fe^{2+} < Ni^{2+} < Pb^{2+} < Al^{3+} < La^{3+} < Y^{3+} < Cr^{3+} < Be^{2+} < Cu^{2+} < Fe^{3+}$. Since the metal cations adsorbed on carbon surface are under the influence of π-electrons their oxidation number can be changed. The change of oxidation state is particularly probable when the introduction of metal cations appears in the carbon bulk. Upon carbonisation, the metal cations are immobilised in the solidified organic precursor and later in the carbon matrix. The reductive influence of π-electrons is so effective that the implanted metal cation are reduced to lower oxidation states. Lukaszewicz[17] found experimental evidences that even cations of alkali metal are reduced to neutral atoms if they are implanted in the carbon matrix. Additional heating of carbons with deposited metal cation in an inert gas atmosphere causes reduction on metal cations to a metallic state. Wang and Lu[18] reported that after deposition of Ni^{2+} ions by immersing of carbon particles in water solution of $Ni(NO_3)_2 \cdot 6H_2O$ and its subsequent thermal treatment at 500 °C in N_2 part of nickel atoms was reduced to metallic state (XRD measurements). Molina-Sabio et al.[19] observed the reduction of copper and chromium ions upon the influence of carbon matrix. Metal cations on a carbon surface often act as active centres catalysing some chemical reactions. This function of deposited metal atoms is particularly important regarding possible sensor applications. Many semiconductor sensor materials are non-stoichiometric. In the case of tin dioxide, the non-stoichiometric character consists in the presence of domains where tin ions are reduced to lower oxidation states including Sn^0. Other modifications of SnO_2—based sensing materials consist in the introduction of metal particles (Pd, Pt, etc.).

Deposited metal cations on a carbon surface can be reduced to element metal atoms by a secondary chemical treatment like heating in a stream of hydrogen. In this manner, one can drive two basic effects:
(1) Reduction of O-containing surface species, and
(2) reduction of the deposited cations to its elemental form.

Numerous papers have been published on metal cation deposition on carbon surface and the influence of the cations on catalytic properties of so modified materials. The reactions that are catalysed by carbon having metal ions/atoms on its surface are listed in Table I. Other catalytic reactions involving metal particles deposited on carbon were reviewed by Auer.[20] Some of these reactions might be applied for the construction of a chemical sensor

Table I. Chemical reactions catalysed by means of carbons containing metal cations and/or atoms.

Carbon	Metal	Catalysed reaction	Phase
From poly(furfuryl alcohol)	Zn^{2+}, Ni^{2+}	Dehydration and dehydrogenation of n-butan-2	Gas
	Oxygen-containing functionalities	Dehydration of 2-methylpropan-2-ol	Gas
	Ni^{2+} oxygen-containing functionalities	Methane reforming with CO_2	Gas
	Fe^{3+} oxygen- and nitrogen-containing functionalities	NO_x reduction	Gas
	oxygen-and nitrogen-containing functionalities	NO_2 reduction	Gas
	oxygen- and nitrogen-containing functionalities	O_2 reduction	solution
Graphite single layers	metallic Pt	Oxidation of H_2	Gas
active carbon	oxygen-containing functionalities	Oxidation of H_2S	Gas

but we have found no reports in the literature that such an idea has been realised. Catalytic removal of SO_x by means of a carbon-supported catalyst is a good example of a potentially useful reaction. Mochida et al.[21] presented the mechanism of H_2SO_4 formation from adsorbed SO_2 molecules. The presence of H_2SO_4 molecules should considerably influence electric conductivity of the whole system (carbon surface under the influence of SO_2) since the molecules of sulphuric acid dissociate and contribute to charge transfer through the sample, see Figure 11.

1.2.3. Intercalation Compounds

Intercalation compounds are a specific group of carbon-based substances. Intercalation consists in the insertion of heteroatoms, ions, or molecules between the layers of graphite by an appropriate chemical treatment.

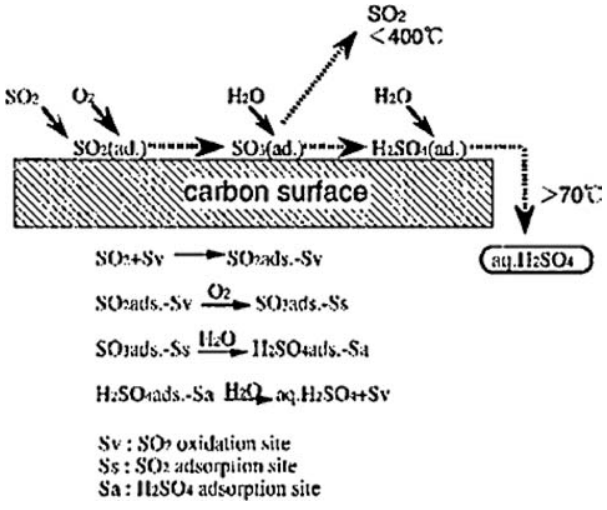

Fig. 11. The mechanism of SO_2 removal over the carbon surface. Reprinted with permission from [21], I. Mochida et al., *Carbon* 38, 227 (2000). © 2000, Elsevier.

The insertion is a result of one of three basic methods:
(1) Intercalation by the action of intercalate vapour at elevated temperatures.
(2) Intercalation by direct reaction between graphite and the intercalate at elevated temperature.
(3) Intercalation by the action of dissolved intercalate (wet method).

Frequently, the proportion between carbon atoms and the number of inserted heteroatoms or molecules is constant. In such a case, the whole system is treated as a stoichiometric compound. The formulas like KC_8, KC_{24}, or $(CF)_n$ are in frequent use. Intercalates and graphite layers can exchange electric charges between them. Inagaki [1]reviewed several examples of such transfer classifying numerous intercalates as donors (Li, Na, K, Rb, Cs, Ca, Sr, Ba, and other metals), acceptors (F, Br, ICl, IBe, IF_5, $FeCl_3$, $NiCl_2$, $AlCl_3$, AsF_5, SbF_5, CrO_3), and intercalates incorporated by coordination bonding. Parallel insertion of two kinds of intercalates is also possible. Intercalation compounds exhibit several unique properties enabling particular functions. One may obtain highly conductive materials, electrode materials (including lithium batteries), catalysts and adsorbents for gas storage. In addition, simple aliphatic hydrocarbons (methane, ethane, propane, *n*-butane, *n*-pentane, etc.) can be accumulated by some intercalation compounds. The process of hydrocarbon adsorption proceeds at elevated temperatures from 90 to 350 °C and is reversible. This property might be applied to mass-sensitive chemical sensing devices.

1.3. Chemical Functionalization of Carbon Nanotubes

Fuctionalization is one of the most important steps in the fabrication of carbon materials for chemical sensors. The specific surface composition of carbons determines phenomena such as adsorption and catalysis, which are essential for the successful detection of chemical

substances. The observed progress in the application of carbon nanotubes to chemical sensing is in part based on some chemical manipulations run on this kind of carbon. One may assume that the further steps in this domain of science will rely on chemical manipulations since the application of bare CNTs seems to be quite limited.

1.3.1. Oxidation of CNTs

The oxidation of CNTs seems to be one of the most important chemical manipulations to be performed on the tubes. Except diamond, the remaining carbon allotropes are characteristic because of the presence (sometimes very limited) of conjugated aromatic rings. Therefore, aromatic rings-containing carbons are predestined to react with electrophilic substances like oxygen, chlorine, fluorine, and free radicals. Carbon in form of SWCNTs or MWCNTs becomes rather easy oxidized in "wet" chemistry processes such as HNO_3 treatment in the presence of H_2SO_4. Kuznetsova and co-workers[22] reported that such treated SWCNTs can incorporate up to 6.7% wt of oxygen, which they assigned to the existence of surface functional groups of carboxyl (–COOH), carbonyl (C═O) and ether (C–O–C) structure at the tube edge. These groups were thermally stable up to 600 °C. Oxygen-containing species were also present at the defect sites like in other carbon materials. The functionalities were removable by an appropriate heat-treatment; heating to 800 °C led to the release of low mass products like CO, CO_2, CH_4, and H_2,[23] with the thermal desorption opening the terminal openings to enhance access to the CNT interior.

Room temperature adsorption of oxygen on CNTs was reported by Collins and co-workers.[24] The report implied the application of the discovered phenomena to the construction of an oxygen sensitive resistor. One found a reversible decrease of electric resistance of SWCNTs-based resistor when it was exposed to a cyclic change from air to vacuum at room temperature (Fig. 12). The results were explained on the same principles as in the case of NO_2 and NH_3 adsorption on *p*-semiconductor SWCNTs. Thus, oxygen was treated as an electrophilic medium. The longer (and frequent) was the exposure to oxygen the more difficult was the recovery of the starting value of CNTs resistance at room temperature. Heat-treatment in vacuum at 110–150 °C led to the expected renewal of the starting properties of CNTs. That indicated the tendency to a slowly proceeding chemisorption of oxygen. The resistance-based observations were supported by the changes of thermoelectric power. The first investigated samples were *p*-type semiconductors but they changed dramatically after an intensive oxidation of SWCNTs. After the treatment, the samples behaved like apparent metallic conductors.

A question may arise how to determine the acidity of CNTs containing oxygen functionalities. Hu et al.[25] investigated acid-base properties of SWCNTs of that kind. The

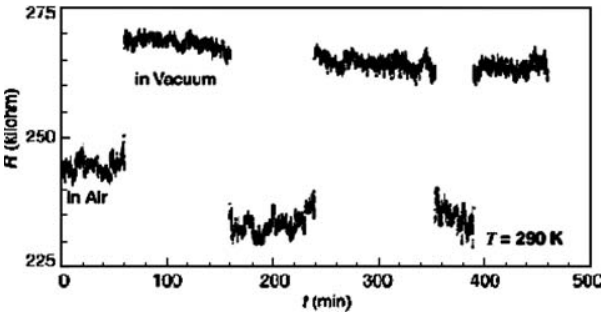

Fig. 12. Sensitivity of the electrical resistance *R* of SWCNT to gas exposure at a temperature (*T*) of 290 K. The nanotube resistance switched by 10 to 15% as the chamber surrounding the sample was alternately flooded with air or evacuated. Identical results were obtained if pure dry oxygen was used rather than air, indicating that oxygen was the source of the effect. Likewise, changing the chamber purge gas between oxygen and any inert gas resulted in similar stepwise changes in *R*. Reprinted with permission from [24], P. G. Collins et al., *Science* 287, 1801 (**2000**). © 2000, AAAS.

method was based on the assumption that the standard method of Bohem, applied widely for other carbon materials, was also applicable to CNTs. Thus, authors employed NaOH and $NaHCO_3$ solutions to determine the total acidity of oxidised sites (NaOH titration) and the content of –COOH groups ($NaHCO_3$ titration). It was found that commercially available SWCNTs contained up to 3% acidic sites that responded to the titration with NaOH. Moreover, almost the whole acidity could be ascribed to –COOH groups. Thus, the acid-base behaviour of oxygen functionalities on CNTs did not differ much from analogous groups on other carbon materials.

The action of fluorine leads to direct reaction between F and C atoms in CNTs. Lee et al.[26] tried to functionalise SWCNTs by treating them with fluorine (direct action on bare tubes). The temperature of the treatment was set at 150–300 °C. At the latter temperature the F/C ratio reached the value of 0.65. XPS investigations revealed a subsequent reduction of the number of sp^2 hybridized carbon atoms. The effect was attributed to the carbon atoms at the ends of the tubes. Extended fluorination led to the formation of $–CF_2-$ and $–CF_3$ groups due to breaking of carbon–carbon bonds. The electric conductance of fluorinated SWCNTs decreased substantially which was ascribed to an electron transfer from the tubes to fluorine atoms. Fluorination positively influenced the solubility of CNTs in alcohols and other solvents.

1.3.2. Metallization and Deposition of Metal Oxides

Metal cluster modified CNTs are of interest for chemical sensing since some metals (as well as their oxides) are regarded as catalyst for many reactions potentially to be employed in sensor operation. Deposition of metal particles on the walls of CNTs and filling them with metal particles or wires were one of the most important problems

solved by groups working on novel carbon materials. Metal or metal oxide introduction to CNTs can be divided into two general categories: insertion and encapsulation. Insertion is when the modifying substance is immobilised inside (or outside) already exiting CNTs. Encapsulation is the process in which CNTs either grow around modifying particles or are synthesised parallel with crystallization of modifiers. Several methods have been announced so far; Chen and co-workers[27] reported a successful application of three basic approaches to solving the problem, so called:
(1) one-step,
(2) two-step, and
(3) two-step by means of metal complexes.

The one-step method of insertion consists of heating MWCNTs in a mixed solution of HNO_3 (azeotropic solution ca. 68% wt) and a metal nitrate. Nitric acid due to its oxidative properties opened the tubes by cup removal at the ends of MWCNTs. Beside that, the action of nitric acid removed some impurities from CNTs like amorphous carbon particles and catalyst residuals. Parallel to the process of MWCNTs "decapitation," ions from the dissolved metal nitrate could penetrate the inner space of CNTs and crystallize after drying. Then, one needed to reflux the excess reactants with water. Subsequent calcination at 400–500 °C of such treated samples in an inert gas atmosphere transformed the deposited metal nitrates into corresponding metal oxides (Fig. 13). At this stage, such treated tubes were in fact metal oxide-modified CNTs and the whole process could be terminated if one intended to synthesise that kind of modified CNTs. A further reduction of oxide-modified CNTs was possible upon hydrogen treatment at 400–500 °C. In this way, metal oxide particles were reduced to metal particles. The one-step insertion was also helpful for filling CNTs with complex oxides like perovskite-type oxides (Table II). That was possible provided the primary modifying solution contained (beside concentrated nitric acid) a stoichiometric mixture of appropriate metal nitrates (dissolved). Heat treatment in an inert gas atmosphere led to crystallization of the complex oxides.

The two-step method of insertion was applicable for filling CNTs with materials (or their derivatives) that were not soluble in water or were not resistant to the action of water vapour, oxygen, carbon dioxide, and HNO_3. The merit of the two-step method consisted in the separation of tube opening from the filling of CNTs with modifying chemicals. Thus, the combined opening and purifying of CNTs by concentrated HNO_3 was the first step. The oxidative treatment of HNO_3 created oxygen functionalities (mostly –COOH and –OH) at the open ends of CNTs. The functionalities blocked the entrance to the interior of the MWCNTs. Therefore the groups often had to be removed by a heat treatment in a stream of inert gas or in vacuum (900–1000 °C) in which the groups were removed and the species like CO_2, CO, H_2O evolved. Such cleaned

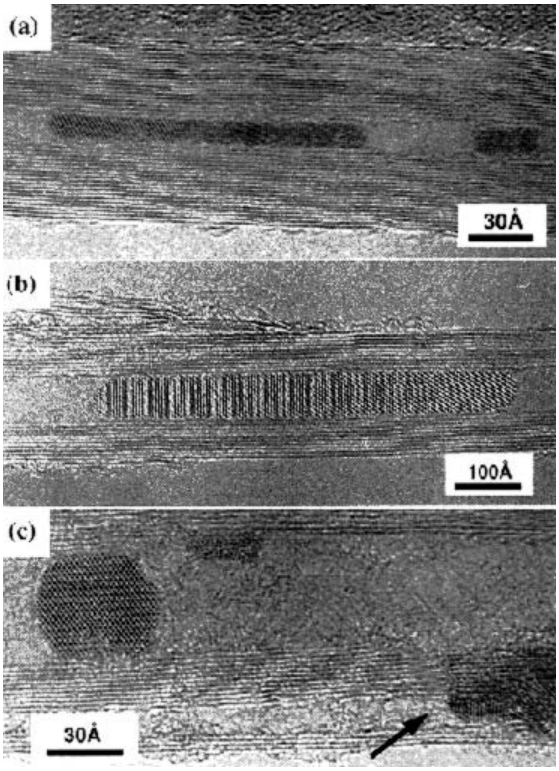

Fig. 13. (a) Nanotube filled with nickel material; the observed fringes of 2.4 ± 0.05 Å correspond to the distance between the (111) planes in NiO. (b) Encapsulated single crystal of Sm_2O_3 with two sets of metal fringes seen inside a carbon nanotube. The Sm_2O_3 lattice fringes 90° to the nanotube wall correspond to the (400) lattice planes of Sm_2O_3. (c) Nanotube containing cavity intercalated crystalline Nd_2O_3 (in the bore of the nanotube) and intralayer intercalated Nd_2O_3 (arrowed). Reprinted with permission from [27], Y. K. Chen et al., *J. Mater. Chem.* 7, 545 **(1997)**. © 1997, Royal Society of Chemistry.

Table II. The list of encapsulated metal and metal oxide particles.

Encapsulated or inserted substance	Starting materials
La_2O_3	$La(NO_3)_3\ 6H_2O$
Pr_2O_3	$Pr(NO_3)_3\ 6H_2O$
CeO_2	$Ce(NO_3)_3\ 6H_2O$
Y_2O_3	$Y(NO_3)_3\ 5H_2O$
Nd_2O_3	$Nd(NO_3)_3\ xH_2O$
Sm_2O_3	$Sm(NO_3)_3\ 6H_2O$
$FeBiO_3$	$Fe(NO_3)_3\ 9H_2O + Bi(NO_3)_3\ 5H_2O$
UO_{2-x}	$UO_2(NO_3)_2\ 6H_2O$
NiO	$Ni(NO_3)_2\ 6H_2O$
MoO_3	MoO_3
MoO_2	MoO_3
ZrO_2	$ZrCl_4$
ZrO_2	$ZrO(NO_3)_2\ xH_2O$
Re	$KReO_4$
Pd	$Pd(NO_3)_2$
Ag	$AgNO_3$
AuCl	$5AuCl_3$
Au	$AuCl_3$
CdO	$Cd(NO_3)_2\ 4H_2O$
CsS	$CdO + H_2S$

Source: Reprinted with permission from [27], Y. K. Chen et al. *J. Mater. Chem.* 7, 545 **(1997)**. © (2005), Royal Society of Chemistry.

CNTs could be brought to contact with the filling substances since there were no geometric and chemical (possible reaction with O-containing functionalities) obstacles. The filling substance could be applied in molten state. The filling could be followed by the measures described in the case of the one-step method, i.e., calcination or calcination with subsequent reduction to achieve metal oxide particles or metal particles respectively.

There was a substantial difference in the form of the modifying substances after their introduction to CNTs, which was dependent on the form of filling substance. The application of solutions resulted in the formation of small (1–5 nm) metal and metal oxide particles while molten modifiers often produced long, continuous metal and metal oxide crystals (wires). Rao et al.[28] also obtained metal wires in SWCNTs by the contact of the tubes with molten salts and subsequent reduction with oxygen. Surface tension of molten modifiers is the main obstacle hindering the process of modifier infiltration when the surface tension is too high. If high surface tension of a molten modifier excluded its application in the way described above, other metal insertion could be employed in the second step. After opening and the removal of O-type functionalities, CNTs were subjected to the penetration by metal complexes in solution. Subsequent calcination or calcination followed by reduction transformed the introduced complexes in metal and metal oxides as formerly mentioned. In general, the above described methods result in the filling of the interior of CNTs with desired species. In some cases on observed the penetration of the interlayer spaces in MWCNTs and subsequent bulge of the materials i.e., the inter lattice distance increased from 0.34 nm to 2 nm.

Liu and co-workers[29] synthesised CNTs decorated with well-dispersed Co particles. The CNTs were obtained by the method of C_2H_2 (in N_2) decomposition over Co catalyst first deposited onto a SiO_2 substrate. Such obtained MWCNTs were treated with a concentrated solution of HNO_3, rinsed and then subjected to impregnation with $Co(NO_3)_2$. The sample was calcinated at 480 °C and reduced with H_2 at 420 °C. Apparently, the route was similar to the two-step method of internal metallization of CNTs described previously but there was one significant difference. There was no step in which the oxygen containing functionalities (certainly present after the HNO_3 treatment) were removed. Thus, the functionalities remained. As in the case of polycrystalline carbons the –COOH and –OH groups are capable for ion exchange. The same groups may be expected at the open ends of oxidized CNTs or defect sites. Liu and co-workers found in TEM investigations that the synthesised MWCNTs and later oxidized tubes had numerous defects at the walls (Figs. 14 and 15).

Some reports suggest[30] the formation of metal particles started from the open end of CNTs and proceeded towards the central part of the tubes. The results obtained

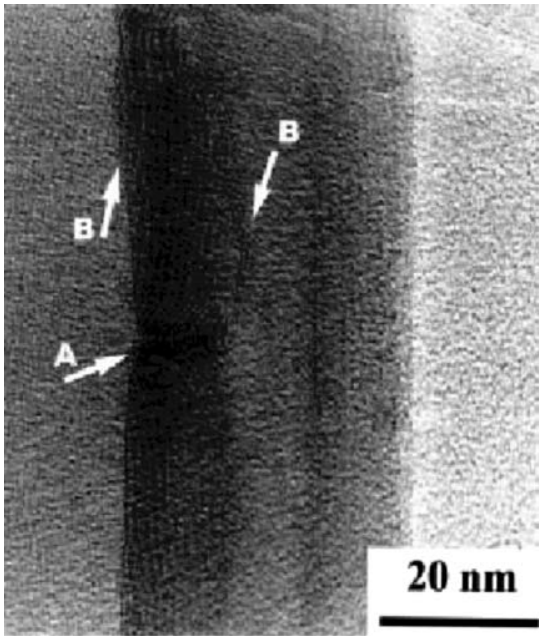

Fig. 14. HRTEM image of a CVD-grown carbon nanotube with defects. Arrow A points out a topological defect and arrows B indicate incomplete graphitic layers. Reprinted with permission from [29], Zong-Jian Liu et al., *Phys. Chem. Chem. Phys.* 3, 2518 (**2001**). © 2001, Royal Society of Chemistry.

by Satishkumar et al.[31] are consistent in full with the above conclusion. The authors achieved a perfect distribution of metal particles (Au, Ag, and Pt) deposited on the oxidized (HNO_3 treatment) SWCNTs by simultaneous reflux with NHO_3 and $HAuCl_4$ (or H_2PtCl_6, $AgNO_3$), and subsequent reflux first with HNO_3 and then with $HAuCl_4$ (or H_2PtCl_6, $AgNO_3$). In this case (MWCNTs), the metal particles were situated outside the tubes. It is to remember that the result reported for SWCNTs claimed an internal metallization of the tubes. It might be a result of different internal diameter of the MWCNTs and SWCNTs. Probably the wider was the tube the easier was metal insertion in the cavity of CNTs. The second method produced also small Au particles but much more uniformly scattered along the tube (Fig. 17). Another method involved the admission of ethylene glycol to the Pt-, Au-, and Ag-containing solution. The yield of metal particles was higher since ethylene glycol acted as a reductor (Fig. 18). The deposited Pt particles were small and of uniform size (ca. 2 nm). Chen and co-workers[27] proved that other species could be deposited in the cavities of CNTs. They transformed the encapsulated metal oxides not only in element metals (reduction by the hydrogen treatment described) but it was possible to change them in metal sulphides under the action of H_2S. For instance, one got CdS by the transformation of CdO.

Metal and their derivatives can be introduced in the CNTs cavity by encapsulation achieved by a modification of the standard arc discharge method of CNTs synthesis. The modification consists in the introduction of metals or

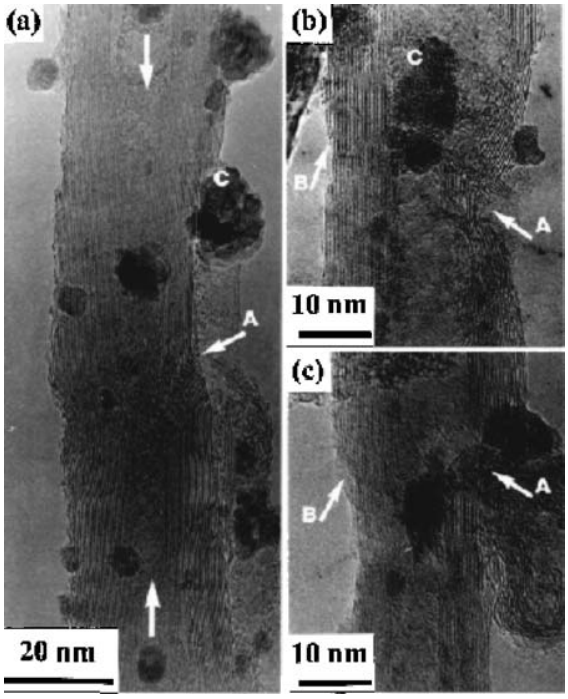

Fig. 15. HRTEM images of Co-deposited carbon nanotubes oxidized by nitric acid. Arrows A indicate the corroded regions and arrows B indicate the open edges of graphitic sheets. (a) A nanotube with its internal diameter decreasing from both the ends along the nanotube axis indicated by two arrows in the middle of the nanotube. (b) Both outer and inner walls of nanotubes after being attacked by nitric acid. (c) A thinned nanotube with a hole in the right side wall. Reprinted with permission from [29], Zong-Jian Liu et al., *Phys. Chem. Chem. Phys.* 3, 2518 **(2001)**. © 2001, Royal Society of Chemistry.

metal derivatives to graphite electrodes, which are employed for lighting the arc. The vaporized electrode (anode) material contains carbon and metal atoms that later can deposit in form of metal filled CNTs. Moreover, the formation of metal carbides also occurs. This method of CNTs metallization seems to be less controllable and less flexible than the presented wet chemistry methods.

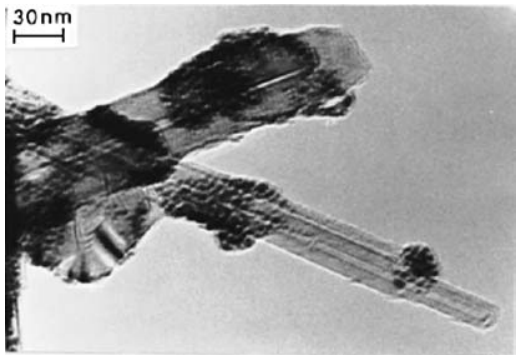

Fig. 16. A TEM image of pristine nanotubes with agglomerated gold particles. Reprinted with permission from [31], B. C. Satishkumar et al., *J. Phys. D: Appl. Phys.* 29, 3173 **(1996)**. © 1996, Institute of Physics IOP Publishing Ltd.

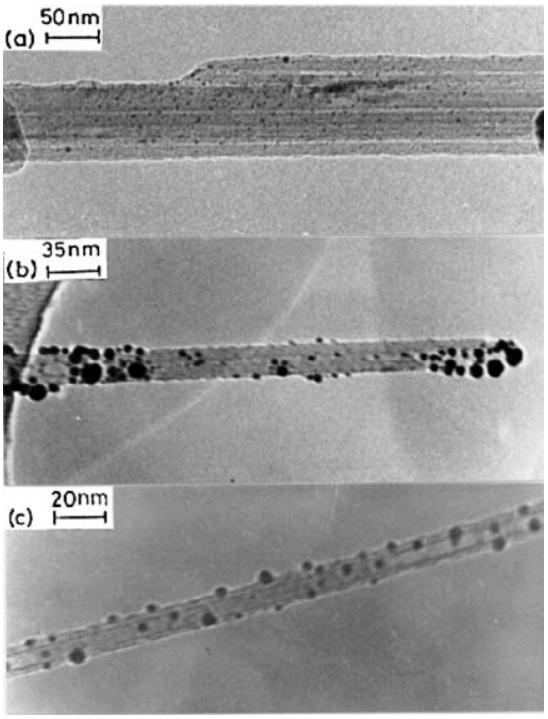

Fig. 17. TEM images of nanotubes decorated by Au nanoparticles; decoration carried out (a) by refluxing with $HAuCl_4$ and HNO_3, (b) by refluxing acid treated nanotubes with $HAuCl_4$ and THPC and (c) by the same procedure as (b) except with mild sonication. Reprinted with permission from [31], B. C. Satishkumar et al., *J. Phys. D: Appl. Phys.* 29, 3173 **(1996)**. © 1996, Institute of Physics IOP Publishing Ltd.

The arc encapsulation of metal was described by Sloan and co-workers.[32] According to numerous quoted literature announcements almost half the elements in the Periodic Table have been introduced into CNTs by the

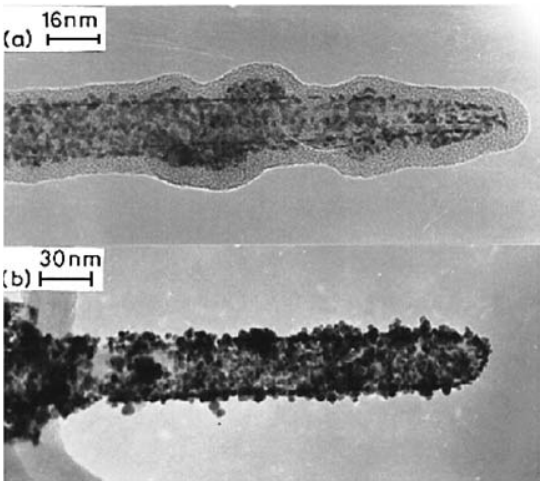

Fig. 18. TEM images of nanotubes decorated by Pt nanoparticles: Decoration carried out (a) by refluxing with H_2PtCl_6 and HNO_3 and (b) by refluxing with H_2PtCl_6 and ethylene glycol. Reprinted with permission from [31], B. C. Satishkumar et al., *J. Phys. D: Appl. Phys.* 29, 3173 **(1996)**. © 1996, Institute of Physics IOP Publishing Ltd.

method: Lanthanides, the first row of transition metals, the platinum group, the main group elements (see references in the review paper).

Metallization of CNTs often occurs during pyrolysis. Bladh and Rohmund[33] fabricated SWCNTs by the catalytic decomposition of a mixture of gases on iron catalyst particles (1000–1100 °C). The mixture consisted of CO, C_2H_2, and H_2. Carbon monoxide was additionally saturated with $Fe(CO)_5$ to the concentration of few ppm. The obtained SWCNTs were characteristic because of iron particles that were encapsulated in the tubes and covered by several graphite layers. The insertion of metal particles into the tubes hinders their direct contact with environment. Therefore, their influence on sensing processes may be questionable. The addition of hydrogen to the gas mixture increased the yield of CNTs due to the reaction: $CO + H_2 \rightarrow H_2O + C$, that supported the standard reaction responsible for the growth of CNTs: $CO + CO \rightarrow C + CO_2$.

Chen and co-workers[34] investigated alkali metal-modified MWCNTs. The nanotubes were obtained by a standard method of catalytic decomposition of methane. The investigated CNTs were then purified from catalyst residuals. After that, the tubes were subjected to the modification with Li and K atoms. The metals were inserted by a solid-state reaction between the nanotubes and lithium (or potassium)-containing compounds like carbonates and nitrates. The basic physical properties of the modified MWCNTs were as follows: Specific surface area ca. 130 m^2/g, density below 1 g/cm^3 (lithium doped). The Li/C and K/C atomic ratios were close to 1/15. Such CNTs were subsequently heated and cooled down to room temperate in H_2 stream. One noticed outstanding hydrogen uptake reaching 20% wt (Li-MWCNTs) and 14% wt (K-MWCNTs) at hydrogen pressure of 1 atm. Comparative samples of Li- and K-modified graphite exhibited a considerable lower affinity to hydrogen i.e., only 35–70% of the H_2-uptake recorded for the modified CNTs. Authors additionally investigated the mechanism of hydrogen adsorption with particular attention to the role of inserted lithium and potassium atoms. It was found basing on FTIR investigations that Li–H bonding preceded the formation of C–H bonds. The dissociative adsorption of H_2 molecules was assumed as the first stage flowed by a spill over of hydrogen atoms. This step was followed by the reaction of atomic hydrogen with carbon atoms in MNCNTs. Thus, lithium atoms were considered as catalytic sites for the formation of atomic hydrogen (in adsorbed form). XRD investigations revealed the formation of CH_x due to the reaction between hydrogen atoms and carbon atoms. It was shown that alkali metals significantly increase the adsorption of hydrogen on modified CNTs. The phenomenon might be applied in mass sensitive devices, however the presented way of hydrogen capture needed elevated temperatures (ca. 500 °C). Such a high temperature is not acceptable by the mentioned mass-sensitive devices as well as the long saturation time (1–2 hours). Fortunately, the K-modified materials could adsorb hydrogen at room temperature. The formation of carbon–hydrogen species on the surface of CNTs may modulate the electric properties of the tubes. That might be a good foundation to employ such modified CNTs as chemiresitors sensitive to hydrogen. Thus, the modification by alkali metals yields interesting material, which has been not intensively explored in sensor research.

Metal oxides can be deposited not only inside CNTs but can cover the walls of the tubes, too. Han and Zettl[35] reported a simple room temperature rout to the functionalization of SWCNTs by covering them with 3–6 nm thick layer of SnO_2. The method is based on the oxidation of Sn^{2+} ions first adsorbed on the walls of the tubes from the solution of $SnCl_2$. The mechanism of SnO_2 formation on the tubes was supposed to be based on the process: $2SnCl_2 + 2H_2O + O_2 \rightarrow 2SnO_2$ 4HCl. Surprisingly the procedure did not need any calcinations at elevated temperature and simple drying in air at room temperature was enough for the formation of oxide coating (Fig. 19).

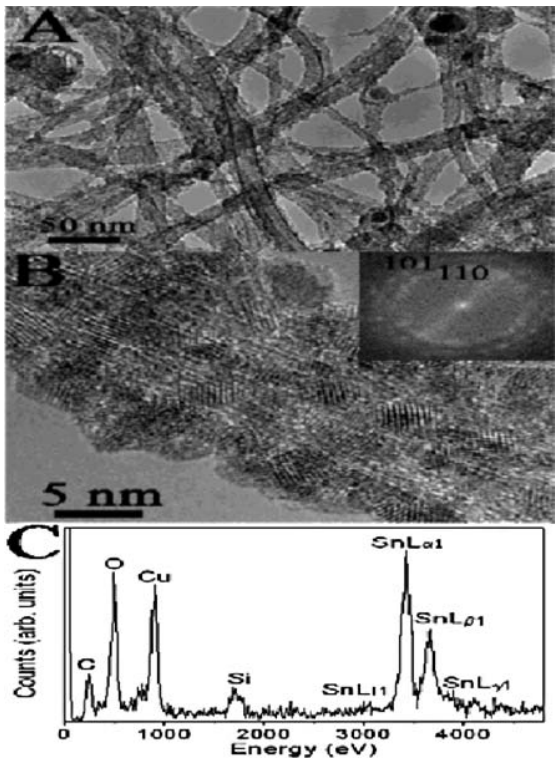

Fig. 19. (A) Low-resolution TEM image of fully coated SWCNTs. (B) High-resolution TEM image of a SWCNT bundle fully coated with SnO_2. The inset is the corresponding FFT diffraction pattern. The three polycrystalline rings correspond to crystal faces of (110), (101), and (200) of tetragonal SnO_2. (C) Typical EDS spectrum of SnO_2-coated SWCNTs. The atomic ratio of O to Sn is near 2. Reprinted with permission from [35], Wei-Qiang Han and A. Zettl, *Nano Lett.* 3, 681 **(2003)**. © 2003, American Chemical Society.

1.3.3. Other Chemical Manipulations

Chemical manipulation of CNTs are not limited to oxidation, metallization, and the deposition of metal oxides. There is long list of other manipulations that are usually performed aiming at better affinity of the tubes to selected substances like water and organic solvents. As will be discussed, the sensing performance of CNTs depend strongly even on non-covalent functionalization.

In the extended report of Seo and co-workers[36] one can find a description of several chemical and physical manipulations of CNTs. Beside widely presented methods for inorganic coating of CNTs (inorganic coating with derivatives of Al–, Ti–, Mg–, and Si– by means of metallorganic and inorganic reactants), one can learn of sidewall covalent alkylation of the tubes that exhibit two basic properties: High affinity towards non-polar organic solvent which eases any further manipulation in such solvents, and susceptibility of the attached alkyl or aryl chains to further chemical modifications. This opens the way for tailoring of basic chemical and physical properties of the modified CNTs. For example, Lim and co-workers[37] elaborated a route to functionalise SWCNTs in which thionyl groups are introduced at the end of the tubes later employed to attach noble metal particles due to the strong affinity of organic thionyl derivatives to metals (Fig. 20). In some other experiments it was shown that –SH groups were isolated from CNTs by long alkyl chains.[38] The phenomenon of CNTs immobilisation on metal surfaces is potentially important for manufacturing of chemical sensors in particular for fabrication of selective electrodes.

Even the alignment of CNTs may be regarded as a kind of functionalization affecting the surface properties of CNTs. Qikun et al.[39] ran amperometric studies on H_2 storage on CNTs obtained by various methods. One investigated CNTs obtained by the arc discharge method, CVD method (C_2H_2 decomposition on an iron catalyst on a Si substrate) and catalytic decomposition of Fe(II) phthalocyanine (self-catalysed decomposition). The results obtained for H_2 adsorption (room temperature, atmospheric pressure) revealed a slow but intensive hydrogen adsorption on the CNTs fabricated by the later method. The maximum hydrogen storage capacity exceeded 8% by weight. Authors quoted reference[40] where one investigated the influence of CNTs alignment on the hydrogen uptake and stated that high hydrogen storage capacity occurred preferable on well-aligned CNTs. In such a case, strong Van der Waals interactions between the tubes positively influenced the adsorption of hydrogen. The adsorption of hydrogen, as concluded from the run of hydrogen uptake curves (Fig. 21) was dependent on the layer structure of the examined MWCNTs.

Sometimes functionalization is used to ease further manipulations with CNTs. Star and co-workers[41] described a route for fabrication of hydrophilic CNTs without any covalent functionalization. Such a non-covalent functionalization does not impair the original properties of CNTs. They adapted the idea originally proposed for the functionalization of fullerenes with cyclodextrines. The method involved sonication of a dispersion containing starch-iodine complex and SWCNTs. The merit of the synthesis consisted in the displacement of I_2 (placed inside a left-handed helix of amylose) by SWCNTs as depicted in Figure 22. The amylose molecules wrap around the tubes allowing stable dispersion of SWCNTs in water. The process seems to be selective to CNTs. Moreover, Star and co-workers showed that the process was reversible and the SWCNTs-amylose complex was destroyed by the hydrolytic action of an enzyme (amyloglucosidase from Rhizopus mold, see Fig. 23).

Zhao et al.[42] proposed another route to functionalise SWCNTs by the attachment of polymer chains to carboxylic groups at the open ends. The process was based on the application of oxalyl chloride to transform –COOH groups into reactive acyl chlorides. The derivatized groups served to anchor polymer chains of poly(m-aminobenzene sulfonic acid)—PABS (Fig. 24). In this way the hydrophobic virgin SWCNTs were changed into a hydrophilic solid due to the polar groups ($-SO_3H$) occurring along the attached chains. The new hydrophilic properties were very helpful for dispersing CNTs in water and other polar solvents. PABS is only one of many possible modifying polymers. According to Zhao and co-workers, the following polymers can be bonded to CNTs, see Table III. An interesting feature of oxygen functionalised CNTs was reported by Sano and co-workers.[43] The oxygen containing functionalities (particularly –COOH groups) at the ends of SWCNTs were forced to condensate that led to the formation of CNT-based rings as presented in Figures 25 and 26. Dicyclohexylcarbodiimide (DCC) was the reagent used to close the CNT-ring by easing the condensation of –COOH and –OH groups. It was also found that the length of SWCNTs prior to the formation of ring had a crucial influence of the process, i.e., if the SWCNTs were shorter than 1 μm only few rings formed. So far, no report has appeared on the application of such cyclic CNTs to chemical sensing where only surface effects may contribute to sensing mechanism and the influence of inner space is excluded.

1.4. Porosity of Carbons

Porosity is an important factor in sensor research since it may positively or negatively influence the sensing properties of a material. Using the term "porosity" in the review one should concentrate on so called open pores, i.e., vacancies in a solid material that are open to environment. Internal vacancies exist in solids but they are of secondary importance. Pores directly influence the adsorption abilities of a solid. Dubinin and other researchers[44] proved that molecules in pores are subjected to much

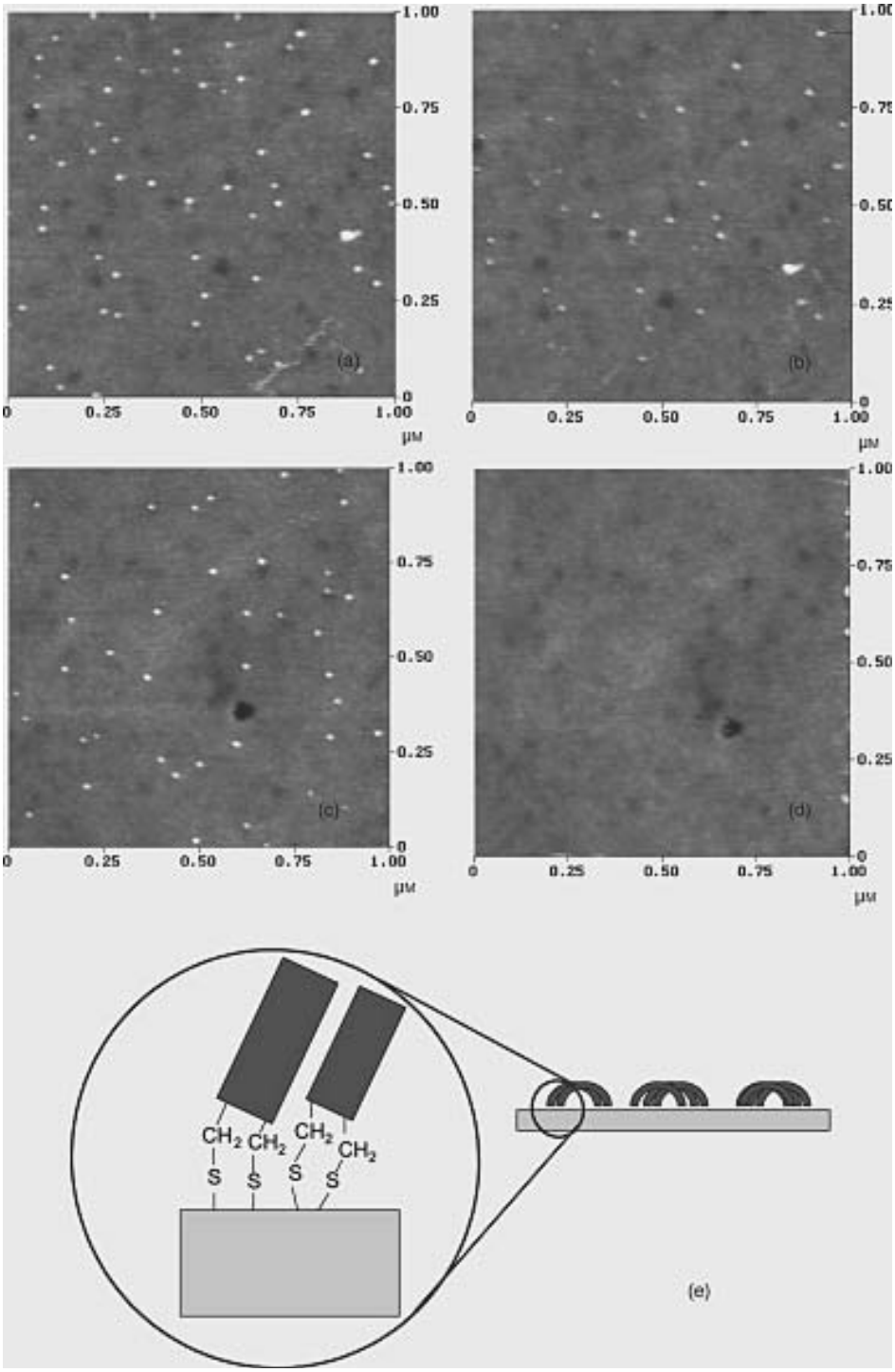

Fig. 20. The AFM images of thiolated CNTs on a gold surface, obtained by a scanning force of (a) 1 nN and (b) 2 nN in the contact mode. The substrate was a silicon wafer coated by a 9 nm thick gold layer, with a 1 nm thick titanium layer in between. The peak-to-valley roughness of the gold surface was within 1 nm. Reduction in the number of the CNTs in (b) reflects their removal from the viewing area by a larger scanning force. The images (c) and (d) were obtained in another region, with a scanning force of 1 and 5 nN, respectively, in the contact mode. The CNTs are seen to be readily removed in (d) by a scanning force of 5 nN. (e) A schematic representation of the vertical view image of (a). The thiolated CNT has thiol groups at both ends, which bind to the gold surface. The flexible tube body of SWNT allows the CNT to conform its geometry for maximum binding energy at the expense of the bending energy. The result is a "bow-type" bundle of the thiolated CNTs. Reprinted with permission from [37], Jong Kuk Lim et al., *Synth. Meter.* 139, 521 **(2003)**. © 2003, Elsevier.

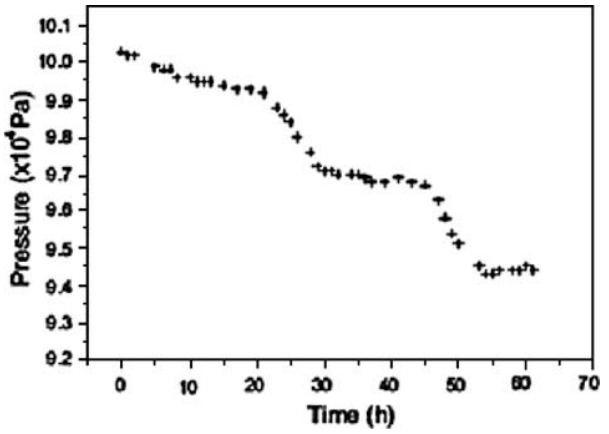

Fig. 21. Uptake of H_2 for sample 3. The plot shows obvious descending steps of the pressure. Reprinted with permission from [39], W. Qikun et al., *Int. J. Hyd. En.* 27, 497 **(2002)**. © 2002, Elsevier.

stronger attraction forces compared to adsorption on a flat surface. The intensive attractive forces are often described as an adsorption potential of pores. The last statement is particularly important in the case of small pores. IUPAC established limits regarding the terms micropore (diameter below 2 nm), mesopore (diameter between 2 and 50 nm) and macropore (diameter above 50 nm). Regarding the sensor related applications open porosity may be the factor supporting sensing properties of the active material applied. For example, the presence of pores increases adsorption of detected molecules from gas or liquid phase. In this way, substances present around a porous material get concentrated on its surface (in pores) much more intensively than on a nonporous solid. On the other hand, immobilization of detected molecules particularly inside micropores is often an irreversible effect at the temperature at which the molecules are adsorbed. Often desorption from micropores must be forced by heating the porous solid.

The importance of porosity in determining the performance characteristics of an adsorbing material was proven by Varghese et al.[45] They studied the effect of pore size and uniformity on the sensing performance of nanoporous alumina films towards water vapour. The porous alumina films were fabricated by anodic oxidation of aluminum film in water solutions of oxalic and sulfuric acid. The pore size was ranging from 2.6 to 60 nm. During extensive sensitivity studies one disclosed that smaller pore size expanded the sensing range (relative humidity RH). The sensitivity of the porous sensors increased in the range of low RH values. The operating range of the sensors could be adjusted to particular needs by the selection of appropriate pore structure of the sensors. The paper points out the importance pore-based effects in sensing phenomena particularly if the adsorbed substance exhibits the tendency to capillary condensation.

Carbon porosity seems to be a natural property regarding the mechanism of graphite formation (nano- and

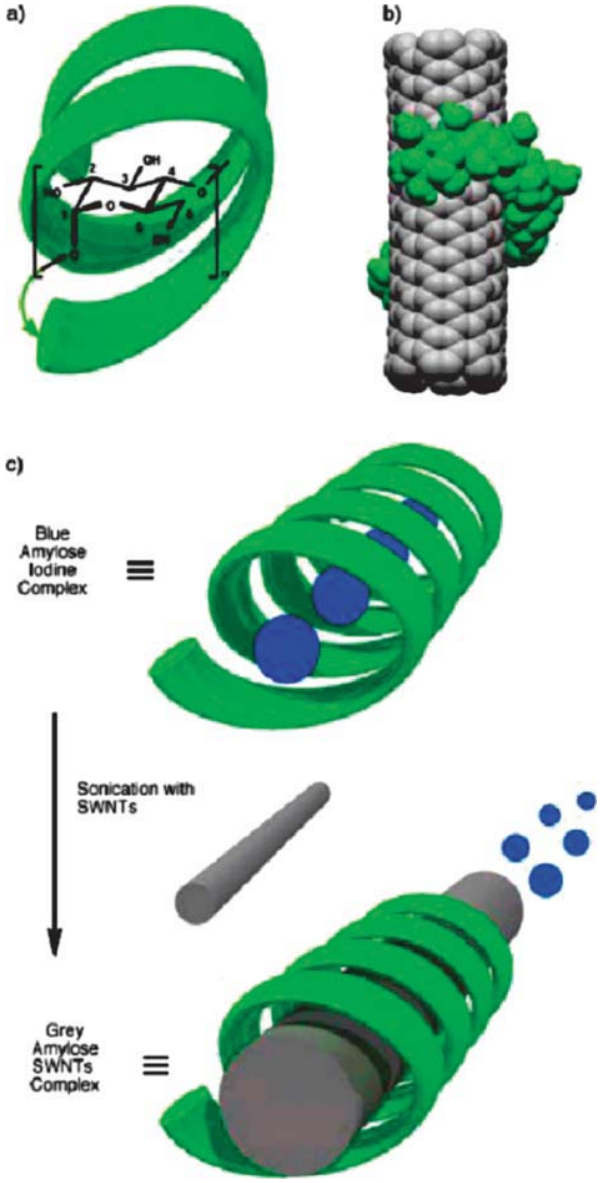

Fig. 22. (a) Schematic representation of the left-handed helix adopted by amylose when it complexes with small molecules. One α-1,4-linked ρ-glucopyranose residue, with its numbering system is overlaid on the helix. (b) Space-filling representation of the result of computer modelling (molecular mechanics and molecular dynamics simulations using the solvation model for water) between a short (6,6)-SWCNT and maltooctaose. (c) Schematic representation of the ™pea-shooting type of mechanism whereby carbon nanotubes displace iodine molecules from the amylose helix. Reprinted with permission from [41], A. Star et al., *Angew. Chem. Int. Ed.* 41, 2508 **(2002)**. © 2002, Wiley-VCH.

microcrystallites) during the carbonisation of some carbon-rich substances. The process of graphite formation is accompanied by an intensive emission of gases and vapours. Mass loss of a heat-treated sample sometimes exceeds 90% of the initial mass, with the atoms involved in the molecules of emitted gases leaving vacancies in the solid. The subsequent aromatisation causes the shrinkage

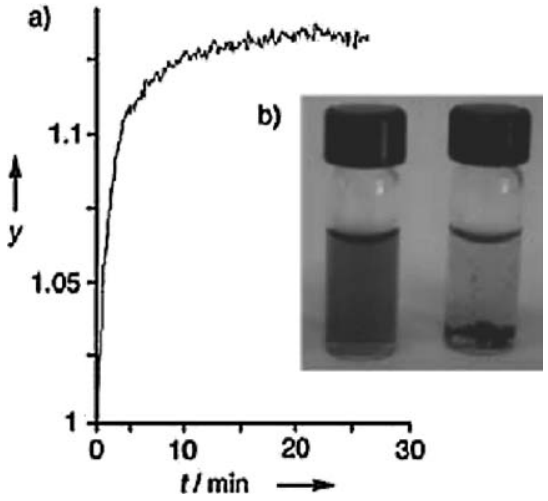

Fig. 23. Enzymatic hydrolysis of the starch-SWNT complex. (a) Changes (y is the refraction in arbitrary units) in light scattering upon addition of amyloglucosidase and (b) a photograph of vials containing the complex before (left) and after (right) addition of the enzyme. Reprinted with permission from [41], A. Star et al., *Angew. Chem. Int. Ed.* 41, 2508 **(2002)**. © (2002), Wiley-VCH.

of some domains in the carbonised material. One assumes the pores in carbon to be slit-type pores.[46] Simplified picture of pores in polycrystalline carbons is presented in the diagram below (Fig. 27).

The porosity of carbons obtained by a direct carbonisation of a selected precursor is often limited. So-called activation is necessary to increase the specific surface area of carbons and to develop their pore structure. There are several classic activation methods like activation by means of gases (and vapours) and activation by the impregnation of precursor. Activation by means of gas consists in the application of gases and vapours causing oxidation and gasification of atoms on carbon matrix. For this method, one may apply O_2, H_2O (steam), and CO_2 at elevated temperatures.

Impregnation of a carbon-rich precursor (or mixing) with substances like $ZnCl_2$, H_3PO_4, NaOH, Na_2CO_3, and Na_2SO_4 can facilitate pore formation.[47] The action of the impregnants consists in their dehydration properties.

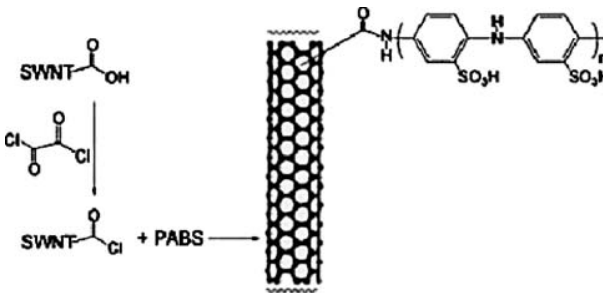

Fig. 24. Reaction of SWCNTs with PABS. Reprinted with permission from [42], B. Zhao et al., *Adv. Fuct. Mat.* 14, 71 **(2004)**. © 2004, Wiley-VCH.

Table III. Polymers attachable to CNTs.

Polymer
Poly(vinyl pyrolidone)—PVP
Poly(styrene sulfonate)—PSS
Poly(m-phenylenevinylidene)–PmPV
Poly(pyrrole)—Ppy
Poly(p-phenylenebenzobisulfonate)—PBO
Poly(vinyl acetate –co-vinyl alcohol)

Source: Reprinted with permission from [42], B. Zhao et al., *Funct. Mat.* 14, 71 **(2004)**. © (2004), Wiley-VCH.

The agents can help to hydrolyse some components of organic substances, e.g., wood. The residuals of the activators should be rinsed with water leaving pores. Means of alkaline activators, particularly NaOH or KOH, reduce the temperature needed to carbonise organic substances. The bases act as oxidants transferring atoms from carbon matrix to the gas phase. One may tailor the pore structure of carbons by the polymer blending method proposed by Ozaki et al.[48] and shown on the below diagram (Fig. 28). The merit of the method is the blending of two kinds of polymer and subsequent carbonisation of the mixture. One of the polymers is a "high carbon yield polymer" (sometimes called a carbonising polymer) that evolves low amounts of volatile products. The second polymer is a "low carbon yield polymer" that is characteristic because of high emission of volatile by-products (sometimes called pyrolyzing polymer). The last one decomposes almost totally and vanishes from the product of carbonisation. The product consists of residuals of the carbonising polymer with empty spaces, i.e., pores left by volatilised polymer. Micropores exist in the carbon matrix formed from carbonising polymer while mesopores are in fact the vacancies left by the decomposed pyrolyzing polymer.

Another way to develop a porous structure in carbon is means of sol–gel technique to obtain carbon-rich foams and carbonise them later. Tamon[49] proposed the way leading to the formation of a polymer aqua gel as presented in Figure 29. Another original method is a template

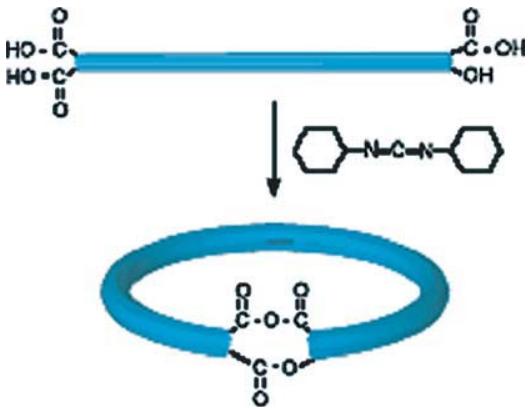

Fig. 25. A possible scheme for the ring-closure reaction with DCC. Reprinted with permission from [43], M. Sano et al., *Science* 293, 1299 **(2002)**. © 2002, AAAS.

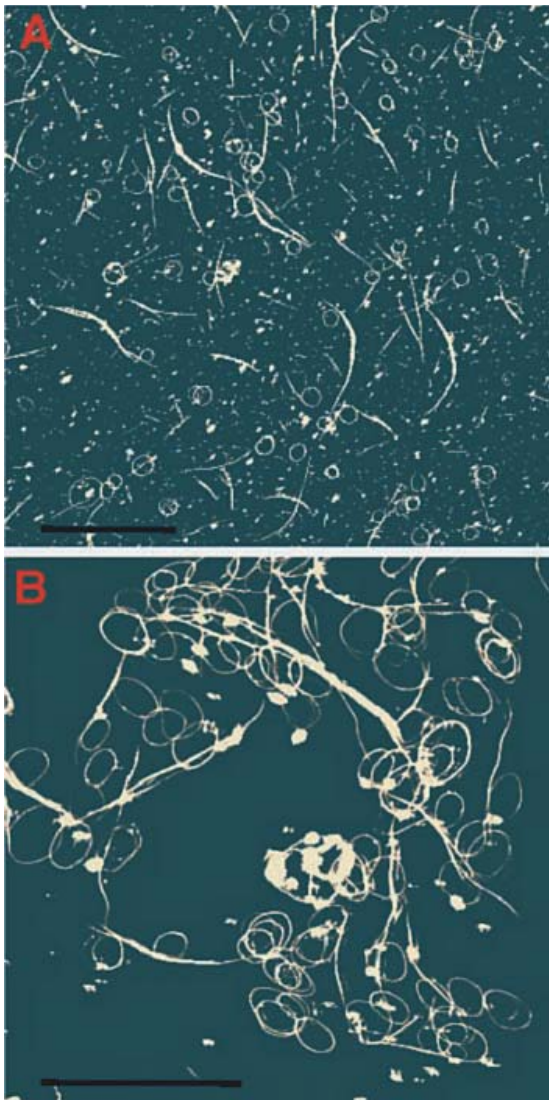

Fig. 26. AFM images of carbon nanotube rings cast on mica. (A) A reaction mixture without any purification. Each ring is dispersed well and is not a part of a long tube. Scale bar, 5 mm. (B) A reaction mixture after washing and filtering through 0.8-mm Tefon Filer. Rings appear to stick to each other after these processes. Scalebar, 2 mm. Reprinted with permission from [43], M. Sano et al., *Science* 293, 1299 **(2002)**. © 2002, AAAS.

carbonisation. The merit of the method is the introduction of a liquid organic precursor (pure or in solution) into an inorganic material having accessible vacancies of nanomeytric dimensions. The liquid precursor penetrates the inorganic template and later both components (organic and inorganic) are subjected to a heat-treatment. Then, the inorganic template may be removed by a selected chemical treatment. Kyotami[50] carbonised polymers in the space between lamellae of a clay. Beside different types of clay, the application of porous silica has been also reported.[51] This methods yields meso- and microporous carbons of high specific surface area. Microporous solids can play the role of a selective membrane that is permeable for

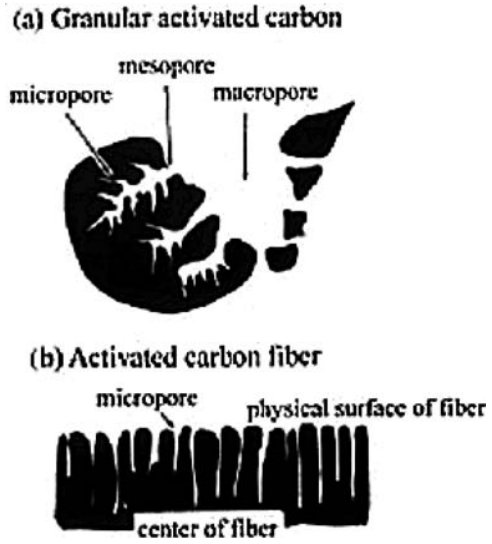

Fig. 27. Pores in granular carbon materials (a) and in carbon fibres (b). Reprinted with permission from [1], M. Inagaki, New Carbons. *Control of structure and functions* **(2000)**. © 2000, Elsevier.

atoms and molecules of an appropriate size and shape. Carbons, if properly prepared exhibit excellent molecular sieving properties. That may be important for some chemical sensors if the problem of cross-sensitivity to undesired molecules occurs.

1.5. Electric Properties of Carbons

From the above-presented phenomena, it is obvious that the heat-treatment conditions must affect the electrical properties of carbons. Usually amorphous carbon is a bad electric current conductor while graphite is a very good

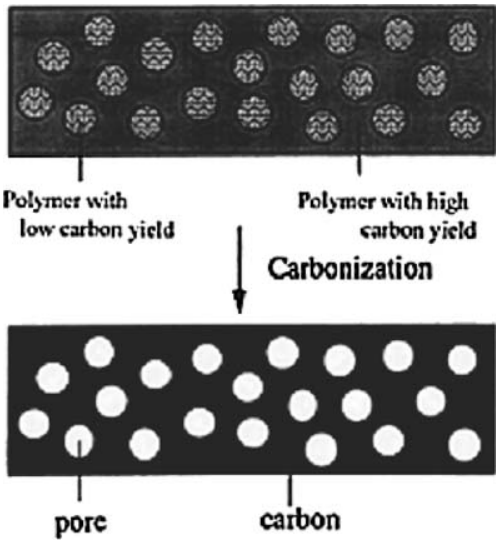

Fig. 28. Visualisation of blending method for developing of carbon porosity. Reprinted with permission from [48], J. Ozaki et al., *Carbon* 35, 1997, 1031 **(1997)**. © 1997, Elsevier.

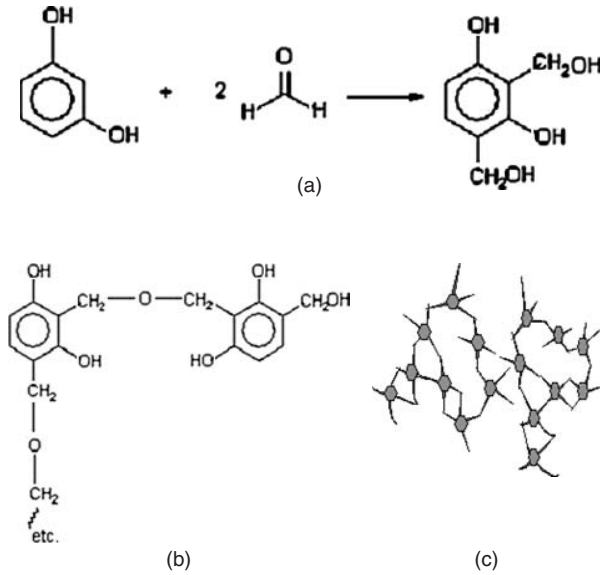

Fig. 29. Formation of organic aqua-gel as a preliminary step to carbon synthesis by sol–gel method as proposed by Tammon.

one when this parameter is measured parallel to graphite planes. Real samples of polycrystalline carbon are a mixture of these two forms of carbon and behave like typical semiconductors. The changes in electronic structure of pyrolyric carbons are summarized in the Mrozowski[52] diagram. The resistivity of pyrolytic carbons decreases dramatically upon increasing temperature of carbonisation.[53] Heat-treatment of CNTs also modifies their electric properties and one may even expect the transformation from *p*-semiconductor to metallic behaviour. Hence it is possible to adjust the electrical properties of carbons for specific applications. Coming from the same raw material one may obtain an insulator, a semiconductor of different energy gap, and an excellent (almost metallic) conductor. No other material offers so much freedom in tailoring of its electrical properties.[54–55] Beside the possibilities offered by heat treatment, carbon materials may be subjected to all modification resulting from doping with foreign atoms.

2. APPLICATION OF CARBONS TO CHEMICAL SENSORS

As mentioned above, carbons may play very differentiated roles in the construction and operation of chemical sensors. In the case of semiconductor chemical sensors, two basic actions must occur to ensure detection of selected species in the gas or liquid phase:
(1) adsorption of detected species on the surface of semiconductor, and
(2) specific interaction of adsorbed-detected species with current carriers in the solid semiconductor.

This phenomenon may proceed by capture or release of current carries by adsorbed species, and through surface reactions between detected species and other molecules as in catalytic oxidation of combustible gases and vapours.

2.1. Carbon Nanotubes as Chemiresistors

The earliest papers announcing successful applications of CNTs to the construction of chemically sensitive devices were published almost ten years ago. Among the works, the paper of Kong, Franklin co-workers[56] is frequently quoted as pioneer one. They investigated *p*-type SWCNTs as chemiresitor sensor for NO_2 and NH_3 detection in air or argon. The obtained results were attributed to the behaviour of single tubes. The CNTs-containing sensors exhibited substantial increase or decrease of electric conductivity upon exposure to the gases. The detected molecules were different regarding their electron affinity. NO_2 was treated as an electron acceptor while electron donor properties were ascribed to NH_3. Thus, one could expect the capture of electron or holes respectively. Since holes were the majority current carriers, their localization (NH_3 adsorption) resulted in an increase of electric resistance. On the contrary, the capture of electrons (NO_2 adsorption) caused the expected decrease of resistance. The examined SWCNTs reacted eagerly with the gases and the response times were short (the order of the of seconds). The ease of adsorption complex formation influenced negatively the time of recovery of the initial resistance, usually reaching the level of hours. Metallic SWCNTs exhibited smaller changes of electric resistance in the same experimental conditions, attributed to the high concentration of current carriers. Metallic SWCNTs exhibited, on the contrary to *p*-semiconductor SWCNTs, a reverse direction of electric resistance change upon adsorption of the gases. Thus, NO_2 adsorption increased the resistance while NH_3 adsorption was responsible for a decreased resistance. The observed behaviour of CNTs obeyed the general rules describing the transfer of charges during adsorption of electron donors or acceptor on semiconductors and metals. As it will be seen, often a peculiar influence of gas adsorption (including NH_3 and NO_2) on the conductance of CNTs has been reported. It particularly deals with the direction of the observed changes of electric resistance, which are not consistent with the general rules and with the results of Kong and Franklin. In most cases, the disagreement is caused by the complex nature of the examined samples. Therefore, one cannot exclude some interparticle-phenomena or an influence of non-CNTs components of hybrid materials.

More recently, Valentini et al.[57,58] investigated the influence of a high temperature exposure to oxygen on the sensing properties of CNTs towards NO_2. The study revealed that intensive oxidation of CNTs at 650 °C causes a dramatic change in the conduction properties of the tubes, with a conversion from a *p*-type semiconductor to metallic. The electric conductivity conversion influenced negatively

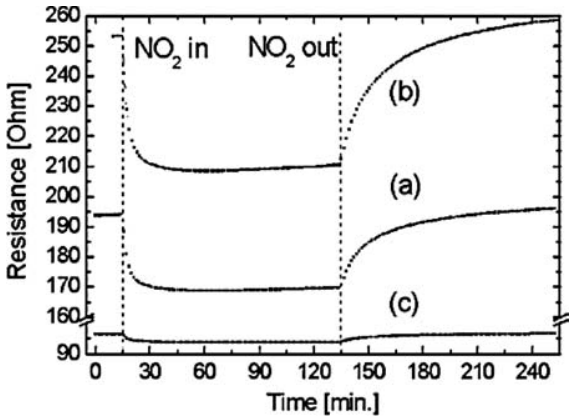

Fig. 30. Resistance changes at an operating temperature of 165 °C in the presence of 100 ppb NO_2 of: (a) As deposited CNTs film after the first thermal treatment; (b) as deposited CNTs film after the second thermal treatment, and (c) CNTs film annealed in air at 650 °C. Reprinted with permission from [56, 57], L. Valentini et al., *Thin Solid Films* 436, 95 **(2003)**. © 2003, Elsevier.

the sensitivity of CNTs towards NO_2. Metallic CNTs (multiwalled, 40–50 nm thick) exhibited rather low sensitivity but still their resistance decreased upon NO_2 adsorption. On the contrary, a gentle heat-treatment at intermediate temperatures (up to 300 °C) helped to develop better sensitivity (Fig. 30).[57, 58] It is suggested that this positive effect resulted from the purification of the as deposited CNTs while defective sites responsible for NO_2 adsorption were still present. The purification consisted in the removal of some graphite particles co-deposited during the growth of CNTs. The high temperature annealing in air (XPS investigations) resulted in the oxidation of nickel cups (residuals of catalyst) to NiO while the carbon atoms were not significantly oxidized. NO_2-sensitivity tests were run at the optimised temperature of 165 °C.

The influence of the catalyst geometry on the growth of CNTs and their electrical response to NO_2 within the range 10–100 ppb have been described.[59] In the study, one compared the sensing properties of two sensors fabricated based on MWCNTs grown on the catalyst layer of different thickness 3 and 5 nm. The thin layer of catalyst led to randomly oriented MWCNTs with diameter of 20–30 nm while the growth on the thick-layer catalyst initiated the formation of uniform MWCNTs but of much wider diameter (Fig. 31).

Compared to oriented MWCNT arrays, randomly oriented nanotubes exhibited relatively high electric resistance, which decreased sharply upon the increase of temperature. The random orientation of MWCNTs resulted in a high sensitivity of such fabricated sensors to the chemical signal of 10–100 ppb of NO_2 in the stream of air. Unfortunately, a drift of base electric resistance was noticed in the case of randomly oriented CNTs, which increased upon increasing number of gas exposures (Fig. 32).

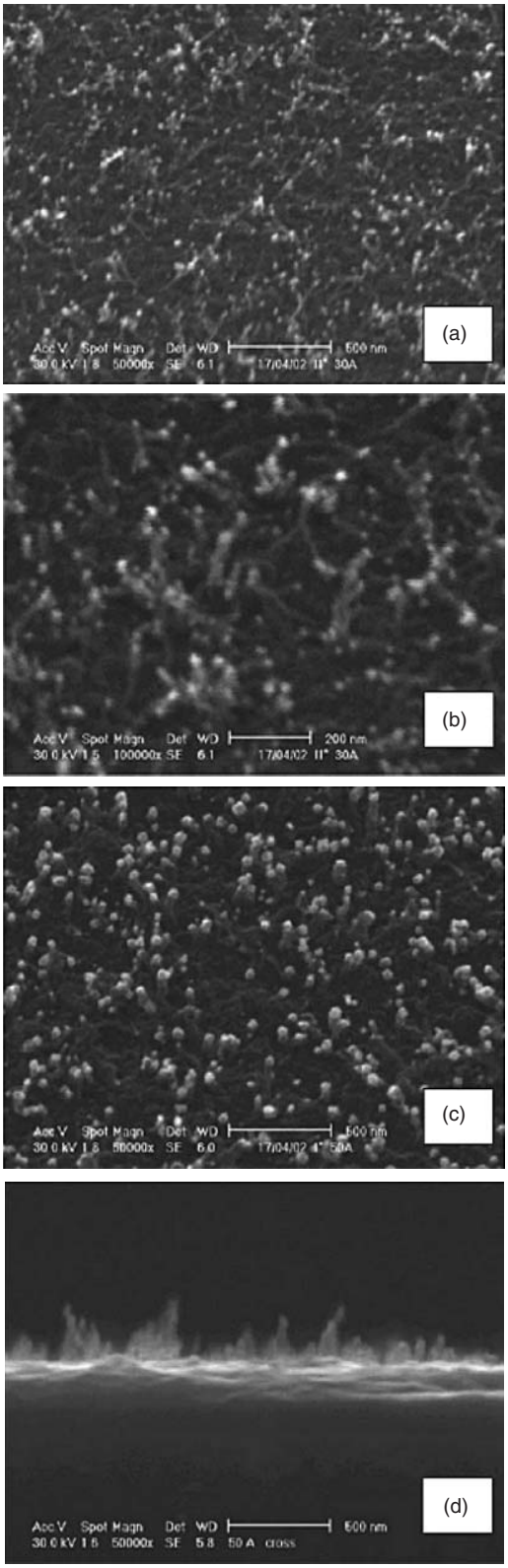

Fig. 31. SEM photograph of CNTs. Top view for sensor A (a) (b), and sensor B (c) cross section for sensor B (d). Reprinted with permission from [59], C. Cantalini et al., *Sens. Actuators B* 93, 333, **(2003)**. © 2003, Elsevier.

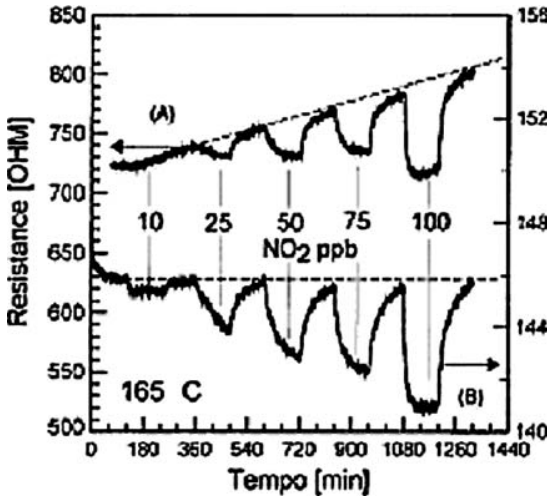

Fig. 32. Dynamic sensor response at 165 °C operating temperature and NO_2 concentrations ranging from 10 to 100 ppb in dry air carrier gas of sensor A and sensor B. Reprinted with permission from [59], C. Cantalini et al., *Sens. Actuators B* 93, 333, (**2003**). © 2003, Elsevier.

The sensors employing well-developed MWCNTs (grown on a thick film of Ni) were less sensitive to NO_2 but reacted faster and gave reversible responses at 165 °C. The behaviour of not-aligned CNTs in the presence of NO_2 was explained basing on the presence of well-developed agglomeration pores and high surface area of CNTs. Thus, the reported work indicates how many factors (physical, chemical, and geometrical) can influence the final sensing profile of the tested CNTs. Li and co-workers[60] investigated a CNT-based chemical sensor for the detection of NO_2 and nitrotoluene vapours. The sensor consisted of SWCNTs deposited on a substrate with interdigitated electrodes. The tubes were synthesised using nickel catalyst, which had to be removed by a standard purification method. Such obtained tubes exhibited extremely high surface area above 1500 m^2/g. The deposition method yielded an ohmic contact between the electrodes and the sensing material made of randomly oriented SWCNTs. No binder was applied and CNTs were only dispersed in dimethylformamide (DMF) and drop-deposited on the sensor background. Authors decided about the use of DMF hoping to debundle CNTs due to the formation of a separation layer of DMF molecules around each individual carbon tube. The initial resistance of the sensing element depended on the number of adhered CNTs, which was controlled by counting the number of dispersion drops set on the substrate. The examined SWCNTs-based sensors responded to the presence of NO_2 within the concentration range 6–100 ppm. The sensors reduced their electric resistance, which effect was qualitatively identical with the result reported by other researchers. There were two distinct drawbacks to the sensors, Figure 33, long recovery and the constant drift of base resistance (a continuous decrease). Li and co-workers proposed to eliminate (or reduce) the negative phenomena by means

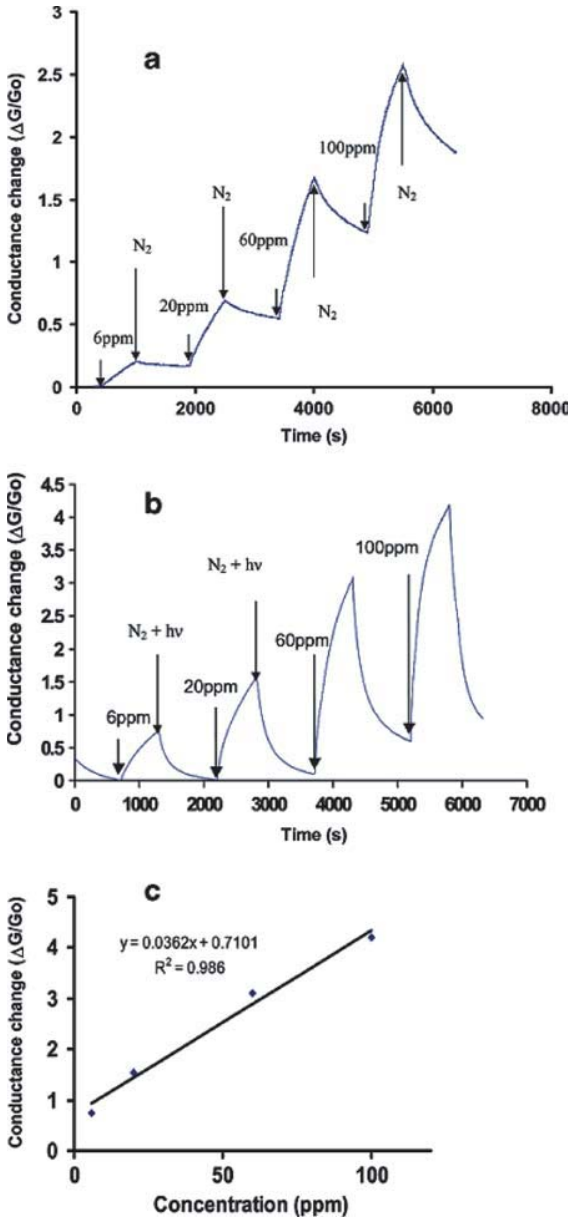

Fig. 33. Representative sensor response for NO_2. Various concentrations of the sample gas and the pure gas injections are shown by arrows. The sample gas is NO_2 in a 400 cm^3/min nitrogen flow at room temperature. Ultrapure nitrogen is used for dilution and purging. (a) Without UV light in the recovery. (b) With UV light for sensor recovery. The UV illumination and N_2 purging start simultaneously. (c) Calibration curve obtained from (b). Reprinted with permission from [60], J. Li et al., *Nano Lett.* 3, 929 (**2003**). © 2003, American Chemical Society.

of UV irradiation during the recovery cycle. That measure reduced the baseline drift and accelerated the recovery to 10 minutes. In the case of nitrotoluene, the response, and recovery proceeded faster while the magnitude of the resistance changes was smaller. In both cases the sensors response was linear versus the gas (vapour concentration) up to 100–150 ppm level. The difference in the response magnitude was explained assuming a

weak bonding (and minor charge transfer) of nitrotoluene to CNTs that resulted from repellent forces between CNTs and aromatic ring in the adsorbate molecules. Additionally, one investigated the influence of benzene and acetone vapours on the resistance of the SWCNTs-based sensors. The extrapolation of the linear sensing characteristic led them to calculate lowest detection limits for both substance which values were 44 ppb for NO_2 and 262 ppb for nitrobenzene. The response to other vapours of different nature like acetone (polar solvent) and benzene (non-polar solvent) were mentioned. The sensitivity to acetone molecules was assumed due to the electron withdrawal from SWCNTs by the interaction with the C=O group. The response to non-polar molecules was a unique finding since hydrocarbon (benzene) adsorption on CNTs was commonly recognized as a minute-charge transfer phenomenon. In such a case, the observed variations of SWCNTs resistance resulted from intertube modulation, i.e., the influence of benzene molecules on the tube-to-tube transport of current carriers. The last phenomenon may be regarded as analogous to the change of interparticle potential barriers in widely investigated (and applied) polycrystalline SnO_2-based chemical sensors for combustible gas detection.

Zhao and co-workers[61] presented a theoretical study on non-covalent functionalization of CNTs by aromatic molecules. The study considered (density functional theory) the interaction between CNTs and selected organic molecules like benzene, cycloheksane, 2,3-dichloro-5,6-dicyyano1,4-bezoquinone (DDQ). Non-covalent functionalization became interesting since it was considered as non-deteriorating for physical and chemical properties of CNTs. Such a functionalization is (in general) considered a reversible process, which can lead to chemical sensing applications. Zhao et al. showed that the adsorption of organic molecules resulted in coupling of π-electrons of adsorbate (if they had such ones) and of adsorbent CNTs. Benzene and cyclohexane were found to be weak electron donors. In general, the theoretical study proved that electronic properties of CNTs were under control by adsorption of organic species, see Figure 34.

The success of SWCNTs application to the detection of NO_2 resulted in theoretical studies describing gas adsorption. Won-Leung Yim[62] investigated the phenomenon by means of the density functional theory. One found that interaction between NO_2 molecule and flat graphene sheets was different from the interaction with rolled up ones. The tensions exiting on the bended spots reduced the stabilization effects of conjugated π-bonds in aromatic rings. That increased the reactivity of the atoms placed in such spots especially in the closing cups at the ends of CNTs. Therefore, the action of NO_2 led to the chemisorption of the molecules at the more reactive sites in SWCNTs. On the contrary, physical adsorption of NO_2 predominated at the walls of CNTs where the state of carbon atoms

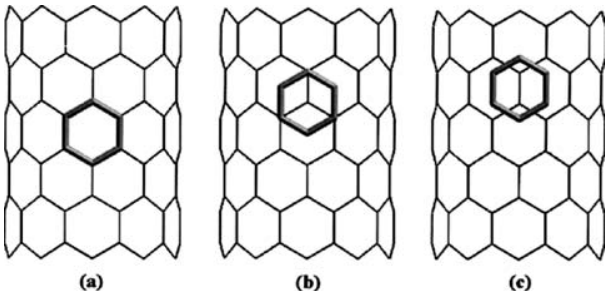

Fig. 34. Three possible sites (a) top, (b) stack, (c) bridge for adsorption of a six-membered ring molecule on a SWCNT. The hydrogen or other atoms on the six-membered ring are not plotted for a clearer visualization. The bridge site is found to be the most favorable. Reprinted with permission from [61], J. Zhao et al., *Appl. Phys. Lett.* 82, 3746 (**2003**). © 2003, American Institute of Physics.

could be described as less reactive. The chemisorption of NO_2 was considered as a direct addition to C=C bonds. The process of chemical bonding of NO_2 was found to be exothermic and hardly reversible while the weak (physical) adsorption was slightly endothermic and therefore reversible. The results may be consistent with the practical observation done during the exposure of SWCNTs to the action of NO_2.

The concept of a novel sensor material was presented by Wei and co-workers.[63] Commercially available SWCNTs were mixed with SnO_2 aiming at the utilization of very well known and widely employed sensing properties of thin (IV) oxide. The composite (containing CNTs) was prepared by the admission a bundle of SWCNTs to the solution of Sn(OOCCH (C_2H_5) C_4H_9), homogenisation and spin coating on a Al_2O_3 substrate with golden electrodes. The sensors were then heat-treated at 500 °C in air. The most important feature of the novel material and sensor was the low operation temperature. The sensor could detect NO_2 in air and nitrogen at room temperature. The observed changes of electric resistance upon the adsorption of NO_2 were completely reversible without any additional cleaning measures like heating or UV irradiation. The sensing characteristics of the sensor, i.e., relative resistance versus NO_2 concentration, were linear up to 1000 ppm. Thus, the presence of SWCNTs in the sensing composite (even in a small amount) caused a spectacular sensitivity increase of the composite sensors with an excellent recovery of the initial electric properties. SEM investigations revealed that SWCNTs were embedded in the SnO_2 matrix, from which Wei and co-workers assumed the existence of two depletion regions in the hybrid SWCNTs/SnO_2 fibres. The material had a fibrillose structure and a cross section of a bundle of the fibres is depicted in Figure 35. The first depletion layer (Fig. 36) existed on the surface of SnO_2 coating. The surface reaction of NO_2 that led to the formation of NO^- may be represented by: $NO_{2(gas)} + O^-_{(SnO_2)} \rightarrow NO^-_{(ads)} + O_{2(gas)}$. The second depletion layer existed near the SnO_2/SWCNTs

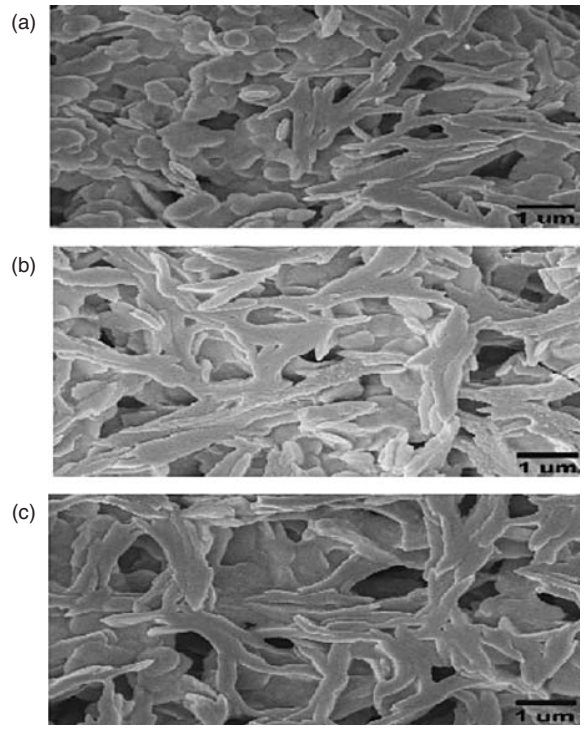

Fig. 35. FE-SEM micrographs of (a) SnO_2 (blank), (b) hybrid SWCNTs/SnO_2 A sensor, and (c) hybrid SWCNTs/SnO_2 B sensor. Reprinted with permission from [63], B. Y. Wei et al., *Sens. Actuators B* 101, 81 **(2004)**. © 2004, Elsevier.

interface. The adsorption of NO_2 molecules proceeded also at that sensitive interface since the sample was porous. Thus, the concentration of electrons in SnO_2 was strongly affected by the depletion layers, which depth increased upon the contact with NO_2. Therefore, the resistance of the hybrid material increased during sensing of NO_2. In the

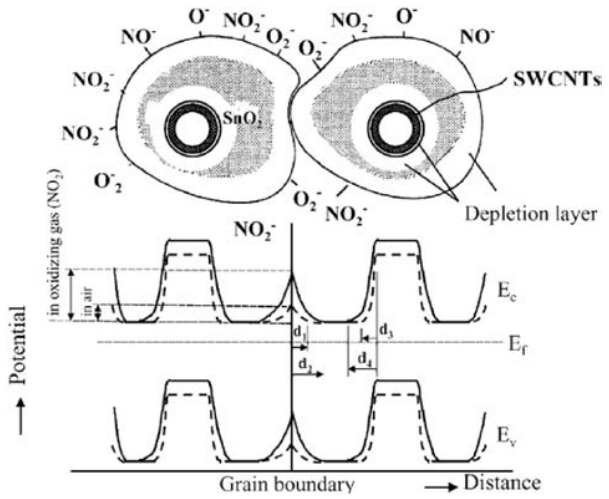

Fig. 36. Model of a potential barrier to electronic conduction at grain boundary for hybrid SWCNTs/SnO_2 sensors. Reprinted with permission from [63], B. Y. Wei et al., *Sens. Actuators B* 101, 81 **(2004)**. © 2004, Elsevier.

case of pure SWCNTs (*p*-semiconductor), the adsorption caused a decrease of electric resistance due to immobilisation of electrons i.e., the minority current carriers. The presented hybrid sensors and the model of its operation assume that the real sensing material was tin (IV) oxide while SWCNTs were only an amplifying substance. It is certainly a novel role ascribed to CNTs in chemical sensing.

Inorganic coatings may be replaced by organic wrapping. An and co-workers[64] embedded SWCNTs in poly (pyrrole) preparing a composite material that was sensitive to NO_2 at room temperature. The hybrid material was fabricated by *in situ* polymerisation of pyrrole mixed with SWCNTs on top of a solid substrate with evaporated electrodes (cyclic drop-wise deposition); the polymer uniformly wrapped the SWCNTs (Fig. 37). The tubes were cross-linked due to the sticking influence of the polymer. In addition, the polymer coating increased the surface area of the nano-composite, which was 3-fold bigger than that of the polymer alone. However, it is not clear how the presence of the polymer influenced the access of gases to the CNTs. The sensitivity of the poly(pyrrole)-SWCNTs composite-based sensors was much enhanced than the sensitivity of a sensor fabricated from SWCNTs only. The adsorption of NO_2 caused an increase of electric resistance of the whole composite. The result was in contrast to other studies on NO_2 adsorption on SWCNTs (described above) without any coating. In these studies NO_2 molecules being in fact radicals, reduced the resistance of *p*-type SWCNTs due to the formation of adsorption complexes, in which electrons from *p*-semiconductor CNTs were immobilized. The peculiar behaviour of the composite (if compared to the reaction of SWCNTs alone) was ascribed to the presence of metallic SWCNTs (beside the semiconductor ones) in the bundle of CNTs that were used for fabrication of the composite sensors. According to the authors, the sample consisted of metallic and semiconductor CNTs and the metallic ones dominated the conduction through the composite material. Authors also assumed that the polymer was modified during polymerisation due to the presence of iron (III) chloride and sodium p-toluene sulfonate (polymer dopant) in an excess amount. Thus, the poly(pyrrole) binder also behaves as an electronic conductor. Although, the sensor was sensitive to NO_2 at room temperature its practical application was affected by a long-term recovery probably caused by NO_2 chemisorption on defected sites on CNTs. It has to be pointed out that the sensing composite became stable and sensitive after annealing at 400 °C for 30 minutes.

Electrical phenomena occurring in solution may be employed to fabricate CNT containing gas sensors. Suehiro and co-workers[65] used dielectrophoresis (DEP) for entrapping of MWCNTs (first dispersed in ethanol) on a selected spot between the interdigitated electrodes. The positive dielectrophoresis force directed the dispersed

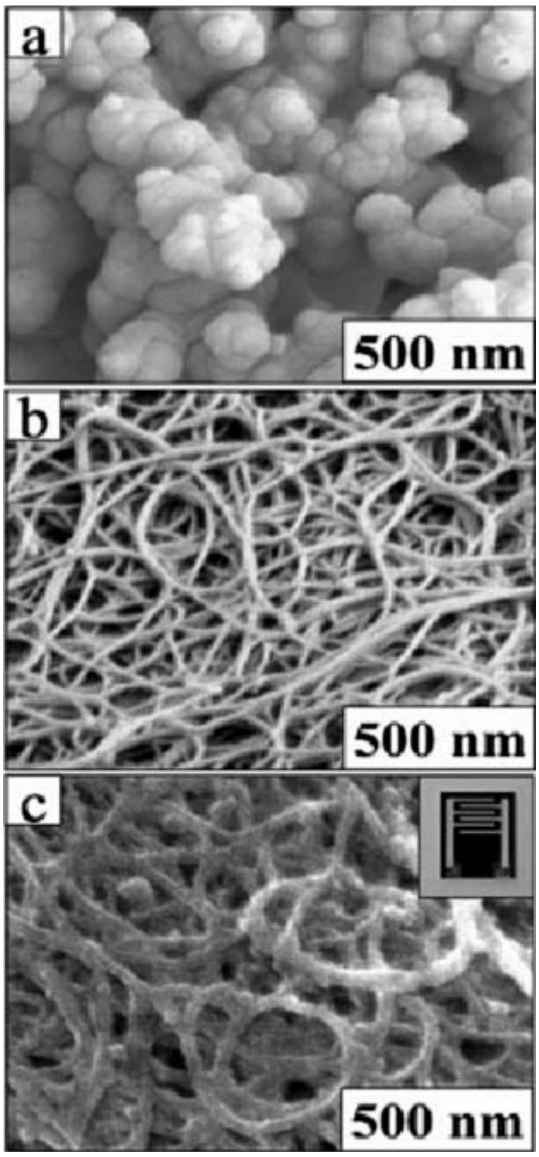

Fig. 37. FE-SEM images of (a) the PPy formed by chemical polymerisation without SWCNTs, (b) the purified SWCNT bundles with a diameter of about 20 nm, and (c) PPy nanocomposite formed by *in situ* chemical polymerisation. Reprinted with permission from [64], K. H. An et al., *Adv. Mater.* 16, 1005 **(2004)**. © 2005, Wiley-VCH Verlag.

MWCNTs towards the region of high intensity of electric field. During dielectrophoresis polarized molecules started to move to a selected spot. Figure 38 shows the schematic diagram of the experimental set-up. The electrodes had a castle-wall pattern in order to create the regions of differentiated intensity of electric field. CNTs were constantly fed to the electrode region where they were entrapped under the influence of AC voltage of 100 kHz and 10 V amplitude. The AC voltage was additionally employed for measuring of the impedance of the sensing layer. After 3 hours, the trapped MWCNTs formed a relatively thick film of randomly oriented CNTs

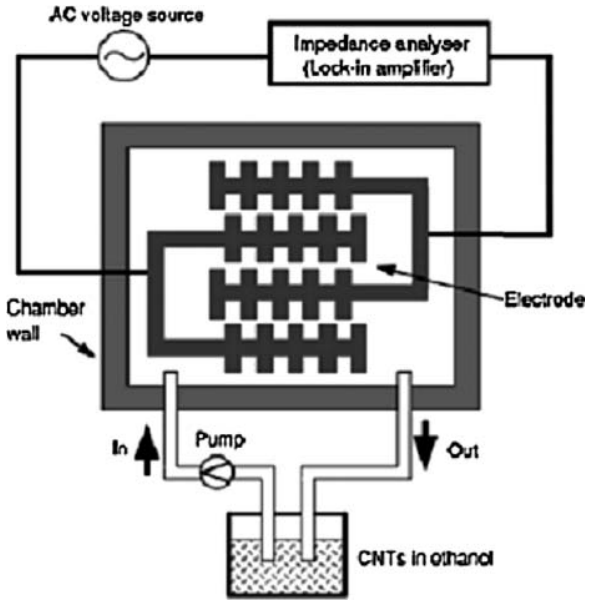

Fig. 38. Schematic diagram of the experimental set-up for MWCNT gas sensor fabrication on a microelectrode using DEP. Reprinted with permission from [65], J. Suehiro et al., *J. Phys. D: Appl. Phys.* 36, L109 **(2003)**. © 2003, Institute of Physics IOP Publishing Ltd.

(Fig. 39). Impedance measurements were employed for the simultaneous observation of the sample's conductance and capacitance during the adsorption of NH_3 (100 ppm at 30 °C). One noticed a reversible decrease of the conductance of the deposited MWCNTs while the capacitance of the CNTs-layer grew. The results are qualitatively consistent with the achievements reported in other studies provided the investigated MWCNTs were *p*-semiconductors. The response of the sensor was linear to the increasing concentration of ammonia in the range up to 10 ppm, beyond which the response diminished.

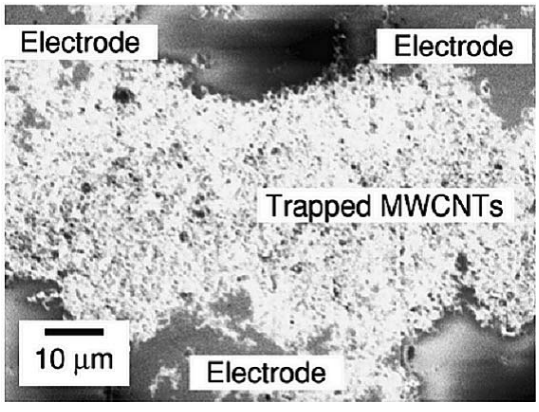

Fig. 39. SEM images of the DEP collection process of MWCNTs on a castellated microelectrode. The amplitude and frequency of the electrode energizing potential were 10 V (peak-to-peak) and 100 kHz, respectively. After 3 h of the DEP process (high magnification). Reprinted with permission from [65], J. Suehiro et al., *J. Phys. D: Appl. Phys.* 36, L109 **(2003)**. © 2003, Institute of Physics IOP Publishing Ltd.

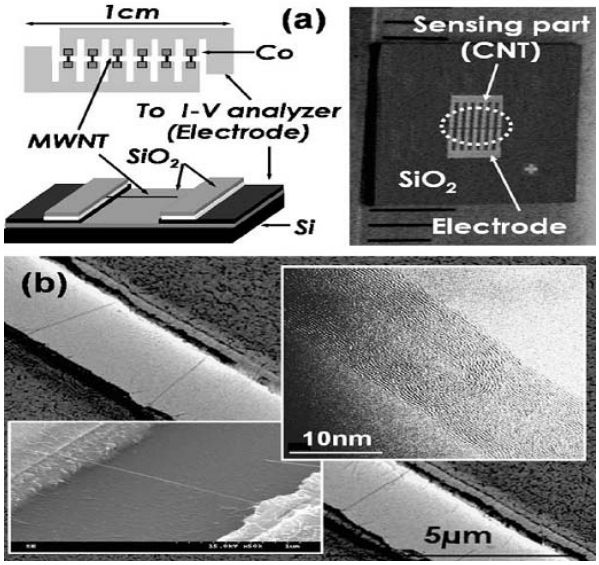

Fig. 40. (a) Photograph of completed MWCNTs based chemical sensor (b) SEM image of aligned CNTs resting on SiO_2 surface after directed growth. The CNTs show clear alignment in the direction of the electric field. The insert shows TEM image of laterally grown CNTs. Reprinted with permission from [66], Yoon-Taek Jang et al., *Sens. Actuators B* 99, 118 **(2004)**. © 2004, Elsevier.

More recently, Jang and co-workers[66] fabricated an ammonia sensor based on laterally grown MWCNTs. The tubes were grown from C_2H_4 by its thermal decomposition between interdigitated electrodes made of nobium. The metal electrodes worked as catalytic sites for the lateral grown of CNTs. The synthesis was additionally accelerated by 3 V bias voltage set across the electrodes. Such obtained tubes were straight MWCNTs that bridged the electrodes as presented in Figure 40. The electrical nature of the CNTs was not homogenous but a combination of metallic and *p*-semiconductor tubes. Since the electric resistance of metallic CNTs do not change significantly upon gas adsorption, all the observed changes were ascribed to *p*-semiconductor CNTs. Oxygen adsorption caused a decrease of electric resistance of the CNTs that was explained as the action of an electron acceptor on minority current carries in a *p*-type semiconductor. On the contrary, electron-donating gas NH_3 caused a reverse phenomenon, i.e., an increase of the electric resistance of the CNTs. The orientation of the tubes suggests that all measured electric effects are results of the adsorbate-CNTs interactions (chemical and physical). The technique proposed by Jang and co-workers seems an excellent approach for fundamental research on CNT gas adsorption.

Valentini and co-workers[67] ran pioneer studies on CH_4 detection by MWCNTs grown on a Ni catalyst. The study was focused on the direct adsorption of both gases on CNTs and the role of Ni catalyst remaining was not considered in detail. Authors proposed the mechanism of charge transfer in the CH_4-CHTs adsorption complexes. After outgassing

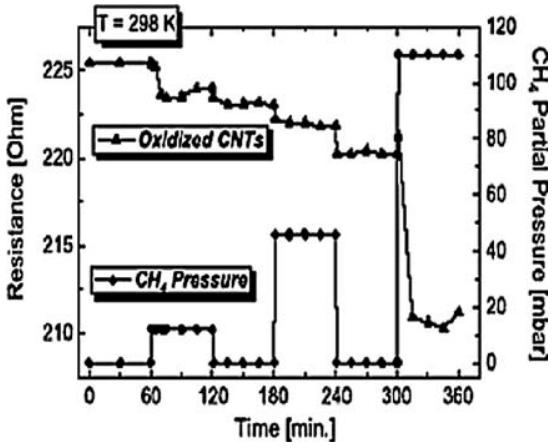

Fig. 41. Dynamic gas response of oxidized CNT films at an operating temperature of 298 K and CH4 partial pressures ranging from 12–110 mbar. Reprinted with permission from [67], L. Valentini et al., *Mat. Sci. Eng. C* 24, 527 **(2004)**. © 2004, Elsevier.

in vacuum, the examined MWCNTs behaved like typical *p*-semiconductors. Methane molecules, being in fact a reducing substance, acted as a donor of electrons. Thus, the adsorption of methane on "clean" CNTs resulted in the capture of holes, increasing the resistance. In another experiment, the CNTs were additionally oxidized before the experiments with methane. The oxidation of CNTs resulted in an increased resistance of CNTs. However, the subsequent adsorption of methane on the oxidised CNTs yielded surprising results, i.e., one observed a decrease of sensor's electric resistance (Fig. 41), the opposite of that obtained for non-oxidized samples. The explanation of the phenomenon based on a formerly published theoretical simulation[68] assumed the presence of oxygen compressed all the holes of semiconductor CNTs. Therefore, oxidized CNTs became an extrinsitic *n*-semiconductor and the adsorption of electron-donators as methane had to decrease the resistance of metallic CNTs. The study announced that the *p*-semiconductor to *n*-semiconductor transition of CNTs is possible not only by heating at elevated temperatures but also on a chemical way, i.e., by oxygen functionalization of CNTs. Moreover, one calculated that methane adsorbs physically on the CNT surface via a minute electron transfer to CNTs (0.027 electron per molecule).

The problem of CH_4 detection in air at room temperature was investigated by Lu and co-workers.[69] The CNTs used in that study differed significantly from those applied in other investigations. It is quite a common practice that CNTs for chemical sensor manufacturing are in a "raw" state. Many employ them "as grown" or at least oxidized. Sometimes one does not realize that often performed purification of CNTs means in fact oxidation of them since the purifying treatment involves the usage of strong oxidants. Thus, Lu and co-workers made a step ahead performing a more complex chemical manipulation. SWCNTs were subjected to metallization by sputtering of Pd particle onto the powder of CNTs. Then the sample was

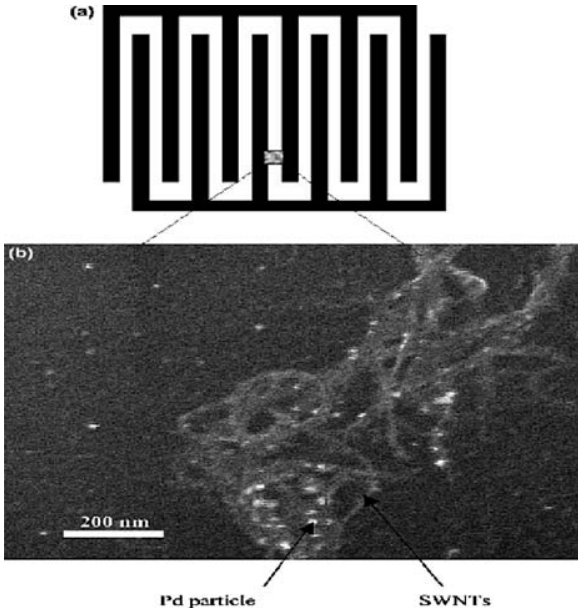

Fig. 42. (a) The interdigitated fingers use a finger width of 10 μm and a gap distance of 8 μm. (b) The scanning electron microscopic (SEM) image of Pd loaded SWCNT bundles dispersed on the interdigitated fingers. The bright spots are Pd particles with measured average size of 10 nm. Reprinted with permission from [69], Y. Lu et al., *Chem. Phys. Lett.* 391, 344 **(2004)**. © 2004, Elsevier.

carefully mixed. The Pd content by weight was close to 1%. The Pd/SWCNTs mixture was dispersed and successively drop-deposited onto a substrate with two interdigitated electrodes as presented in Figure 42. The fabrication procedure provided that the particles of Pd were small (ca. 10 nm in diameter) and well dispersed among the bundle of SWCNTs. The operation of the sensor was tested towards 0–100 ppm of methane in air at temperatures ranging from 25 to 150 °C. The resistance of the Pd-SWCNTs-containing resistors was tested upon the contact with CH_4 when 1 V bias voltage was set on the electrodes. A sensing mechanism was proposed to explain the observed resistance changes. As depicted in Figure 43. Pd particles were expected to donate electrons to adsorbed CH_4 molecules, which became charged negatively. Thus, the Pd particle was charged positively against the surface of a carbon tube. Therefore, Pd particles could restore the transferred electrons by attracting the electrons from CNTs. According to authors, the semiconductor SWCNTs were loosing minority current carriers, i.e., electrons. Thus, the conductance of CNTs had to increase as observed in practice. There was a problem with the renewal of the base resistance after exposure to pure air. The baseline was hard to recover suggesting that some durable adsorption complexes had to appear. Therefore, one applied UV irradiation to return to the starting resistance. The UV irradiation caused a significant increase of sensor's resistance probably due to deterioration of numerous surface species existing on Pd particles and CNTs.

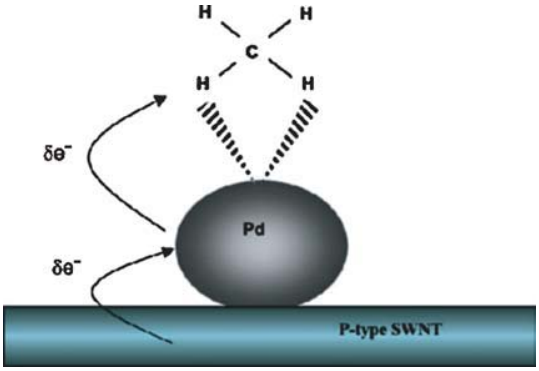

Fig. 43. The proposed sensing mechanism for room temperature methane detection using Pd-SWCNT sensors. Pd tends to form weakly bound complex Pd-(CH_4) at room temperature. When loaded on a SWCNT, the SWCNT can facilitate the formation of the complex by transfer charge to methane. As a result, *p*-typed SWCNT gains more holes as carriers for increased conductance. Reprinted with permission from [69], Y. Lu et al., *Chem. Phys. Lett.* 391, 344 **(2004)**. © 2004, Elsevier.

Novak and co-workers[70] fabricated a CNTs-based transistor and showed that the device was sensitive to many substances (ammonia, xylene vapour, and hexane vapour). Additionally, they investigated the sensitivity towards DMMP vapours (dimethyl methylphosphate) in the region of sub-ppm concentrations. The test using DMMP is one of pioneer works regarding the properties of the substance, which is a simulant for the nerve agent Sarin. The sensor design was equivalent to a chemically sensitive transistor (Fig. 44). It was achieved by the direct growth of SWCNTs onto a SiO_2 layer covering a Si substrate that

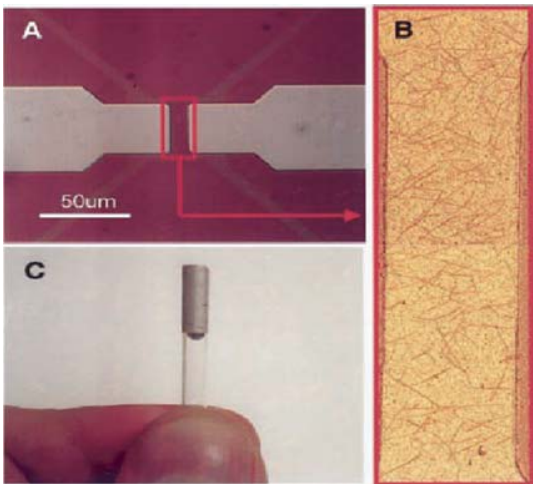

Fig. 44. (a) Optical micrograph of a SWCNT device. Ti contacts were evaporated on top of a SWCNT film grown on thermal SiO_2. The source/drain channel dimensions are 10×30 μm^2. The Si substrate serves as a back gate. (b) Representative AFM image of a SWCNT network that shows multiple conduction pathways via interconnected CNTs. (c) Optical micrograph of a SWCNT flow-cell chemiresistor sensor made from 1/8 in. outer diameter quartz tubing. Reprinted with permission from [70], J. P. Novak et al., *Appl. Phys. Lett.* 83, 4026 **(2003)**. © 2003, American Institute of Physics.